A FLEXIBLE STATISTICAL FRAMEWORK FOR THE CHARACTERIZATION AND MODELLING OF NOISE IN POWERLINE COMMUNICATION CHANNELS

by

Abraham Mutunga Nyete

Thesis submitted in fulfillment of the requirement for the degree

DOCTOR OF PHILOSOPHY IN ENGINEERING: ELECTRONIC ENGINEERING

SCHOOL OF ENGINEERING

UNIVERSITY OF KWAZULU-NATAL

SUPERVISOR: PROF. THOMAS J.O. AFULLO

CO-SUPERVISOR: DR. INNOCENT E. DAVIDSON

DECEMBER 2015

As the candidate's supervisors, we have approved this thesis for submission.

Signed…….. Date……

Name: Prof. Thomas J.O. Afullo

Signed…….. Date……

Name: Dr. Innocent E. Davidson

Declaration 1 - Plagiarism

I, **Abraham Mutunga Nyete**, declare that

1. The research reported in this thesis, except where otherwise indicated, is my original research.

2. This thesis has not been submitted for any degree or examination at any other university.

3. This thesis does not contain other persons' data, pictures, graphs or other information, unless specifically acknowledged as being sourced from other persons.

4. This thesis does not contain other persons' writing, unless specifically acknowledged as being sourced from other researchers. Where other written sources have been quoted, then:

   a. Their words have been re-written but the general information attributed to them has been referenced

   b. Where their exact words have been used, then their writing has been placed in italics and inside quotation marks, and referenced.

5. This thesis does not contain text, graphics or tables copied and pasted from the Internet, unless specifically acknowledged, and the source being detailed in the thesis and in the References sections.

Signed…….Date……..

Declaration 2 – Publications

The following list of papers have been published/submitted for review and constitute part of the work in this thesis:

Journal papers under review:

[J1] A.M. Nyete, T. J. O.Afullo, and Davidson, I. E., "In-building power line noise modelling and characterization using nonparametric kernel density estimators," *SAIEE Africa Research Journal,* (*under review*).

Published conference papers:

[C1] A.M. Nyete, T. J. O.Afullo, and I.E. Davidson, "Performance evaluation of an OFDM-based BPSK PLC system in an impulsive noise environment," *In PIERS Proceedings*, pp. 2510-2513, August 25-28 2014, Guangzhou, China, ISBN: 978-1-934142-28-8.

[C2] A.M. Nyete, T. J. O. Afullo, and I.E. Davidson, "On Rayleigh approximation of the multipath PLC channel: Broadband through the PLC channel," *In 2014 Southern Africa Telecommunication Networks and Applications Conference (SATNAC) Proceedings*, Port Elizabeth, South Africa, pp. 265-270, 31 August-3 September 2014, ISBN 978-0-620-61965-3.

[C3] A. M. Nyete, T. J. O. Afullo,, and I.E. Davidson, "Intra-building Power Network Noise Modelling in South Africa," *In Proceedings of the 23rd Southern African Universities Power Engineering Conference*, University of Johannesburg, Johannesburg, South Africa, 28-30th January 2015, pp. 468-472, ISBN 978-0-86970-786-9.

[C4] A. M. Nyete, T. J. O. Afullo, and I.E. Davidson, "Statistical Models of Noise Distribution in Broadband PLC Networks," *In Proceedings of PIERS 2015 in Prague*, July 6-9 2015, Prague, Czech Republic, pp. 423-429, ISBN: 978-1-934142-30-1.

[C5] A. M. Nyete, T. J. O. Afullo, and I.E. Davidson, "Power Line Noise Measurements and Statistical Modelling in the Time Domain," *In Proceedings of PIERS 2015 in Prague*, July 6-9 2015, Prague, Czech Republic, pp. 1569-1574, ISBN: 978-1-934142-30-1.

[C6] A.M. Nyete, T. J. O. Afullo, and I.E. Davidson and A.C. Britten, "A nonparametric approach for noise modelling in power line networks for PLC applications," *2015 Eskom Power Plant Engineering Institute Students Conference*, Eskom Academy of Learning, Midrand, South Africa, 8-9th June 2015.

[C7] A.M. Nyete, T. J. O. Afullo, and I.E. Davidson, "Statistical analysis and characterization of power line noise for telecommunication applications," *In Proceedings of the IEEE AFRICON 2015 Conference*, Addis Ababa, Ethiopia, 14–17 September 2015, pp. 213-217, ISBN: 978-1-4799-7497-9.

[C8] A.M. Nyete, T. J. O. Afullo, and I.E. Davidson, "On the application of non-parametric estimation methods for low voltage PLC network noise modelling," *In Proceedings of the Southern Africa Telecommunication Networks and Applications Conference (SATNAC) 2015*, Arabella Hotel & Spa, Western Cape, South Africa, 6-9 September 2015, pp. 59-63, ISBN: 978-0-620-67151-4.

Acknowledgements

I wish to thank the Almighty God for the opportunity to pursue graduate studies and for granting me the resources to accomplish this dream; above all good health. I would also like to thank my supervisors Prof. Thomas T.J.O. Afullo and Dr. Innocent E. Davidson for their guidance and support throughout the study period. The many and long periods of time spent in discussing the progress and direction of the research cannot go unmentioned. I will forever be indebted to them for the way they have shaped my life up to now. Your humility and wisdom is a big inspiration to many.

Additionally, I want to thank my colleagues Dr. Peter Akuon, Dr. Akintunde Alonge and Mr. Mike Asiyo for the role they played in introducing me to academic research. Also I wish to acknowledge Fulatsa Zwane and Dr. Chrispin Mulangu for breaking the ground on this research area in our research group. I also wish to acknowledge my colleagues Mary Nabangala Ahuna and Steve Awino. I also wish to thank Mr. J. Gumede and Steven Awino for their assistance with the equipment handling during the noise meausements.

Also, I wish to thank my parents, brothers and sisters for their support and love through out my life. I also wish to thank the love of my life Lilian Kenyuri Nyamwamu in a special way for painstakingly taking care of our two sons; Allan Mutunga and Alvin Mutunga for the period I have been away on graduate studies. Her support in many respects is higly appreciated. I also thank Allan Mutunga and Alvin Mutunga for being nice and supportive to mummy during the period of my absence. Good to see that you guys have grown now and can help mummy with house chores!

Lastly, I would also wish to acknowledge the German Academic Exchange Service (DAAD) for providing support for this work through the African Network of Scientific and Technological Institutions (ANSTI). I am also very grateful to ESKOM for supporting this work through their EPPEI programme.

To all of you, may the Lord God Almighty continue to shower his blessings on you!

Abstract

One communication medium that has received a lot of interest in recent years is the power line channel, especially for the delivery of broadband content. This channel has been traditionally used to carry electrical power only. But with the recent advancements in digital signal processing, it is now possible to realize communications through the power grid, both in narrowband and broadband. The use of the power line network for telecommunication purposes constitutes what is referred to as powerline carrier communications or simply powerline communications (PLC). The biggest incentive for PLC technology use is the fact that the power line network is already in place, which greatly reduces the communication network set up cost, since no new cabling layout is required. PLC technology is widely applied in home networking, broadband internet provision and smart grid solutions. However, the PLC channel presents a very hostile communication environment. And as such, no consideration has been made in the design of traditional power line network to accommodate communication services. Of all the PLC channel impairments which include frequency-dependent attenuation, frequency selectivity, multipath and noise, noise is the biggest threat to communication signals. This noise manifests itself in form of coloured background noise, narrowband interference and impulsive noise. A thorough understanding of this noise distribution is therefore crucial for the design of a reliable and high performing PLC system. A proper understanding of the noise characteristics in the PLC channel can only be realized through noise measurements in live power networks, and then analyzing and modeling the noise appropriately. Moreover, the noise scenario in power line networks is very complex and therefore cannot be modeled through mere analytical methods. Additionally, most of the models that have been proposed for the PLC noise previously are mere adaptations of the measured noise to some existing impulsive noise models. These earlier modeling approaches are also rigid and model the noise via a fixed set of parameters.

In the introductory work in this thesis, a study of orthogonal frequency division multiplexing (OFDM) as the modulation of choice for PLC systems is presented. A thorough survey of the salient features of this modulation scheme that make it the perfect candidate for PLC modulation needs is presented. In the end, a performance analysis study on the impact of impulsive noise on an OFDM based binary phase shift keying (BPSK) system is done. This study differs from earlier ones in that its focus is on how the elementary parameters that define the impulsive noise affect the system, a departure from the usual norm of considering the overall noise distribution. This study

focuses on the impact of interarrival times (IAT), pulse amplitudes as well as pulse widths, among other parameters.

In the first part of the main work in this thesis, results of an intensive noise measurement campaign for indoor low voltage power line noise carried out in various power line networks, in the Department of Electrical, Electronic and Computer Engineering buildings at the University of KwaZulu-Natal, Howard campus are presented. The noise measurements are carried out in both time and frequency domains. Next, the noise measurements are then analyzed and modeled using two very flexible data modeling tools; nonparametric kernel density estimators and parametric alpha stable (α-stable) distributions. The kernel method's ability to overcome all the shortcomings of the primitive histogram method makes it very attractive. In this method, the noise data structure is derived straight from the data itself, with no prior assumptions or restrictions on the data structure, thus effectively overcoming the rigidity associated with previous noise models for power line channels. As such, it results in density estimates that "hug" the measured density as much as possible. The models obtained using the kernel methods are therefore better than any parametric equivalent; something that can always be proven through goodness of fit tests. These models therefore form an excellent reference for parametric modeling of the power line noise. This work forms the author's first main contribution to PLC research.

As a demonstration of the kernel models suitability to act as a reference, parametric models of the noise distribution using the alpha stable (α-stable) distribution are also developed. This distribution is chosen due to its flexibility and ability to capture impulsiveness (long-tailed behaviour), such as the one found in power line noise. Stable distributions are characterized by long/fat tails than those of the Gaussian distribution, and that is the main reason why they are preferable here since the noise characteritics obtained in the kernel technique show visible long/heavy tailed behavior. A parameter estimation technique that is based on quantiles and another on the empirical characteristic function are employed in the extraction of the four parameters that define the characteristic function of the α-stable distribution. The application of the α-stable distribution in other signal processing problems has often been over-simplied by considering the symmetric alpha stable distribution, but in this thesis, the general α-stable distribution is used to model the power line noise. This is necessary so as to ensure that no features of the noise distribution are missed. All the models obtained are validated through error analysis and Chi-square fitness tests. This work forms the author's second main contribution to PLC research. The author's last contribution in this thesis is the development of an algorithm for the synthesis of the power line as a Levy stable stochastic process. The algorithm developed is then used to generate the PLC noise process for a

random number of alpha stable noise samples using the alpha stable noise parameters obtained in the parametric modeling using stable distributions. This algorithm is generalized for all admissible values of alpha stable noise parameters and therefore results for a Levy stable Gaussian process are also presented for the same number of random noise samples for comparison purposes.

Table of Contents

List of Figures

List of Tables

Table of abbreviations/acronyms

Abbreviation	Full name/Meaning
PLC	Powerline communications
OFDM	Orthogonal frequency division multiplexing
BPSK	Binary phase shift keying
IAT	Interarrival times
α-stable	Alpha stable
QAM	Quadrature Amplitude Modulation
TCM	Turbo Coded Modulation
DSO	Digital storage oscilloscope
FFT	Fast Fourier Transform
RLC	Resistor-inductor-capacitor
EMC	Electromagnetic Compatibility
EMI	Electromagnetic interference
NB-PLC	Narrowband PLC
BB-PLC	Broadband PLC
BER	Bit error rate
SNR	Signal to noise ratio
SRC	Series resonant circuit
AWGN	Additive white Gaussian noise
AM	Amplitude modulation
GIR	Gaussian-to-impulse noise power ratio
BPF	Band Pass Filter
MLSE	Maximum likelihood estimator
APP	*a posteriori probability*
MAP	*maximum a posteriori*
LLR	log likelihood ration
CDMA	Code-Division Multiple Access
SF	Spreading factor
MCSS	Multicarrier Spread Spectrum
THSS	Time Hopping spread spectrum
DSSS	Direct Sequence Spread Spectrum (DSSS)
FHSS	Frequency Hopping Spread Spectrum
IDFT	Inverse discrete Fourier transform
IFFT	Inverse fast Fourier transform
FFT	fast Fourier transform
EM	Electromagnetic
EMS	Electromagnetic susceptibility
EME	Electromagnetic emission
CE	Conducted emission
RE	Radiated emission
CS	Conducted susceptibility
RS	Radiated susceptibility
FCC	Federal Communications Commission
CISPR	*Comité International Spécial des Perturbations Radioélectrique*s
TVSS	Transient voltage surge suppressor
pdf	probability density function

Abbreviation	Full name/Meaning
cdf	cumulative frequency distribution
MISE	mean integral square error
AMISE	asymptotic MISE
DF	degrees of freedom
SL	significance level
PSD	power spectral density
i.i.d	independent and identically distributed
DSP	digital signal processing
ML	maximum likelihood
MoM	method of moments
RMSE	root mean square error

Chapter One

1. Introduction

1.1 General introduction

Communication technologies have evolved over the years; both wired and wireless. This evolution has been driven by the desire to develop faster and more reliable communication networks as well as reduce costs. One such communication technology which has received a lot interest from researchers and industry players is power line communications (PLC). PLC entails the utilization of power lines for the transfer of information from the transmitter to the receiver. This technology is attractive due to the fact that no additional network layout is required to be able to send information; apart from coupling devices. Thus, it is possible to carry both voice and data traffic together with electricity in the same channel using this technology. PLC technologies are mainly classified into two; narrowband and broadband, depending on the frequency band of operation. Usually, broadband PLC operate in the frequency range between 1 MHz to 300 MHz. Narrowband PLC operate in the frequency range between 3 KHz to 500 KHz [1]**.** Power lines terminate at almost every home and this enables the use of the low voltage network as a last mile access solution for communication purposes. PLC is useful in automation of meter reading services, pre-paid billing services, automation of fault detection, load management, high data rate internet access and home Television carrier services. PLC networks also form part of local area networking solutions [2, 3]. The PLC channel is defined by attenuation, channel transfer function, noise as well as multipath.

Different channel modeling approaches have been fronted in an effort to demystify the complexity associated with PLC channels. These models are mainly based on a bottom up approach in describing the channel in terms of the constituent power line components by employing scattering parameters or four pole impedance and admittance matrices. These models utilize detailed knowledge of the power line network components to determine the necessary matrix elements. Their main drawback is the large number of parameters required to build the matrices, which often is hard to determine with sufficient accuracy. Other channel models have been fronted which employ a top down approach; in which case the communication channel is treated as a black box and then its transfer characteristics are determined from channel measurements [4-9]. Some PLC

standards that are currently in use include the CENELEC standard, IEEE 1901 Standard, ITU-T G.hn and HomePlug AV [1].

However, the PLC channel is however a hostile environment for use as a communications media. This is primarily so because the channel characteristics are highly varying with frequency, time, loads and topology. The channel is also plagued with different sources of noise which are difficult to effectively describe both parametrically and nonparametrically. The main noise types in PLC include background noise, narrowband interference and impulse noise. As again, the channel characteristics of the PLC network are difficult to model parametrically in terms of the network elements as the complexity of such as task grows magnificently as the network size increases. The channel impedance also varies with the number of loads and is also frequency dependent. Also the signal is attenuated as it traverses the channel from the transmitter to the receiver. This attenuation is mainly dominated by frequency selective fading. Of all the PLC channel impairments, noise is the biggest threat to communication signals. This noise in all its form is detrimental to communication signals; especially during impulsive noise events where data is lost in bits or bursts. This noise therefore affects the channel performance as well as reliability. In this thesis, the main focus is to study the PLC noise in indoor low voltage PLC networks through measurements, analysis, modeling, characterization, and synthesis. The noise is modeled both parametrically and nonparametrically and then synthesized as a Levy stable stochastic process [8-14].

1.2 Motivation

The power line network provides a ready medium for communication, owing to its extensive coverage, both outdoor and indoor. This in turn greatly reduces the cost of rolling out a communication network. The use of the PLC network as a communication medium brings with it a lot of challenges since the power line network is originally designed to carry electrical power. These challenges range from noise impairments, difficulties in properly characterizing the channel non-parametrically and parametrically, implementation of robust error control techniques and modulation schemes, and proper coupling of the signal to the network. Until now we still don't have any universal models that can be used to model and characterize the frequency, amplitude, phase, impedance and noise charcateristics of the PLC channel.

PLC channels are time-varying and have frequency-dependent loads connected and is also plagued by different noise types. One of the biggest problems in PLC channels is the impulsive nature of the noise which is usually a direct consequence of switching ON or OFF of the electrical appliances on

the network as well as transients generated during faults. All in all, the complex environment provided by power networks for communication purposes calls for the proper understanding of the channel characteristics so as to ensure that the error performance and reliability of the network is improved while at the same time not comprising on other key performance metrics like throughput and delay.

Currently, all the models that have been proposed for modeling noise in PLC channels are parametric. These models are derived using fixed and limited forms of distributions which renders them rigid. This rigidity means that the fitting of measured noise data using such models could lead to some of the salient fetaures of the noise distribution being missed out. To counter this shortcoming associated with parametric models, in this thesis, a novel application of nonparametric kernel density estimators for the modeling of noise measured in low voltage indoor PLC networks is presented. The density estimate in this technique is obtained directly from the data without any restrictions being imposed and/or making any assumptions pertaining the underlying data structure. The kernel density technique is the most popular and robust nonparametric estimator. The models derived using this modeling tool are seen to "hug" the measured noise very closely, and going by the error statitics obtained as well as consistency results obtained using the Chi-square tests, these models are reference models. They are reference models in that they model the data as it is, without forcing it to fit into some form of known parametric distribution.

And again, to demonstrate the ability of the kernel models to act as reference models, and to further investigate the long-tailed behavior observed in the kernel models, a very flexible stochastic modeling tool is applied to model the noise data parametrically. This tool is a four parameter distribution that is able to model very impulsive (evident from the heavy tails observed in the kernel models) to non-impulsive Gaussian cases. As such, the distribution is loosely a generalized Gaussian distribution. This modeling tool is the alpha (Levy) stable distribution. Alpha stable distributions are characterized by long/heavy tails and are therefore the perfect choice for investigating the long tails of the noise distribution. This work constitutes the author's second contribution to PLC research. Also, to generalize and further understand the PLC noise process, to the extend that we no longer resort to noise measurements to characterize the long-tailed nature of PLC impulsive noise, there is need for a PLC noise synthesis process. Having confirmed that the noise in PLC networks can be modelled as an alpha stable process, a PLC synthesis framework for PLC noise as a Levy stable process is then very necessary. Thus, such a framework is developed in the last part of this thesis and a demonstration of its applicability to synthesize the PLC noise for a random number of alpha stable noise samples is also presented. This framework is applicable for

any level of noise impulsiveness that may be experienced in PLC networks. This framework is able to regenerate the noise process from the modelling results obtained from measurements. This work constitutes the author's third contribution to PLC research.

PLC technology is expected to be the key driver of internet connectivity through the power grid, especially for connecting people living in rural/remote areas. The uptake of PLC technology has been slow due to lack of universal standards/models, especially in broadband PLC, and the incompatibility between the few available standards developed by different bodies.

1.3 Research questions

The following research questions have guided this research:

1.What are the inherent characteristics of the power line channel that hinder optimal communication through the channel?

2. How does the power line channel transfer characteristic behave and what influences it?

3. Which are the current power line noise models and what are their strengths and weaknesses?.

4. What techniques can be applied for the development of better noise models for the optimization of the power communication channel?

5. Is it possible to develop a stochastic process for noise synthesis in PLC channels?

1.4 Research Objectives

The research areas to be looked into include (but not limited to) the following:

1. Study of parametric and non-parametric models of the PLC channel characteristics.
2. An assessment of the power line channel performance under various noise conditions.
3. Study and characterization of different types of noise inherent PLC channel.
4. Development of better noise models that applicable in the redesign and/or optimization of the power line communication channel both parametrically and no-parametrically.
5. Development of a noise synthesis algorithm for PLC channels

1.5 Research methodology

The following steps were adopted to ensure successful completion of this research work:

1. A thorough literature review of the PLC channel characteristics.
2. A literature survey of the different noise and channel models that have been proposed by different researchers in an effort to characterize the PLC channel.
3. Noise measurements in indoor low voltage network enviroments.
4. Analysis, characterization, modeling and synthesis of the acquired noise measurements.
5. Validation of all the models developed through error analysis and Chi-Square tests.

1.6 Contributions

The following are the main contributions to this important research field:

1. Development of novel nonparametric low voltage power line noise models derived from noise measurements using kernel density estimators.
2. Development of parametric low voltage power line noise models that are benchmarked on the most optimal nonparametric kernel models using stable distributions.
3. Development and testing of a novel Levy stable PLC noise synthesis framework

The following are minor contributions to the area of PLC research:

1. A performance evaluation study of impulsive noise on an OFDM-based BPSK system.
2. Development of a Rayleigh approximation channel model of the power line channel transfer function.

1.7 Thesis organization

The rest of this thesis is organized as follows:

In Chapter two, a survey of power line communications is provided. This survey covers the channel transfer function, power line noise, modulation, as well as EMC/EMI issues in PLC. Also, a performance evaluation study of impulsive noise on an OFDM-based BPSK system is done.

In Chapter three, the noise measurement procedures as well as the measuring equipment description are presented. The coupling circuit design as well as its transfer function is presented as well. Also,

the measurement environment where some of the noise measurements were done is described. Finally, a snap shot of a few of the noise measurement results is presented at the end of the chapter.

In Chapter four, a novel application of nonparametric kernel density estimators for the modeling of the noise data obtained in Chapter three is presented. The features and properties of this flexible nonparametric stochastic tool are outlined before its application in the derivation of reference models for the measured noise characteristics in both time and frequency domains. The models tests for goodness of fit and reliability are also presented.

To demonstrate the kernel models ability to act as reference models, and to further investigate the long tails observed in the kernel models, in Chapter five, the very flexible stable distribution is applied in the modeling of the measured noise characterictics. This distribution is used because of its superior flexibility compared to other impulsive noise models, as well as its ability to capture the impulsive nature of power line noise. The impulsiveness found in many phenomena results in heavy/long tails in their marginal distributions; something that stable distributions are well-known to capture perfectly. All the models in this chapter are referenced on their optimal kernel models counterparts, and therefore their fitness as well as consistency test results are presented as well.

Upon confirmation that the noise process in PLC systems is actually an alpha stable (Levy) process as seen in the results in Chapter five, in Chapter six, a PLC noise synthesis framework is developed based on the nonlinear transformation of an independent exponential variable and an independent uniform variable, as well as the proof of equality in law of a skewed random variable. All results are compared to those obtained from measurements in Chapter five, and therefore their stability/reliability as well as goodness of fit results are also presented.

In Chapter seven, an executive summary of the contents of this thesis is presented together with possible directions for future work.

Chapter references

[1] L.T Berger, A. Schwager and J.J. Escudero-Garzas, "Power line communications for smart grid applications," *Journal of Electrical and Computer Engineering*, vol. 2013, Article 712376, 16 pages.

[2] H.C. Ferreira et al., "Power line communications: An overview," *IEEE AFRICON 1996*, 24-27 September 1996, Stellenbosch, South Africa, pp. 558-563.

[3] A.M. Nyete, T. J. O. Afullo, and I.E. Davidson, "Statistical analysis and characterization of power line noise for telecommunication applications," *In Proceedings of the IEEE AFRICON 2015 Conference*, Addis Ababa, Ethiopia, 14–17 September 2015, pp. 213-217.

[4] M. Zimmerman and K. Dostert, "A multi-path signal propagation model for the power line channel in the high frequency range," *Proceedings of the 3rd International Symposium on Power Line Communications and Applications*, 1999, Lancaster, U.K. pp. 45-51.

[5] A.M. Nyete, T. J. O. Afullo, and I.E. Davidson, "On the application of non-parametric estimation methods for low voltage PLC network noise modelling," *In Proceedings of the Southern Africa Telecommunication Networks and Applications Conference (SATNAC) 2015*, pp. 59-63.

[6] M. Zimmermann and K. Dostert, "A Multipath Model for the Power Line Channel", *IEEE Transactions on Communications*, vol. 50, no. 4, pp.553-559, April 2002.

[7] J. Anatory, M.M. Kissaka and N.H. Mvungi, "Channel model for broadband power line communication," *IEEE Transactions on Power Delivery*, vol. 22, no. 1, pp. 135-141, January 2007.

[8] A. D. Familua and L. Cheng, "Modelling of in-house CENELEC A-band PLC channel using Fritchman model and Baum-Welch algorithm," *2013 IEEE International Symposium on Power Line Communications and Applications*, pp. 173-178.

[9] A.M. Nyete, T. J. O.Afullo, and I.E. Davidson, "Performance evaluation of an OFDM-based BPSK PLC system in an impulsive noise environment," *In PIERS Proceedings*, August 25-28 2014, Guangzhou, China, pp. 2510-2513.

[10] P. Mlynek et al., "Power line cable transfer function for modeling of power line communication system," *Journal of Electrical Engineering*, vol. 62, no. 2, pp. 104-108, 2011.

[11] A. M. Nyete, T. J. O. Afullo,, and I.E. Davidson, "Intra-building Power network noise modelling in South Africa," *In Proceedings of the 23rd Southern African Universities Power Engineering Conference*, University of Johannesburg, Johannesburg, South Africa, 28-30th January 2015, pp. 468-472.

[12] E. Biglieri, "Coding and modulation for a horrible channel," *IEEE Communications Magazine*, pp. 92-98, May 2003.

[13] A.J. Han Vinck and J. Haring, "Coding and modulation for power-line communications," *ISPLC 2000*, pp. 265-272.

[14] H.C. Ferreira et al., “Permutation Trellis Codes,” *IEEE Transactions on Communications*, vol. 53, no. 11, pp. 1782-1789, November 2005.

Chapter Two

2. Powerline Communications Survey

2.1 Introduction

Power lines are designed to carry electric power. However, the extensive coverage that the power lines have reached in recent years has attracted the attention of communication engineers who see it as the cheapest medium for modern day communications. This has led to the emergence of power line communications [PLC]; which essentially refers to the transfer of voice, data and video signals between the transmitter and the receiver over the electrical power network. PLC technology is primarily attractive because the power line network is already in place, which greatly brings down the cost of setting up a communications network. Hence, many research efforts have been fronted that are geared towards the investigation of the characteristics of the PLC channel. These efforts range from the study of the channel frequency response, attenuation, noise characteristics, multipath effects, throughput as well as coding and modulation options that best suit this channel [1-20]. A simplified diagram of a power line communication network is shown in Figure 2-1.

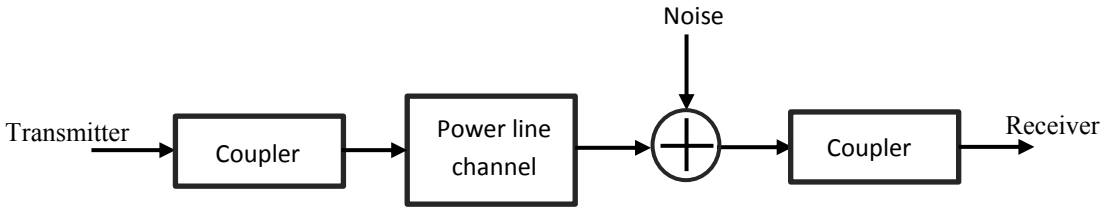

Figure 2- 1: A simplified block diagram of a power line communication network

Currently, PLC applications can be are categorized into two broad categories: the “last mile” and the “last inch” access. The “last mile” application in networking solutions refers to the use of the PLC channel in providing a communications link between the last point of connection at the distribution layer (may be the local distribution transformer) and the customer premises. Fig. 2-2 below shows an example of such an application. On the other hand, the “last inch” application refers to the use of PLC technology in providing networking communication channel inside the

customer premises; see Fig. 2-3 for an illustration. PLC technology is not necessarily better than other communication technologies, neither are these other technologies without challenges of their own, or to put in other words; superior to PLC technology. However, PLC has a clear edge over the other technologies owing to the fact that a socket terminates at every room in every house that is connected to the power grid, thus providing readily available medium of communication [1, 15]. The power line network is by far be the most expansive and ubiquitous in the world both at the core, distribution and access layers.

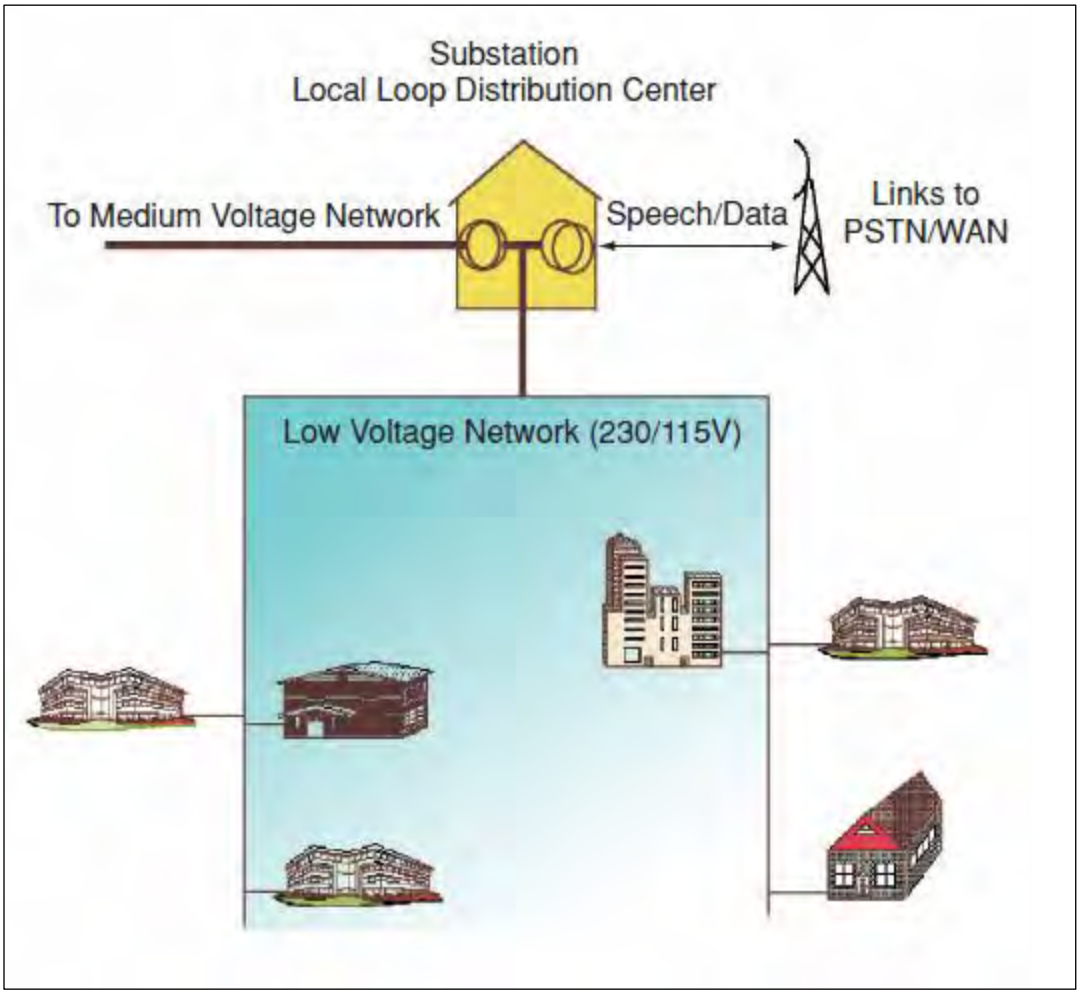

Figure 2- 2: The "last mile" broadband connection to homes and offices from a local distribution center [16]

PLC technology is broadly divided into two categories depending on the frequency band and the data throughput rate. These are the narrowband and broadband PLC. Narrowband PLC (NB-PLC) operates in the frequency band 3-500 KHz while broadband PLC (BB-PLC) usually operates at

frequencies between 1-300 MHz. Further, NB-PLC can be sub-classified into low data rate and high data rate applications. NB-PLC applications have a throughput that is limited to a few kbit/s and are also based on single carrier technology. This category of PLC system is mainly applied in automation of metering solutions, low data rate interconnections and control of home appliacnces through power sockets in every room, street lighting control, ground-lights control in airport runways, home automation and application in control data communication with 40 kbit/s in street car/subway systems on 750V direct current networks . BB-PLC data rates are in the megabit per second range. Broadband PLC networks are an ideal solution for advanced information technology applications such as high speed data transfer, real-time video streaming and high definition television (HDTV) as well as voice connections [1, 17-21].

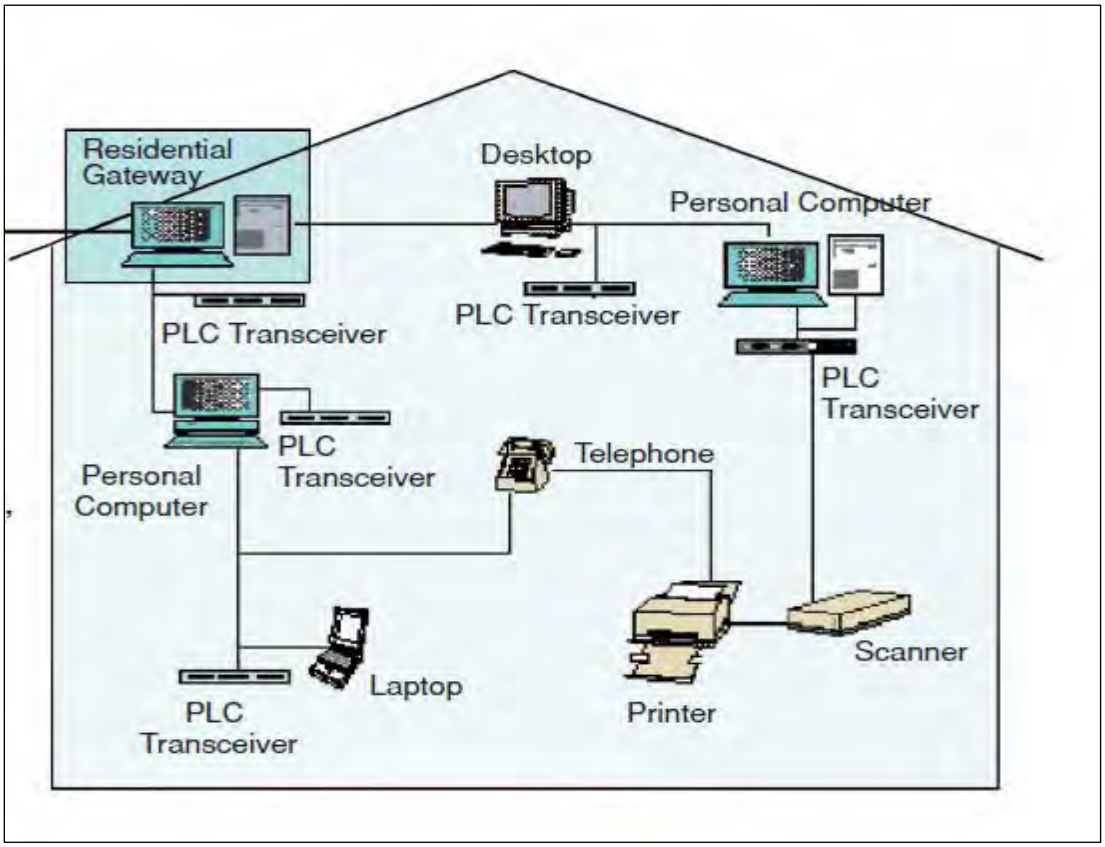

Figure 2- 3: The “last-inch” access or in-house networking [16]

The fact that the power lines were designed with the primary goal of transmitting electrical power means that the channel is not that favorable for communication purposes. Thus the PLC channel is

hostile in as far as communication needs are concerned. This is so because the channel is plagued by impedances that vary both with time and frequency, attenuation that is frequency dependent, multipath effects that arise from multiple branches and nodes, different noise types as well as electromagnetic compatibility issues that limit the transmit power [17,19]. Thus there is need to study and understand the channel behavior in different loading conditions and noise types. The studies would range from obtaining the channel transfer function, throughput analysis and modeling, noise measurements and modeling, and study of the channel response when different coding and modulation schemes are used to enhance the channel performance [6, 12, 15, 17-19, 22]. The channel performance can be measured in terms of the bit error rate (BER) and the signal to noise ratio (SNR).

However, the biggest problem in the characterization of the PLC channel properties would be to come up with a model that describes all the channel characteristics and incorporates all the measurements into a mathematical model, and still remains physically meaningful in terms of the distribution both in space and time, and also remains simple to the point that any required statistics can be extracted for solving any problem to do with signal transmission and reception. Thus the characterization of the PLC channel, like any other communication channel, is a tradeoff between system complexity and performance. All in all, there is no universally accepted channel and noise models for the PLC channel currently, and efforts to get some are an on-going exercise. Different researchers and academicians have proposed models of the PLC channel base on analytical derivations and/or from measurements.

2.2 Powerline channel modeling

2.2.1 PLC channel modeling approaches

Power line networks differ in terms of structure, topology and the physical properties from other transmission media such as coaxial cables, fiber-optic cables and twisted pair cables, and wireless channels, among other media. The power line environment is hostile when used for data and voice communication. The channel is very dynamic both in time and space, which means that the channel properties are hard to accurately predict and/or model. For practical purposes, models of the channel frequency response, channel availability and reliability as well as noise models are of interest. In contrast though, most of the models developed to define the above channel characteristics are very limited in terms of their practical value [6].

For the channel transfer characteristics (frequency response), most of the models are limited due to the fact that they are based on bottom-up approaches which means that the network behavior is described in terms of a large number of distributed components. Normally, such components are described in form of matrices which describe their properties, based on either scattering parameters or admittance and four-pole values [6, 22, 23]. This means that the details of all the network components, that is, cables, connected devices and joints (nodes) are needed for the setting up of the above matrices. But, from a practical perspective, it would be impossible to determine all the parameters associated with each of these network elements with sufficient precision.

On the contrary, a more practical approach would be to measure the channel transfer function between the input and the output by assuming that the network is a black box. This approach is usually referred to as the top-down method. This approach is the one adopted in [4-6, 24]. In [24], an attenuation and noise model is presented based on measurements. This model is narrowband in that its frequency range is restricted to below 150 KHz. The model described in [6] describes the channel transfer characteristics in the range of frequencies between 500 KHz and 20 MHz; thus this model can be used for broadband applications. The model describes the channel multipath properties in very few relevant parameters, as compared to complexity associated with the bottom-up strategy. The channel parameters are derived from measurements. The basic idea in this approach were first explored in [4] and at the same time a less precise though simpler multipath model derived in [5].

Only in the simplest of cases, that is a single branch network, can the physical explanation for the measured results be identified in terms of the cable losses, transmission as well as reflection factors. In real networks, comprising of many branches and nodes, the back-tracing of the observed results to the physical nature of the network would be an impossible task. Thus the top-down methodology is a more realistic and simpler approach.

2.2.2 PLC Channel Models

The power line channel is one of the most complex channels to describe in terms of the constituent elements in the network as described above. Thus, most of the models that are in existence today are based on the measured network response which is then related to particular known electric or electronic phenomena. Alternatively, the phenomena are used to predict the PLC channel response and then measurements are done to test how close the measurements and predictions come. Earlier models of the channel frequency response are the multipath model of Zimmermann and Dostert [4,

6], the echo model of Philipps [5], Meng *et al.* model [9], Anatory *et al.* model [7, 25] and the Esmaillian model [26], among others.

2.2.2.1 Zimmermann and Dostert Multipath Model

A typical power distribution network consists of numerous branches and nodes. If the power network is used as a communication channel, the signal is bound to suffer from multiple reflections and at the end of the day, it will undergo multipath propagation. The various nodes (interconnection points) within the network act as possible scattering/reflection points for the signal. Thus the signal travels back and forth before reaching the final destination. This is primarily so because the different branches that are interconnected from one node have different complex impedances. It is on this basis that Zimmermann and Dostert [4, 6] proposed a multipath model for the powerline channel.

If we consider the signal that travels through a complex power line network, it becomes rather obvious that there is no direct line of sight path between the transmitting and receiving antenna. Thus, different copies (echoes) of the signal that are attenuated and delayed in different proportions arrive at the receiving antenna. The kind of fading experienced in this case is frequency selective. The model was first developed by considering the simplest of a power network that can be; a single node network with one branch. This is illustrated in Fig. 2-4 below. The network consists of three elements (1), (2) and (3) with lengths L_1, L_2 and L_3 and the characteristic impedances Z_{L1}, Z_{L2} and Z_{L3} respectively. With the assumption that points A and C are matched, which makes $Z_A = Z_{L1}$ and $Z_C = Z_{L2}$, the reflection points are B and D, with the reflection coefficients r_{1B} , r_{3B}, r_{3D} and the transmission coefficients are t_{1B}, t_{3B}.

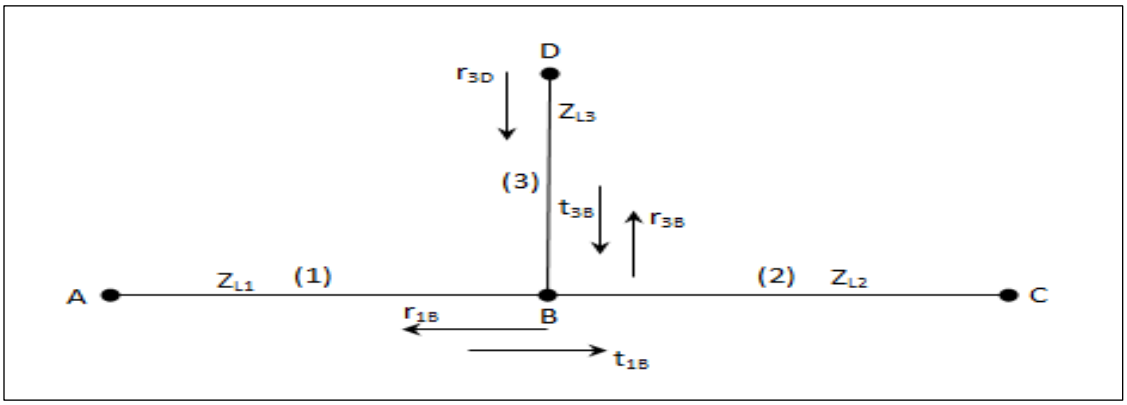

Figure 2- 4: Multipath propagation: Cable with one tap [6].

With these assumptions in place, the link may have an infinite number of propagation paths. Each path i, has a weighting factor g_i which represents the product of the reflection and transmission coefficients along the particular path. In [27], Gotz *et al.* have shown that after a reasonable number of paths, typically between 5-50 paths, the weight factor becomes negligible and the model is computed with a finite number of paths. From complex channel transfer function measurements, the authors came up with the following expression for the channel frequency response as a multipath environment [6]:

$$H(f) = \sum_{i=1}^{N} g_i \cdot e^{-(a_0 + a_1 f^k)\cdot d_i} \cdot e^{-j2\pi f \tau_i} \tag{2.1}$$

Where, N is the number of propagation paths, $g_i$is the weighting factor, a_0 , a_1 and exponent k are the parameters that define the frequency-dependent attenuation, d_i is the path length, τ_i is the path delay given by the following expression:

$$\tau_i = \frac{d_i}{v_p} = \frac{d_i\sqrt{\varepsilon_r}}{c_0} \tag{2.2}$$

Where ε_r is the insulating material's dielectric constant, c_0 is the speed of light, d_i is the length of a path and v_p is the propagation speed. Thus we can see from (2.1) that the model is characterized by three different components; the weighting factor, the attenuation portion and the delay portion. The factor $e^{-(a_0 + a_1 f^k)\cdot d_i}$ determines the amount of attenuation that takes place during signal transmission in the PLC channel. The factor $e^{-j2\pi f \tau_i}$ is the delay portion. The transmission and reflection coefficients are always less than one, and so, it goes without saying that the net product of all the transmission and reflection coefficients is also less than one, viz a viz:

$$|g_i| \leq 1 \tag{2.3}$$

The attenuation factor is obtained from the complex propagation constant by using transmission line analogy, that is:

$$\gamma = k_1\sqrt{f} + k_2 f + jk_3 f \tag{2.4}$$

Where $k_1\sqrt{f} + k_2 f$ is the attenuation constant and $k_3 f$ is the phase constant.

The constants k_1, k_2 and k_3 summarize the geometrical and material properties of the network. Thus it can be seen from (2.4) that the attenuation increases with frequency. The weighting and the delay factors are obtained when the frequency response of the PLC channel is converted into time domain. The weighting factor is inversely proportional to the delay factor. This is due to the reduction in signal power as the signal travels through different points of discontinuity. This is depicted in Fig. 2-5 below. For the single branch network, reflection coefficients are obtained from:

$$r_{1b} = \frac{Z_{L2}||Z_{L3} - Z_{L1}}{Z_{L2}||Z_{L3} + Z_{L1}} \tag{2.5}$$

$$r_{3d} = \frac{Z_0 - Z_{L3}}{Z_0 + Z_{L3}} \tag{2.6}$$

$$r_{3b} = \frac{Z_{L2}||Z_{L1} - Z_{L3}}{Z_{L2}||Z_{L1} + Z_{L3}} \tag{2.7}$$

Where Z_0 is the characteristic impedance,.

Consequently, the transmission coefficients are obtained from:

$$t_{1b} = 1 - |r_{1b}| \tag{2.8}$$

$$t_{3b} = 1 - |r_{3b}| \tag{2.9}$$

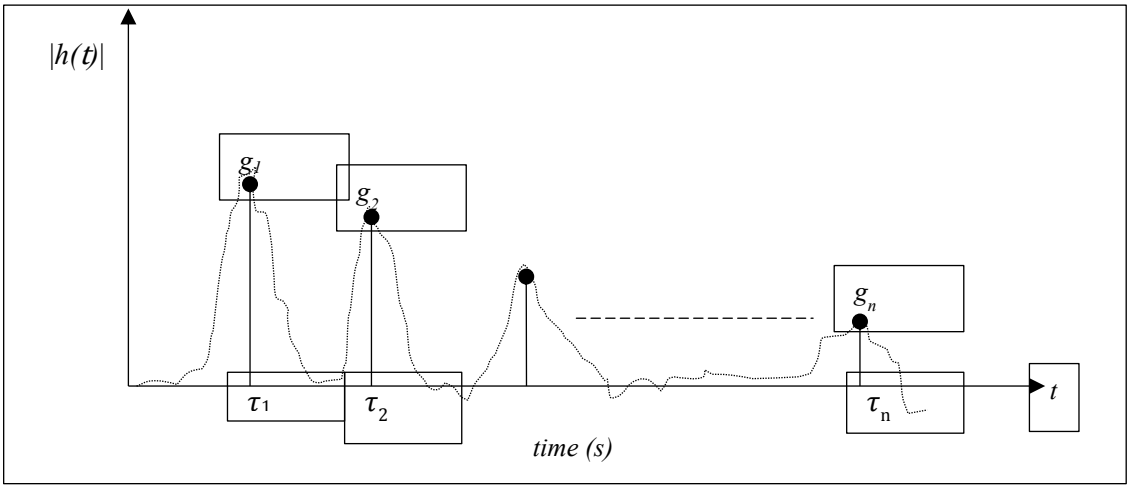

Figure 2- 5: The impulse response of a single branch topology

However, it is noted that the complexity of this approach increases as the number of branches and nodes increases. Table 2.1 summarizes the expressions for obtaining the three components of the Zimmermann and Dostert model for **N** paths.

Table 2. 1: Model parameters for an N-path network [4]

path no.	signal direction	path length (d_i)	weighting factor (g_i)
1	$A \rightarrow B \rightarrow C$	l_1+l_2	t_{1b}
2	$A \rightarrow B \rightarrow D \rightarrow B \rightarrow C$	$l_1+2l_3+l_2$	$t_{1b} \times r_{3d} \times t_{3b}$
3	…	…	…
N	$A \rightarrow B \rightarrow (D \rightarrow B)^{N-1} \rightarrow C$	$l_1+2(N-1)\cdot l_3+l_2$	$t_{1b} \times r_{3d} \times (r_{3d} \times r_{3d})^{N-2} t_{3b}$

2.2.2.2 Philipps' models

The impedance characteristics of a PLC channel is highly variable with frequency and ranges between a few ohms to a few kilo ohms. The characteristics display the presence of both peaks and notches. At the peaks, the channel behaves like a parallel resonant circuit. In much of the frequency band, the impedance is either inductive or capacitive. The characteristic impedance of a powerline cable is around 90 Ohms. However, the net impedance in the network is determined by the topology of the network as well as the loads that are connected to it, whose impedances may be highly dependable on the frequency as well. Phillips also noted that the signal that is sent through the PLC channel will undergo reflections at points of impedance discontinuities and as a result echoes of the transmitted signal are produced. Thus, the powerline is regarded as an environment where multipath effects are prominent. This tallies with the views of Zimmerman and Dostert [4, 6].

Based on these observations concerning the powerline channel behavior, from extensive measurements by Philipps [28], two models were proposed for the PLC channel transfer characteristics; the echo model and the series resonant circuit model [5].

2.2.2.2.1 Echo model

The echo model is based on the multipath nature of the PLC channel which leads to direct as well as indirect transmission of the signal. Thus, the signal that gets to the receiver is a summation of several copies (echoes) of the transmitted signal, and not just one direct signal from the transmitter to the receiver. This means that different signals are delayed and attenuated differently. This fact led to the development of the echo model, which happens to be in good agreement with the parameters that constitute the network.

If we assume that there are N paths that the signal travels through to the receiver, then, on the path v, the signal will suffer the amount of delay equal to τ_v and also be attenuated by a complex factor ρ_v. The complex path attenuation is given by [5]:

$$\rho_v = |\rho_v| \cdot e^{-j\varphi_v} \tag{2.10}$$

where:

$$\varphi_v = tan^{-1}\left(\frac{Im(\rho_v)}{Re(\rho_v)}\right) \tag{2.11}$$

Then, the impulse response $h(t)$ is obtained as a sum of N dirac pulses which are multiplied by ρ_v and delayed by τ_v, that is:

$$h(t) = \sum_{v=1}^{N} |\rho_v| \cdot \delta(t - \tau_v) \tag{2.12}$$

The channel transfer function is obtained as a Fourier transform of the impulse response, from which we have:

$$H(f) = \sum_{v=1}^{N} |\rho_v| . e^{j\varphi_v} \cdot e^{-j2\pi f \tau_v} \tag{2.13}$$

The graphical representation of the echo model is shown in Fig. 2-6. For each path, there are three parameters that have to be defined. Hence, for a model with N paths, a total of $3N$ parameters will be required to completely define the model. These parameters are the delay factor τ_v, the phase shift φ_v and the attenuation factor ρ_v. The said model can be optimized by using an evolutionary strategy as described in [5] which essentially minimizes the root mean square error and maximizes the correlation factor between the measured and modeled functions.

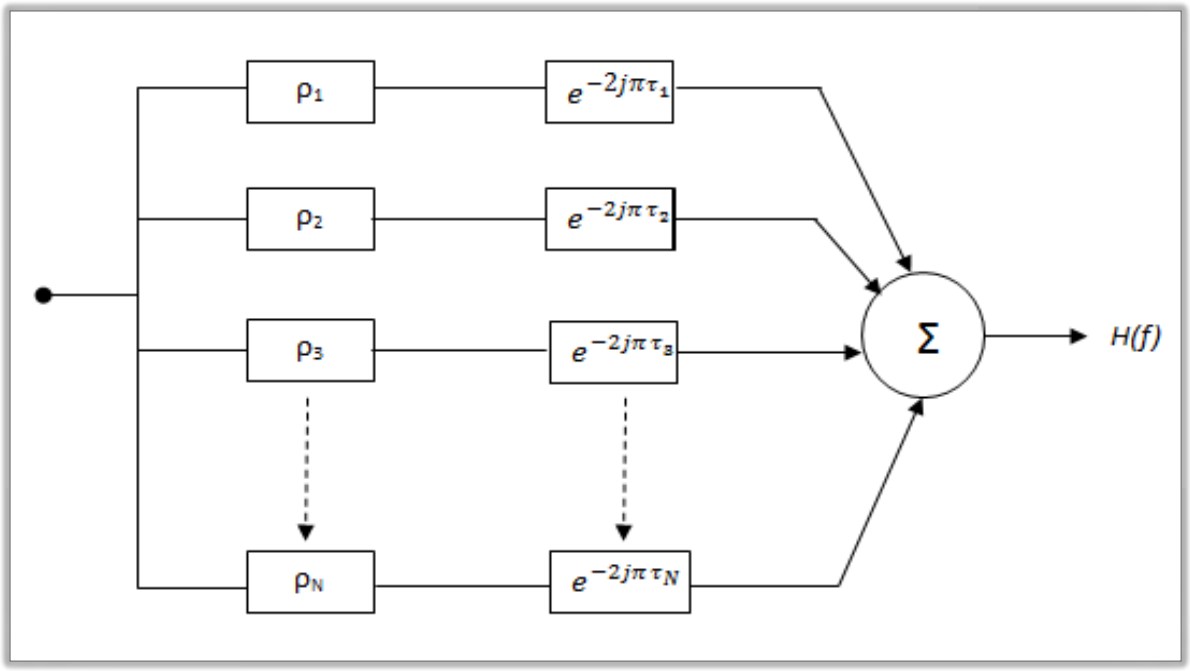

Figure 2- 6: Graphical representation of the Echo model

2.2.2.2.2 Series resonant circuit model

Electrical load impedance measurements have been shown to behave like one or few series resonant circuits whose constituent elements are a resistance R, inductance L and a capacitance C. This is due to the fact that many appliances incorporate a capacitance at the input for preventing interference and also possess a feeder line that is both resistive and inductive. Since in most cases the loads are very much far apart, they do not influence one another. Hence it would be realistic to model the powerline channel as a cascade of series resonant circuits (SRC) that are decoupled. Fig 2-7 below shows a single RLC resonant circuit connected to line of a load impedance Z.

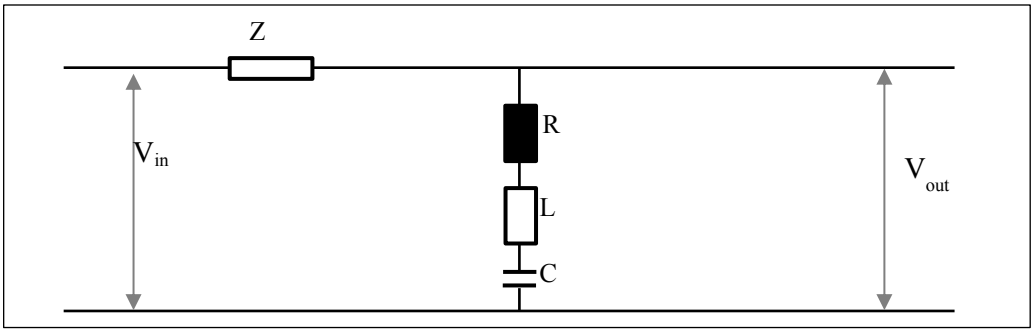

Figure 2- 7: Series RLC resonant circuit

The frequency-dependent impedance of the series RLC resonant circuit is calculated as :

$$Z_S = R + j \cdot 2\pi f \cdot L + \frac{1}{j \cdot 2\pi f \cdot C} \tag{2.14}$$

At resonance, the capacitive and inductive reactances are equal, and the circuit is purely resistive (minimum impedance). The resonant frequency is then computed from:

$$f_{res} = \frac{1}{2\pi\sqrt{L.C}} \tag{2.15}$$

Then, the channel frequency response is given by:

$$H(f) = \frac{1}{1 + \frac{Z}{Z_S(f)}} \tag{2.16}$$

The channel frequency response is shown in the Fig. 2-8 below; where we see that a notch occurs in the amplitude transfer function at resonance. The value of the amplitude characteristic at lower and high frequencies is almost 1. The depth of a notch is a function of the resistance R and the impedance Z.

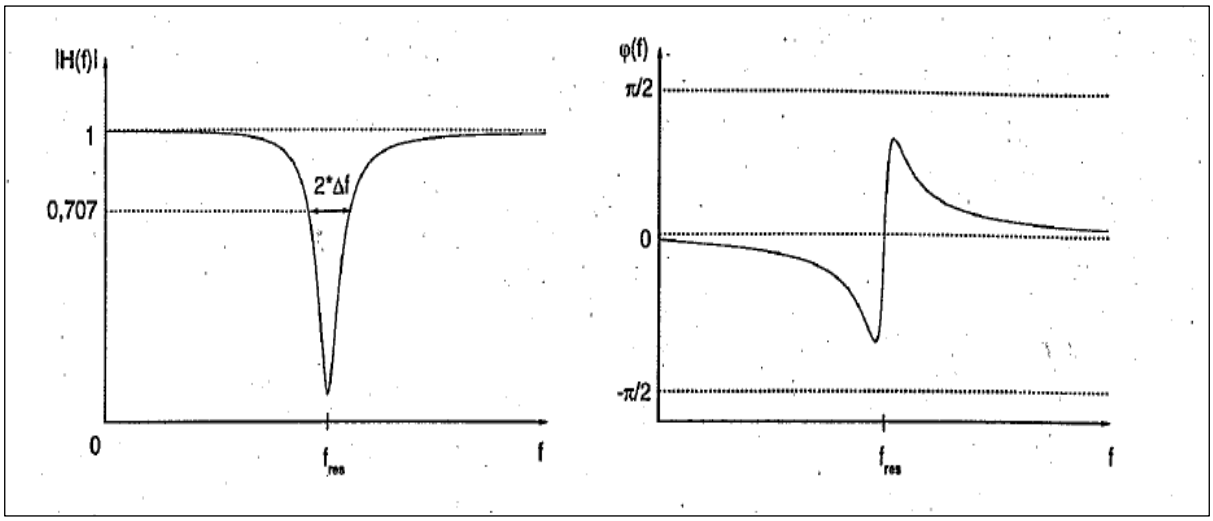

(a) Amplitude response (b) Phase response

Figure 2- 8: The amplitude and phase response of a series RLC Circuit [5]

The quality factor (Q factor) of the circuit is given by:

$$Q = \frac{f_{res}}{2.\Delta f} = \frac{1}{R}\sqrt{\frac{L}{C}} \tag{2.17}$$

The quality factor is a function of the notch width; the narrower the notch, the higher the quality factor. In the phase response, we see that there is a steep rise at resonance. The phase is capacitive at lower frequencies while it is inductive at higher frequencies. The overall frequency response characteristic is modeled as a series of cascaded decoupled series resonant circuits, and is given by:

$$H(f) = \prod_{i=1}^{n} H_i(f) \tag{2.18}$$

In order to fit the model, 3*N* parameters should be optimized. The same approach adopted for the echo model can be used for the optimization. Table 2.2 shows the parameters that were obtained for a maximum of five series resonant circuits; that have been determined by using the evolutionary strategy.

Table 2. 2: Set of parameters of series resonance circuits model

No	R (Ohm)	L (µH)	C(nF)	f_{res} (MHz)	Q
1	21.4	0.137	10.8908	4.122	0.165
2	12.1	8.264	0.1334	4.793	20.640
3	67.9	18.919	0.0197	8.238	14.431
4	46.4	11.948	0.0103	14.324	23.183
5	19.6	1.008	0.0273	30.357	9.799

The frequency response of this kind of circuit is shown below.

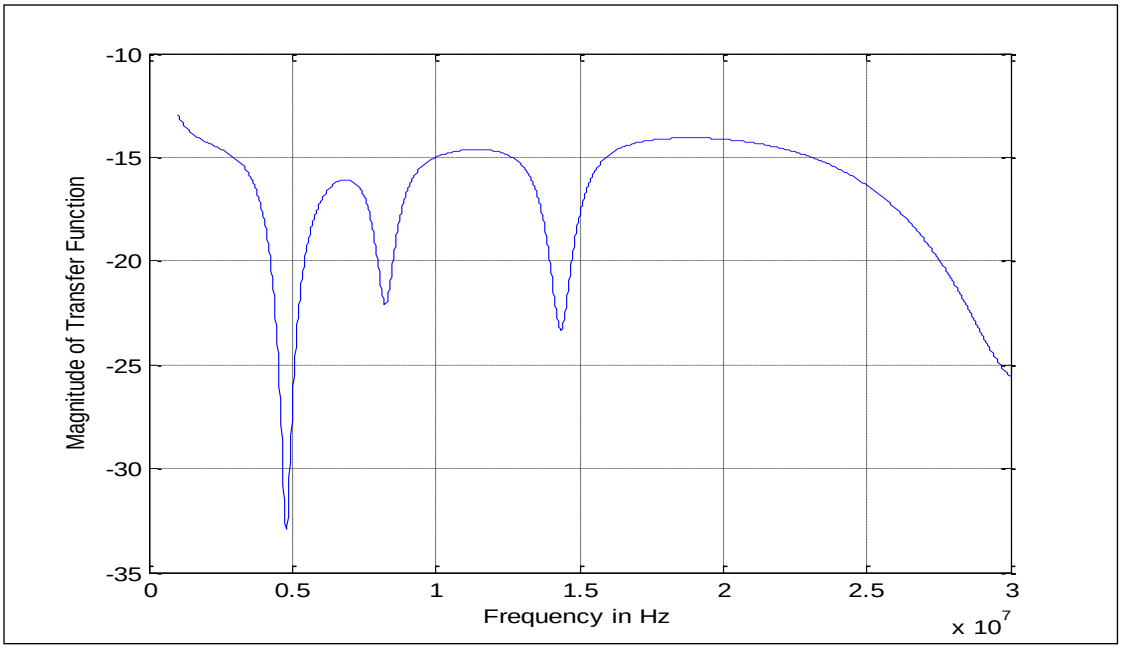

Figure 2- 9: Channel transfer characteristic for a five series resonant circuits model

2.1.2.3 Meng et al. model

Meng *et al.* [9] applied transmission line theory to come up with a transfer characteristic model of the power line for a low voltage network. To validate the model, a sample network comprising of several branches and connected to different household appliances was constructed and the channel measurements were done. A simplified in-house powerline network with *N* branches is shown in Fig. 2-10 below.

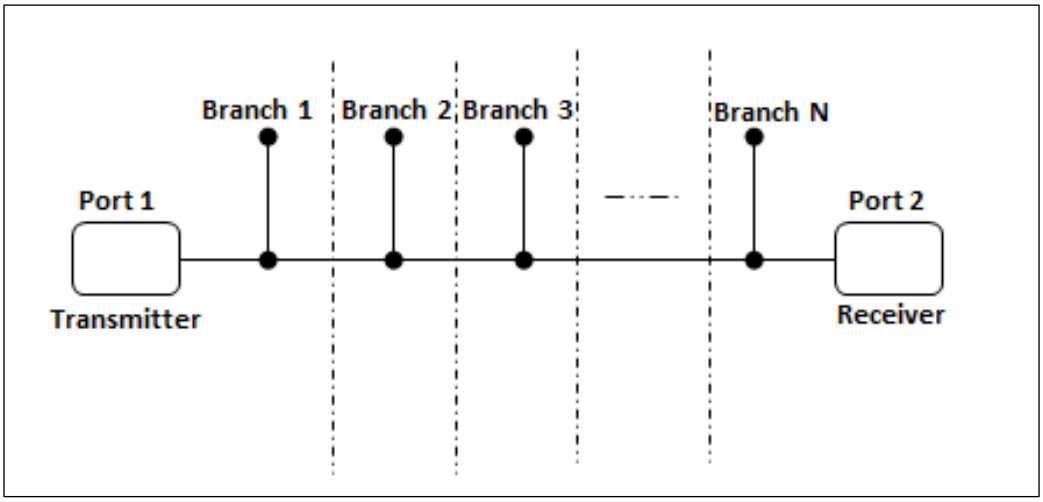

Figure 2- 10: A simplified in-house powerline network with *N* branches

Four key parameters for the line are determined first, that is, the line resistance R, the line inductance L, the line capacitance C and the line conductance G. These primary parameters are necessary in the determination of the two model parameters; the propagation constant γ and the characteristic impedance Z_o. The mathematical procedure for the primary line parameter determination is a outlined below for each element:

1. **Resistance**

Due to skin effect, when there is an ac current flow in the conductor, where more current flows near the conductor surface as opposed to towards the center. This is caused by the self-inductance within the conductor [9, 29]. This phenomenon causes an increase in the cable resistance which even becomes worse as the frequency of the current increases. Even though there is uniform current distribution throughout the cable cross section, when computing the cable resistance, it is normal to

make the assumption that all the current flows within the cable "skin depth". The skin depth δ is computed as [9, 30]:

$$\delta = \sqrt{\frac{1}{\pi f \mu_c \sigma_c}} \tag{2.19}$$

Where μ_c is the permeability of the conductor, σ_c is the conductivity of the conductor, and f is the current frequency. Hence, for a transmission line consisting of two wires with a solid core conductor, its resistance is computed as:

$$R_{solid} = \frac{1}{\pi a \delta \sigma_c} \left(\frac{Ohms}{m}\right) \tag{2.20}$$

Where a is the conductor radius. If however the conducting wires are stranded, then the current flow area is reduced due to the gaps between the wire strands. In such cases, the solid cable resistance is multiplied with a correction factor. This correction factor is given by [9]:

$$X_R = \left[Cos^{-1}\left(\frac{r_{wire}-\delta}{r_{wire}}\right) \times {r_{wire}}^2 - (r_{wire}-\delta) \times \sqrt{{r_{wire}}^2 - (r_{wire}-\delta)^2}\right] / (2 \times (r_{wire} \times \delta) \tag{2.21}$$

Where r_{wire} is the a single wire strand radius, and δ is as defined in (19) above. Thus, the net resistance of the stranded conductor is given by [9]:

$$R = X_R \times R_{solid} \left(\frac{Ohms}{m}\right) \tag{2.22}$$

2. Inductance

For a transmission line comprising of two wires, its net inductance is a summation of the self-inductance per conductor and the mutual inductance between them. The self-inductance L_s is calculated as follows [29]:

$$L_s = \frac{\mu_c}{8\pi} \quad \left(\frac{H}{m}\right) \tag{2.23}$$

Also, the mutual inductance is computed using the following expression [29]:

$$L_m = \frac{\mu_c}{\pi} In\left(\frac{D-a}{a}\right) \quad \left(\frac{H}{m}\right) \tag{2.24}$$

Where D is the distance between the conductors. So, the net inductance is given as [29]:

$$L = L_s + 2L_m = \frac{\mu_c}{\pi}\left[\frac{1}{4} + In\left(\frac{D-a}{a}\right)\right]\ \left(\frac{H}{m}\right) \tag{2.25}$$

3. Capacitance

The two-wire cable capacitance is a function of the cable to cable capacitance per unit length, C_{cable}, and the capacitance due to the coupling effects from both the metal conduit, $C_{conduit}$ and the earth cable. The capacitance between the metal conduit and the earth cable is zero because both of them are grounded which means that the potential between them is zero also. The cable capacitance per unit length, C_{cable} is given by [29]:

$$C_{cable} = \frac{\pi\varepsilon}{In[\left(\frac{D}{2a}\right) + \sqrt{(\frac{D}{2a})^2 - 1}]} \quad \left({}^{F}/_{m}\right) \tag{2.26}$$

Where ε is the dielectric material permittivity between the conductors. The capacitance due to the coupling effects from the metal conduit, $C_{conduit}$, is given by [9]:

$$C_{conduit} = \lim_{N\to\infty} \sum_{k=1}^{N} \frac{1}{N} \times \frac{2\pi\varepsilon_k}{In(\frac{b_k}{a})} \quad ({}^{F}/_{m}) \tag{2.27}$$

Where ε_k and b_k are dielectric material permittivity and the metal conduit inner radius for the sector *k*. The net capacitance, *C* is then obtained from [9]:

$$C = C_{cable} + \frac{C_{cable}}{2} + \frac{C_{conduit}}{2} = \frac{3C_{cable}}{2} + \frac{C_{conduit}}{2}\ \left({}^{F}/_{m}\right) \tag{2.28}$$

4. Conductance

From [29], we see that if the medium is homogeneous, then the following expression holds true:

$$\frac{C}{G} = \frac{\varepsilon}{\sigma} \tag{2.29}$$

which implies that,

$$G = \frac{\sigma C}{\varepsilon} \tag{2.30}$$

Where σ is the dielectic material conductivity and G is the cable conductance per unit length. In the approach taken by Meng *et al.*, the dielectric material is assumed to be a mixed content and the space inhomogeinity is neglected to make the model more tractable.

Based on the lumped-element circuit model of the transmission line, the propagation constant γ and the characteristic impedance Z_o can be computed as [9, 29]:

$$\gamma = \alpha + j\beta = \sqrt{(R + j\omega L)(G + j\omega C)} \tag{2.31}$$

$$Z_o = \sqrt{\frac{R + j\omega L}{G + j\omega C}} \tag{2.32}$$

Where ω is the angular frequency. The real part of the propagation constant α is the attenuation constant while the imaginary part is the phase constant β. Thus we see that these parameters can be used to characterize any transmission line regardless of its length. The input impedance Z_{in} of a transmission line whose length is *l* and is terminated by a load impedance Z_L is given by:

$$Z_{in} = Z_o \frac{Z_L + Z_o \tanh(\gamma . l)}{Z_o + Z_L \tanh(\gamma . l)} \ \ (Ohms) \tag{2.33}$$

If the load is a short circuit, then $Z_L = 0$, which gives:

$$Z_{is} = Z_o \tanh(\gamma . l) \ \ (Ohms) \tag{2.34}$$

If however the load impedance is replaced by an open circuit, then $Z_L = \infty$, and we have:

$$Z_{io} = Z_o \coth(\gamma . l) \ \ (Ohms) \tag{2.35}$$

From the Equations (2.34) and (2.35), we can obtain the characteristic impedance and the propagation constant as follows:

$$Z_o = \sqrt{Z_{is} Z_{io}} \tag{2.36}$$

$$\gamma = tanh^{-1} \sqrt{\frac{Z_{is}}{Z_{io}}} \tag{2.37}$$

The diagram shown in Fig. 2-11 is used for the s-parameters evaluation for a single-branch network. In the derivation that follows, the path line is defined as the direct path for the signal (excluding the branches). Line 1 is the path power line with line parameter Z_o, γ, Line 2 is the branch power line with line parameter Z_o, γ, Line 3 is the transmission line with 50Ω characteristic impedance. By applying the theory of the transmission line, Z_{in1}, Z_{in2}, Z_{in}, Γ_1 and Γ_2 are determined as follows [9]:

$$Z_{in1} = Z_o \frac{Z_L + Z_o \tanh(\gamma . l_3)}{Z_o + Z_L \tanh(\gamma . l_3)} \ (Ohms) \tag{2.38}$$

$$Z_{in2} = Z_o' \frac{Z_b + Z_o' \tanh(\gamma . l_2)}{Z_o' + Z_b \tanh(\gamma . l_2)} \ (Ohms) \tag{2.39}$$

$$Z_{in} = Z_o \frac{(Z_{in1} // Z_{in2}) + Z_o \tanh(\gamma . l_1)}{Z_o + (Z_{in1} // Z_{in2}) \tanh(\gamma . l_1)} \ (Ohms) \tag{2.40}$$

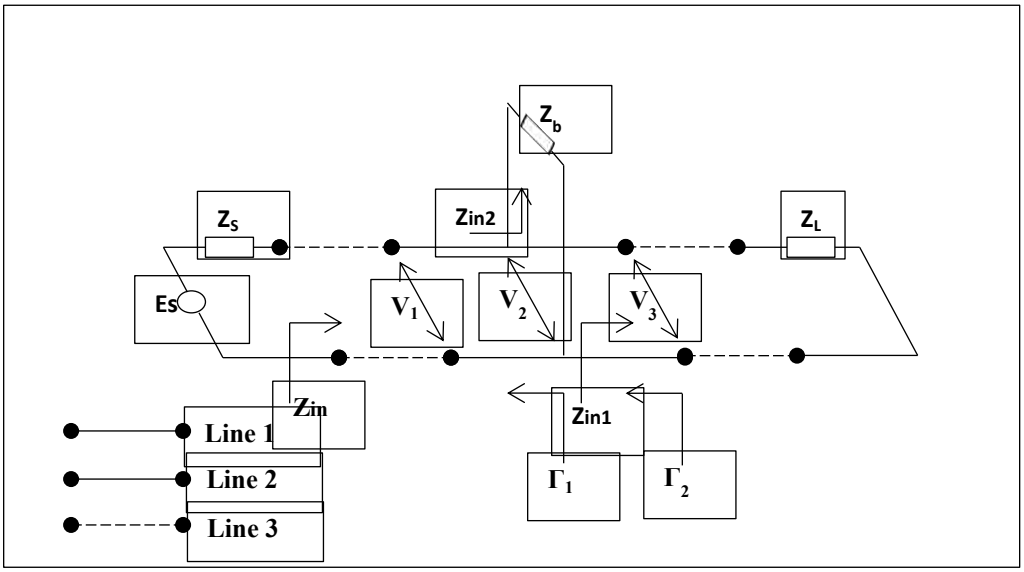

Figure 2- 11: Single-branch network diagram

Where Z_s is the source impedance, Z_L is the load impedance, Z_b is the load impedance at the branch end, Z_{in1} is the input impedance of the network on the right of the tap, Z_{in2} is the input impedance of the branch network, Z_{in} is the input impedance of the single branch network, Γ_1 is the reflection coefficient from path end, and Γ_2 is the reflection coefficient from tap point calculated as:

$$\Gamma_1 = \frac{Z_L - Z_0}{Z_L + Z_0} \tag{2.41}$$

And,

$$\Gamma_2 = \frac{Z_{in1} || Z_{in2} - Z_0}{Z_{in1} || Z_{in2} + Z_0} \tag{2.42}$$

The s-parameters S_{11} and S_{21} are obtained using the following equations [31]:

$$S_{11} = \frac{Z_{in} - 50}{Z_{in} + 50} \tag{2.43}$$

$$S_{21} = 2\,\frac{V_3}{E_g} \tag{2.44}$$

The S_{21} parameter can also be calculated indirectly according to the following equation:

$$S_{21} = 2\,\frac{V_3}{V_2}.\,\frac{V_2}{V_1}.\,\frac{V_1}{E_g} \tag{2.45}$$

Where,

$$\frac{V_1}{E_{g_1}} = \frac{Z_{in}}{Z_{in} + Z_g} \tag{2.46}$$

From [30], the shifting of reference planes yields the following:

$$\frac{V_3}{V_2} = \frac{(1 + \Gamma_1)\, e^{-\gamma l_3}}{1 + \Gamma_1 e^{-\gamma l_3}} \tag{2.47}$$

$$\frac{V_2}{V_1} = \frac{(1 + \Gamma_2)\, e^{-\gamma l_1}}{1 + \Gamma_2 e^{-\gamma l_1}} \tag{2.48}$$

After determining the S-parameters above, we can then obtain the scattering matrix for an entire network comprising several cascaded single branch networks. There are two methods that can be applied to do this. One is the use of signal flow graphs while the other one is the use of the chain scattering matrix (T-matrix). For ease of computation, the latter is used in this case. The overall T-matrix for the whole cascaded network is a product of the individual T-matrices for each single branch network. The following is the relationship between the S-matrix and the T-matrix [9]:

$$[T] = \begin{bmatrix} \frac{1}{S_{21}} & -\frac{S_{22}}{S_{21}} \\ \frac{S_{11}}{S_{21}} & S_{12} - \frac{S_{11}S_{22}}{S_{21}} \end{bmatrix} \tag{2.49}$$

And then the total T-matrix for an entire network is calculated as [9]:

$$[T] = \prod_{k=1}^{N} [T_k] \tag{2.50}$$

Where T_k is the T-matrix of the k^{th} cascaded element in network. The S-matrix for the whole network can then computed as [9]:

$$[S] = \begin{bmatrix} \frac{T_{21}}{T_{11}} & T_{22} - \frac{T_{21}T_{12}}{T_{11}} \\ \frac{1}{T_{11}} & -\frac{T_{12}}{T_{11}} \end{bmatrix} \tag{2.51}$$

The S_{21} term gives the transfer function of the network.

2.2.2.3 Anatory et al. Model

The Anatory *et al.* model [7, 25] is based on the fact that at a particular node, part of the signal will be transmitted and another part will be reflected. The model also takes into consideration the loads connected to the network, their distances from the path line and the number of nodes. For a multiple branch transmission line at a single node as shown in Fig. 2-12, where Z_S is the impedance of the source, Z_n is the characteristic impedance of any terminal , and V_S and Z_L are source voltage and load impedance respectively, Anatory *et al.* developed the following transfer function for the PLC channel [7, 25, 32, 33]:

$$H_m(f) = \sum_{M=1}^{L} \sum_{n=1}^{N_T} T_{LM} \alpha_{mn} H_{mn}(f) \qquad n \neq m \tag{2.52}$$

Where: $N_{T,}$ is the total number of branches connected at node B and terminated in any arbitrary load, n is any branch number, m is any referenced (terminated) load, M is the number of reflections (with a total L number of reflections),

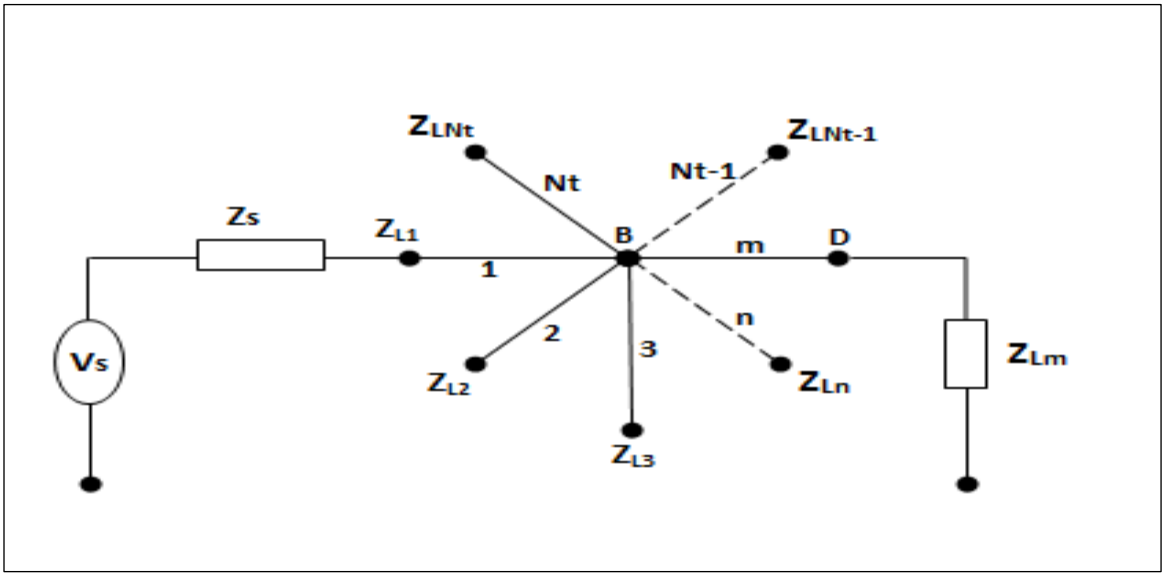

Figure 2- 12: Single node power line network with multiple branches [32]

H_{mn} *(f)* is the transfer function between line *n* and a referenced load m, and T_{LM} is the transmission factor at the referenced load m, respectively. α_{mn} is the signal contribution factor given by:

$$\alpha_{mn} = P_{Ln}^{M-1} \rho_{nm}^{M-1} e^{-\gamma_n (2(M-1) l_n)} \tag{2.53}$$

Where ρ_{mn} is the the reflection factor at node B between line *n* and the referenced load *m*, and γ_n is the propagation constant of line *n* that has line length L_n. All terminal reflection factors P_{Ln} in general are given by:

$$P_{Ln} = \begin{cases} \rho_s & n = 1(source) \\ \rho_{Ln}, & otherwise \end{cases} \tag{2.54}$$

except at the source where $\rho_{L1} = \rho_S$ is the source reflection factor. The authors extended the above results for any power line network with spread branches as shown in Fig. 2-13.

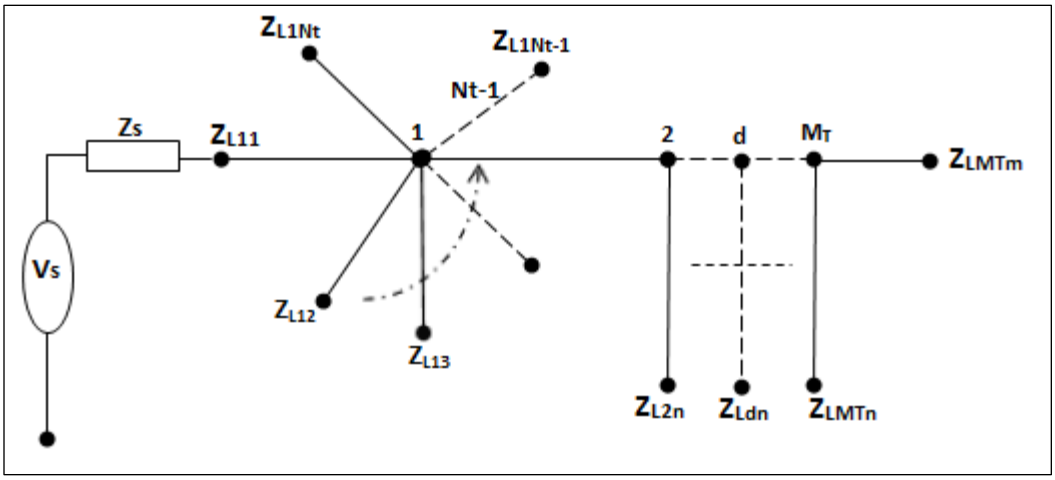

Figure 2- 13: Power-line network with distributed branches

They obtained the transfer function of such a network as:

$$H_{mM_T}(f) = \sum_{d=1}^{M_T} \sum_{M=1}^{L} \sum_{n=1}^{N_T} T_{LM} \alpha_{mnd} H_{mnd}(f) \qquad n \neq m \tag{2.56}$$

$$\alpha_{mnd} = P_{Lnd}^{M-1} \rho_{nmd}^{M-1} e^{-\gamma_{nd}(2(M-1)l_{nd})} \tag{2.57}$$

$$P_{Lnd} = \begin{cases} \rho_s & d = n = 1(source) \\ \rho_{Lnd}, & otherwise \end{cases} \tag{2.58}$$

Where all the parameters used have the same significance as mentioned above and, M_T is the total number of distributed nodes, d is any referenced node (1… M_T), and $H_{mnd}(f)$ is the transfer function from line *n* to a referenced load *m* at a referenced node *d*.

2.2.2.4 Mulangu and Afullo model

Recently Mulangu and Afullo [34], investigated the effect of the number of branching nodes in a power line network and derived a PLC channel model that is based on Mie scattering theory [35]. The basis of this model is on the assumption of a multitude of scatterers that are randomly spread in the channel vicinity, requiring a sufficient number of impedance discontinuity points. The power line is considered as one single element, and then it is subdivided into a grid of scattering points

(small areas) whose dimensions range from 0.5 to 3 mm. A power law mathematical formulation that relates specific attenuation in the channel to the number of branching nodes is then derived.

If an electromagnetic wave of known amplitude travels through a volume, containing *N* scattering particles that are identical with diameter *D*, its amplitude decreases by the factor of $e^{-\gamma l}$, at any distance l. The coefficient of attenuation γ is calculated as [34]:

$$\gamma = NQ_{ext}(D) \tag{2.59}$$

The wave attenuation in dB is then given by:

$$A_{dB} = 10\log\frac{1}{e^{-\gamma l}} = 4.343\gamma l \tag{2.60}$$

While the specific attenuation in dB/km computed as:

$$A_s = 4.343\gamma \tag{2.61}$$

$$A_s[dB/km] = 4.343 \times 10^3 \int_0^\infty N(D)Q_{ext}(D)dD \tag{2.62}$$

Equation (2.62) can also be rewritten as:

$$A_s[dB/km] = 0.25\pi \int_0^\infty D^2N(D)Q_{ext}(D)dD \tag{2.63}$$

The power law form of the specific attenuation is given as:

$$A_s = \varrho K^{\xi} \tag{2.64}$$

where ϱ and ξ are powerline specific coefficients and K is the branching nodes number.

2.2.2.5 Zwane and Afullo model

A series of resonant circuits (SRCs) can be used to describe the power line channel [5]. From channel measurements, a correlation of the notch locations to the SRC branch parameters was obtained. The transmission line theory for two extreme cases, that is, short circuited and open circuited branches, was used. Through the analysis of the input impedance characteristics around a resonant wavelength λ_r, the short and open circuited circuits behaved like a series RLC circuit. For the open circuited end, the cable length is in odd multiples of $\lambda_r/4$ while for the short circuited end, the cable length is in even multiples of $\lambda_r/2$. Table 2.3 presents a summary of the series RLC parameters determination formulations obtained.

Table 2. 3: Series resonance RLC parameters [36]

Resonance	Quarter wavelength ($\lambda_r/4$) Open circuit	Half wavelength ($\lambda_r/2$) Short circuit
R	$\frac{1}{4}Z_0\alpha\lambda_r$	$\frac{1}{2}Z_0\alpha\lambda_r$
L	$\frac{\pi Z_0}{4\cdot\omega_0}$	$\frac{\pi Z_0}{2\cdot\omega_0}$
C	$\frac{4}{\pi\omega_0 Z_0}$	$\frac{2}{\pi\omega_0 Z_0}$
Q	$\frac{\beta_r}{2\alpha}$	$\frac{\beta_r}{2\alpha}$

Where in the above table, Z_0 is the characteristic impedance of the line, ω_0 is the resonant angular frequency, α is the attenuation constant of the line, λ_r is the wavelength at resonance and $\beta_r = \pi/l$. From Equation (2.16), each resonant circuit is described by a transfer function $Hr_i(f)$ and the overall transfer function is given as:

$$H(f) = A\prod_{i=1}^{n} Hr_i(f) \tag{2.65}$$

Where n is the number of series resonant circuits forming the total transfer functionand A is the average path loss factor from transmitter to receiver distance determined by $e^{-\gamma d}$.

2.3 Noise in PLC Channels

The PLC channel is plagued by different noise types that are generated by different sources. These noise components vary in terms of their severity and features. Some of the noise components have power levels that vary with time for every second or minute or hour and they are broadly referred to as colored background noise. On the hand, we have noise components that are periodic impulses and either synchronous or asynchronous with the mains. The channel also suffers from non-periodic asynchronous noise [37]. Impulsive noise tends to be more dominant than the other noise types and its levels that are usually several decibels above the background noise. Impulsive noise is characterized by its amplitude, inter-arrival time and the width of the bursts.

PLC noise measurements and characterization has been studied by several authors [38-41]; but regardless of the measurement methodology and the equipment used, they have reported the presence of between three to five noise components. The authors have broadly classified the noise as background noise, narrowband interference and impulsive noise. From a telecommunications perspective, we therefore conclude that the PLC receiver is affected in the time domain by a superposition of all the noise components. Work done on PLC channel noise is limited as compared to that on channel transfer function measurements and modeling. The noise in PLC channel is different from the classic additive white Gaussian noise (AWGN). The noise in PLC has two main sources; noise generated by electrical appliances that are connected to the power network and that which is ingressed into the network from external sources either through radiation or conduction.

The following are the three broad classes of PLC channel noise [39, 40, 42-44]:

1. Impulsive noise: This category of noise is subdivided into different noise components depending on whether or not they are periodic or aperiodic and synchronous or asynchronous to the mains frequency. Impulsive noise is subdivided as follows:

    a) *Impulsive noise that is synchronous with the mains frequency and is periodic*: This type of impulsive noise is cyclostationary and is synchorous with the mains frequency. It is generated by silicon controlled rectifiers in different power supplies.

    b) *Impulsive noise that is periodic but asynchronous with the mains frequency*: This category of impulsive noise is generated by periodic impulses whose repetition rates are between 50 to 200 KHz. However, repetition rates that are outside this range have been found in some other measurements [38]. On the other hand, apart from the high repetition rates, this kind of impulsive noise also exhibits an underlying period equal to the mains one, which then qualifies it to be categorized as cyclostationary.

    c) *Asynchronous impulsive noise*: This kind of impulsive noise is very unpredictable and is the most dominant. It exhibits no regular occurrence and mainly arises from transients that originate from the connection or disconnection of electrical appliances from the power line network. The impulses can last for between some microseconds and a few milliseconds with a random occurrence. The power

spectral density of this kind of noise can go as high as 50 dB above the background noise. It is also sometimes referred to as sporadic impulsive noise.

2. Narrowband interference: This type of PLC noise is formed by modulated or sinusoidal signals originating from different electrical devices with a transmitter or receiver that cause spurious disturbances, and also ingress from broadcast stations, etc. Its severity normally varies from hour to hour, and in some cases may also vary synchronous with the mains. Some of its components can also be treated as cyclostationary. This noise can be subdivided into two depending on the shape of the power spectral density, as follows:
   a) Narrowband interference with multiple discrete frequency components: The power spectral density of this type of narrowband interference is made up of several equally spaced components (less than 5 KHz bandwidth). However these components are not harmonically related, that is, denoting by f_j, with *j=0, 1, ...,* the frequencies of the spectral peaks, then, its happens that $f_j - f_{j-1} = f_{j+1} - f_j$ but there is no f_0 that satisfies $f_j = pf_o$ for *j=0, 1, ...* and $p \in N^+$. This category of noise is observed above 4 MHz and frequency spacings up to 50 KHz have been observed. Fig. 2-14 shows an example of the estimated power spectral density of this kind of interference.

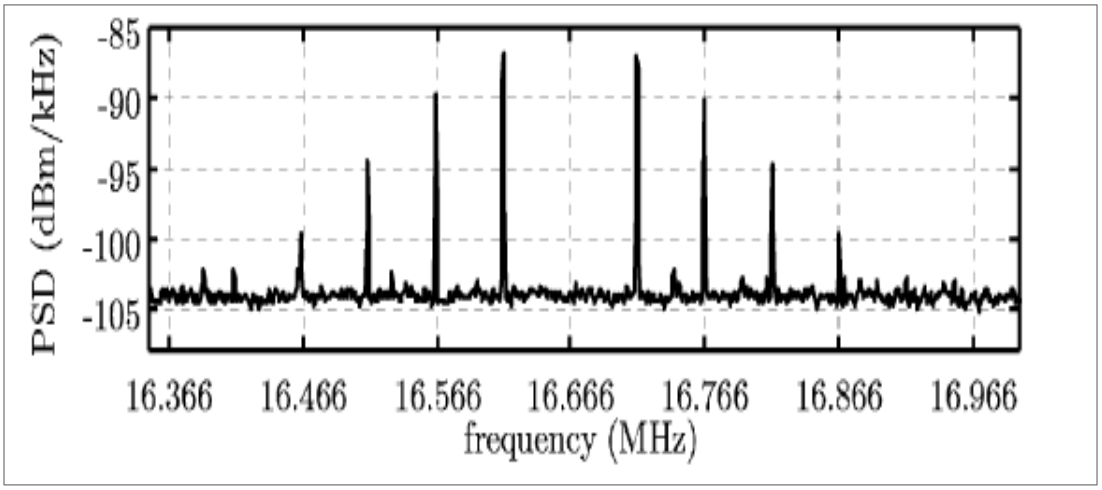

Figure 2- 14: Power spectral density of narrowband interference with multiple frequency components [42]

This figure shows that this kind of interference has the shape of a double-sided modulation of a periodic signal. The corresponding time domain representation is showm in Fig. 2-15 below.

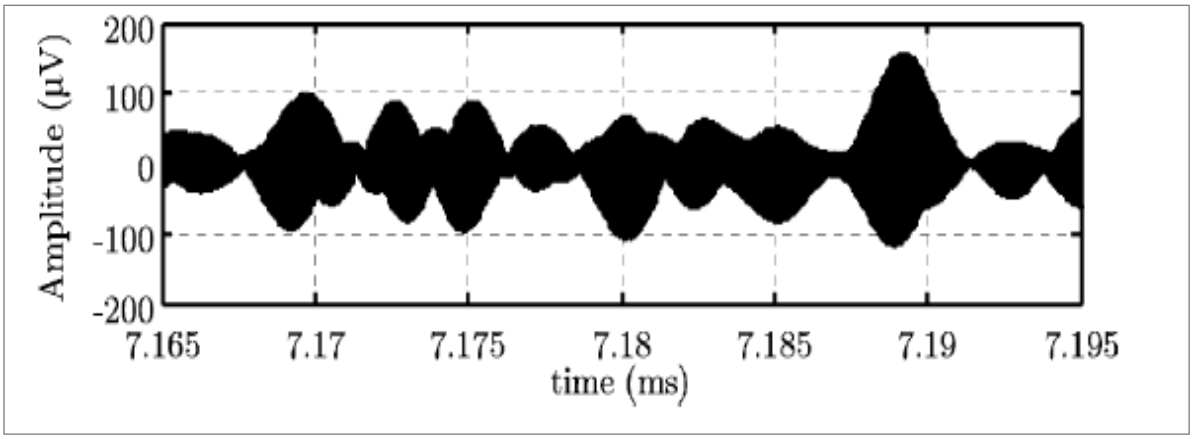

Figure 2- 15: Time-domain power spectral density of narrowband interference with multiple frequency components [42]

b) Single frequency component interference: The power spectral density of this kind of interference is comprised of a single narrowband term (bandwidth below 20 KHz) and is significantly higher than the background noise (by even more than 30 dB). This interference component is usually prominent below 2 MHz and above 20 MHz. Interference from commercial AM radio stations is one type of this interference.

Additionally, the interference can also be grouped into two categories depending on the statistical properties.:

a) Stationary: This kind of interference may comprise of multiple equally space components or only a single component term but their levels do not change with the mains cycle. Much of narrowband interference fall under this category.

b) Cyclostationary: This type of interference may also comprise of a single or several equally spaced components. The key distinguishing feature is its synchronous behavior with the mains. Fig. 2-16 shows a time-domain diagram of this kind of noise. This diagram gives a detailed view of a 76 KHz cyclostationary narrowband interference that happens just before two periodic synchronous impulses with high amplitude. An AM interference with a smaller amplitude and carrier frequency of 88 KHz is also visible in the diagram.

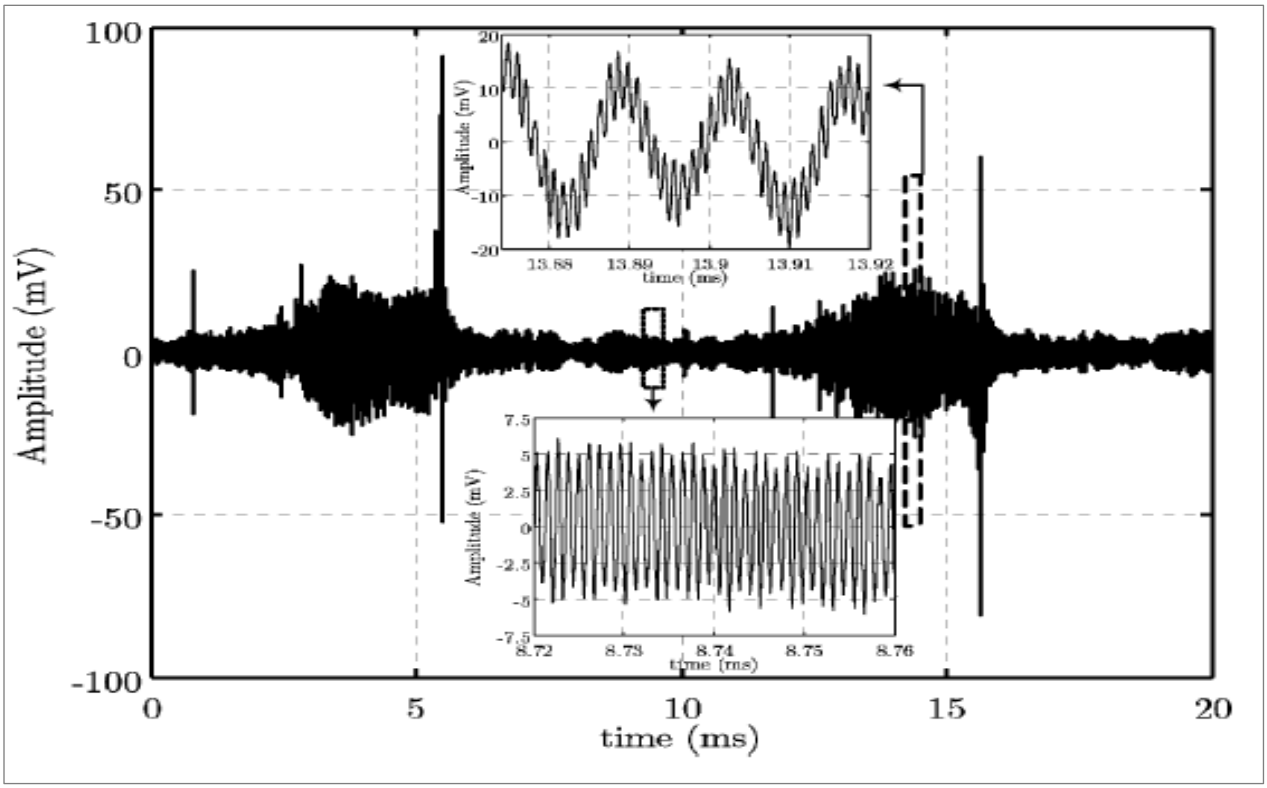

Figure 2- 16: Time-domain diagram of cyclostationary narrowband interference [42]

3. Colored background noise: This kind of noise originates from various sources with low power spectral density that varies with frequency, and their origin is usually unknown. Some of these sources may even be situated outside the premises and in such a case the noise is ingressed into the network via radiation or conduction. This noise can also be assumed cyclostationary with a level that strongly depends on the type and number of the electrical appliances connected to the network. This noise has a power spectral density that varies over time in terms of minutes or even hours.

Colored background noise, narrowband noise and periodic impulsive noise asynchronous to the mains frequency are usually stationary over periods ranging between seconds and minutes or even hours, and can be generally referred to as background noise. However, impulsive periodic noise that is synchronous with the mains frequency and asynchronous impulsive noise are time variant from microseconds to milliseconds. During such impulses, the power spectral density of the noise rises significantly and may result in bit or burst errors during transmission of data [39, 43]. Thus, impulsive noise is the biggest threat to the optimal performance of PLC systems and is discussed further below.

2.3.1 Impulsive noise

When analyzing impulse noise from the perspective of its impact on the PLC channel in terms of data transmission, there are two key questions that must be answered; they are [43]:

(i) When do the impulses take place?

(ii) What is the strength of the impulses?

In order to address the first question, the assumption of an impulse that is rectangular in shape offers a reasonable and simple approach; which makes the characterization of the impulse possible with only a few parameters being used. These basic parameters are the impulse width t_w, arrival time t_{arr} and interarrival time t_{IAT} or the impulse distance t_d. The second question can be sufficiently dealt with by analyzing the amplitude of the impulse, energy of the impulse, and power or the specific power spectral density. These characteristics of the impulses are demonstrated in Fig. 2-17 with a rectangular envelope of some sample impulses.

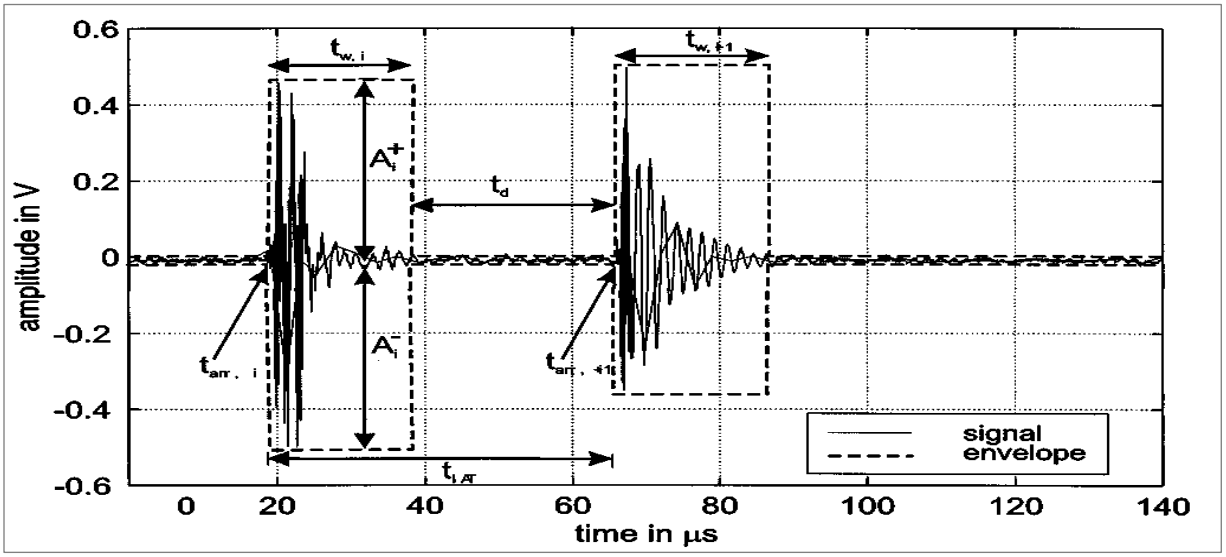

Figure 2- 17: Time-domain impulse representation and envelope with characteristic parameters [43].

In this figure, $A = max\{A_i^+,\ A_i^-\}$. The separation distance between two impulses is described by the impulse distance t_d or interarrival time t_{IAT} which are related according to the following expression [43]:

$$t_{IAT} = t_w + t_d = t_{arr,i+1} - t_{arr,i} \tag{2.66}$$

Using an general impulse function $imp(t)$ with a unit amplitude and unit width, a train of impulses can be described by[43]:

$$n_{imptrain}(t) = \sum_{i=1}^{N} A_i \,.\, imp\left(\frac{t - t_{arr,i}}{t_{w,i}}\right) \tag{2.67}$$

Where $n_{imptrain}(t)$ is the train of impulses. The parameters $A, t_w \; and \; t_{arr}$ are random variables whose statistical properties can be obtained through measurements. From these parameters, secondary parameters can be obtained that are crucial in analysis of impulse noise and studying its behavioral characteristics over time. One of these secondary parameters is the impulse rate, given by:

$$r_{imp} = \frac{N_{imp}}{T_{win}} \tag{2.68}$$

Where N_{imp} is the number of impulses that occur within a given window of observation T_{win}. With the right choice of the window of observation, it is possible to determine the current frequency of the impulse events in terms of the number of impulses per second. A figure of the actually disturbed time can be determined from the "disturbance ratio"; which by definition is the ratio of the sum of the widths of all impulses generated within a window of observation, and the length of the window of obervation, that is [43]:

$$disturbance\; ratio = \frac{\sum_{i=1}^{N_{imp}} t_{w,i}}{T_{win}} \tag{2.69}$$

Impulse-free time percentage, which is the complement to the disturbance ratio, can then be derived from the above equation.

2.3.2 Analog and digital impulses mathematical concepts

Considering a pulse of unit area, $p(t)$, as shown in Fig. 2-18 (a), the pulse tends to an impulse as its width, ε, tends to zero [38]. The impulse function shown in Fig. 2-18 (b) is an infinitesimal time width pulse defined as [15]:

$$\delta(t) = \lim_{\varepsilon \to 0} p(t) = \begin{cases} 1/\varepsilon, & |t| \le \varepsilon/2 \\ 0, & |t| > \varepsilon/2 \end{cases}, \tag{2.70}$$

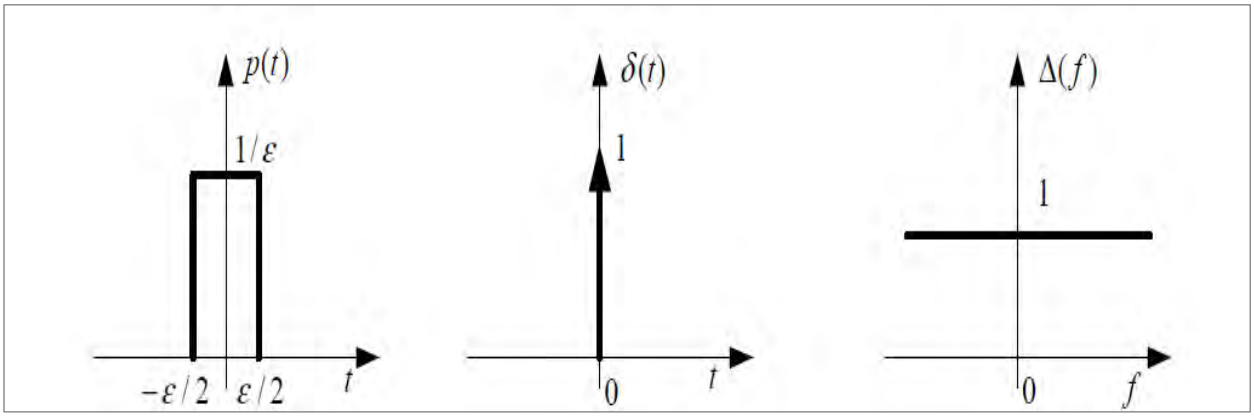

(a) (b) (c)

Figure 2- 18: (a) A pulse of unit area (b) An impulse as pulse width, $\varepsilon \to 0$ for the pulse (c) The impulse function spectrum.

The impulse function integral is given by:

$$\int_{-\infty}^{\infty} \delta(t)\, d(t) = \varepsilon \times \frac{1}{\varepsilon} = 1 \tag{2.71}$$

And, the impulse function Fourier transform is computed as:

$$\Delta(f) = \int_{-\infty}^{\infty} \delta(t) e^{-j2\pi f t}\, d(t) = e^0 = 1, \quad -\infty < f < \infty \tag{2.72}$$

Where f is the frequency variable. An impulse that is digital, $\delta(m)$, is defined as a signal with an "on" duration of one sample, and is expressed as follows:

$$\delta(m) = \begin{cases} 1, & m = 0 \\ 0, & m \neq 0 \end{cases} \tag{2.73}$$

Where m is the discrete-time index. Making use of the Fourier transform relation, the digital impulse frequency spectrum is given by:

$$\Delta(j\omega) = \sum_{m=-\infty}^{\infty} \delta(m) e^{-j2\omega m} = 1, \quad -\infty < \omega < \infty \tag{2.74}$$

In a communication system, real noise that is impulsive lasts for a duration that is usually greater than one sample period. Impulse noise usually originates at particular time and space, and will then be propagated all the way to the receiver. Noise that is impulsive is a non-stationary, binary-state impulses sequence whose amplitudes are random and also occurs at random positions. This non-stationary nature of impulsive noise can be analyzed by considering the noise process power spectrum with a few impulses per second; the process has zero power when the noise is absent, and the noise power is the impulse power when the impulse is present. Hence, power spectrum and autocorrelation of impulsive noise are time-varying, binary state processes.

2. 3.3 Impulsive noise statistical models

In this subsection, we review a number of statistical models that have proved useful in the characterization and modeling of impulsive noise processes. A sequence of impulsive noise, $n_i(m)$, is made up of pulses that have short durations and have random amplitudes, random durations and random occurrence times, and may be modeled as a P-tap filter output, given by [45]:

$$n_i(m) = \sum_{k=0}^{P-1} (h_k \, n(m-k) b(m-k)) \tag{2.75}$$

Where $b(m)$ models the occurrence time of the impulsive noise and is a binary-valued random sequence, $n(m)$ models the amplitudes of the impulse and is a random process that is continuous-valued, and h_k models the each impulse duration and shape and is a filter impulse response. There are two popular statistical and basic processes that have been applied in impulsive noise modeling as a binary sequence that is amplitude-modulated, which are: the Bernoulli-Gaussian and Poisson-Gaussian processes. The two processes are discussed next.

2.3.3.1 Impulsive noise Bernoulli-Gaussian model

In this model of the impulsive noise, a Bernoulli process, $b(m)$, is used to model the impulses random occurrence time and a Gaussian process is used to model the impulse amplitudes. A Bernoulli process, $b(m)$, is a process that is binary-valued and takes a value of "1" with a probability of α and a value of "0" with a probability of $1-\alpha$. The mass function of the probability (pmf) of a Bernoulli process is hence given by [15]:

$$P_B[b(m)] = \begin{cases} \alpha, & for\ b(m) = 1 \\ 1 - \alpha & for\ b(m) = 0 \end{cases} \tag{2.76}$$

The random amplitude impulsive noise Gaussian probability density function (pdf) whose mean is zero is given as [15]:

$$p_N[n(m)] = \frac{1}{\sqrt{2\pi\sigma_n}} exp\left\{-\frac{n^2(m)}{2{\sigma_n}^2}\right\} \tag{2.77}$$

Where ${\sigma_n}^2$ is the noise amplitude variance, and σ_n is the noise amplitude standard deviation. Then, the Bernoulli-Gaussian model pdf of the impulsive noise, $n_i(m)$, is given by [15]:

$$p_N^{BG}[n_i(m)] = (1 - \alpha)\delta[n_i(m)] + \alpha p_N[n_i(m)] \tag{2.78}$$

Where $\delta[n_i(m)]$ is the Kronecker delta function. The function $p_N^{BG}[n_i(m)]$ is a mixture of a discrete probability mass function $\delta[n_i(m)]$ and a continuous pdf $p_N[n_i(m)]$.

2.3.3.2 Impulsive noise Poisson-Gaussian model

In this model of the impulsive noise, the impulsive noise event occurrence probability is modeled as a Poisson process, while a Gaussian process is used to model the random amplitude distribution of the impulsive noise. The Poisson process, described in [46], is a random-event counting process. The occurrence probability of *k* impulsive events in a time interval *T* in a Poisson model is given by:

$$P(k, T) = \frac{(\lambda T)^k}{k!} e^{-\lambda T} \tag{2.79}$$

Where λ is a rate function with the following properties:

(i) Probability of one impulse in a small time interval $\Delta t = \lambda \Delta t$

(ii) Probability of zero impulse in a small time interval $\Delta t = 1 - \lambda \Delta t$

The assumption here is that not more than one impulsive noise event can occur in a time interval Δt. In this model, the impulsive noise pdf in a small time interval Δt is given as [15]:

$$p_N^{PG}[n(m)] = (1 - \lambda\Delta t)\delta[n_i(m)] + \lambda\Delta t p_N[n_i(m)] \tag{2.80}$$

Where $p_N[n_i(m)]$ is the Gaussian pdf as before.

2.3.4 PLC impulsive noise models

As earlier mentioned, PLC noise can be classified broadly into three; narrowband interference, background noise, impulsive noise and corona noise. Impulsive noise tends to be more dominant in low voltage networks, and slightly less in medium voltage networks. However, noise in high voltage networks tends to be dominated by corona noise. This types of noise has been previously modeled using different models; but, the most commonly used ones are derived from the two models discussed above. These models are the two-term mixture Gaussian model and the Middleton's class-A impulsive noise model.

2.3.4.1 The two-term mixture Gaussian model

This model is popular in PLC due to its simplicity. This model is derived from the Bernoulli-Gaussian model discussed above. The impulsive noise occurrence probability is a random process which is Bernoulli while a Gaussian distribution controls the noise amplitudes. Another Gaussian distribution is used to model the background noise. Thus, the impulsive noise probability density function of the two-term mixture Gaussian model is given by [15, 47]:

$$p_N(n) = (1-\epsilon)N(0,\sigma^2) + \epsilon N(0,k\sigma^2) \tag{2.81}$$

Where ϵ is the impulse noise probability of occurrence, $N(0,\sigma^2)$ is the zero-mean Gaussian distribution with a variance σ^2 that represents the background noise, $N(0,k\sigma^2)$ models the impulsive noise component that is also Gaussian distributed but its variance is k times greater than that of the background noise. Even though this model is simple and is used frequently in the analysis of PLC systems [47-50], it is deficient in that it does not provide a very accurate representation of the true impulse noise. Another model, the Middleton's class-A impulsive noise model, which is also widely used and counters the shortcomings of this model, is discussed next. The model is also limited in its ability to model long tailed processes, like PLC noise.

2.3.4.2 Middleton's class-A noise model

This is a rather simple model based on Poisson-Gaussian model and incorporates both background and impulsive noise. This model, which is also widely referred to as the Middleton's class-A impulsive noise model suggested in [51]. Due to its relative accuracy in the modeling and characterization of real impulsive noise, this model has been employed by several authors in the analysis of the performance of PLC systems [52-54]. This model represents the background and impulsive noise using the Poisson-Gaussian model. A Poisson random process is used to model the impulsive noise probability of occurrence; with the probability of having *m* impulsive noise events in a given interval *T* given by [15, 47, 51]:

$$P = \frac{(\lambda T)^m}{m!} e^{-\lambda T} \tag{2.82}$$

A Gaussian random process is used to model the impulsive and background noise amplitudes. If we let $A = \lambda T$ and simply refer to it as the impulsive index, then the pdf of Middleton's class-A impulsive noise model is given by [47, 51]:

$$p_A(n) = \sum_{m=0}^{\infty} e^{-A} \frac{A^m}{m!} \frac{1}{2\pi\sigma_m^2} exp\left(-\frac{|n|^2}{2\sigma_m^2}\right) \tag{2.83}$$

Where $\sigma_m^2 = \sigma^2 \frac{m/A+\Gamma}{1+\Gamma}$ is the *m*th impulse power, σ^2 is the total noise power (inclusive of the powers of the Gaussian background noise and impulsive noise), $\Gamma = \sigma_G^2/\sigma_I^2$ is the Gaussian-to-impulse noise power ratio (GIR), σ_G^2 is the power of the Gaussian noise, and σ_I^2 is the power of the impulsive noise. The impulsiveness of the noise reduces if *A* is increased, and the noise is very close to Gaussian in such a case. The above equation indicates that impulsive noise sources have a Poisson distribution, and for each source of impulse noise, a characteristic Gaussian noise with a different variance is generated. If we let $N_o = 2\sigma^2$ be the total white noise one-sided power spectral density, then the probability density function of the impulse noise can be written in terms of *A*, Γ , and N_o as follows [15]:

$$p_A(n) = \sum_{m=0}^{\infty} e^{-A} \frac{A^m}{m!\,\pi N_o} \frac{A(1+\Gamma)}{m+A\Gamma} exp\left(-\frac{A(1+\Gamma)}{m+A\Gamma}\frac{|n|^2}{N_o}\right) \tag{2.84}$$

However, this model does not tell us whether or not the noise is impulsive in the time domain. Also, it is limited in that it cannot model the fat tails in PLC systems sufficiently. Also, it was developed for general impulsive infeterference and not for PLC noise.

2.4 PLC Systems modulation

To optimize on the performance of PLC systems, techniques for combating the two key types of noise in PLC channels are necessary. Most of the techniques used in wireless communication systems afflicted by AWGN have been adapted for use in PLC systems. The performance of the PLC system under the application of these techniques can then be compared with one other, and even with the system performance without their application. The main techniques for enhancing system performance in the wired environment are coding and modulation. Different coding and modulation techniques or a combination of both improve the system performance in different ways. Some of the methods applicable in the PLC environment are discussed below.

2.4.1 Single Carrier Quadrature Amplitude Modulation (QAM)

This modulation scheme is known to provide a spectral efficiency that is high in digital communication systems [55]**.** However its performance under the Middleton's class-A impulsive noise environment was first explored in [56]. However the work reported in [56] suffers a serious drawback in that a conventional receiver (the receiver designed for AWGN channels) is employed in determining the impact of the impulsive noise on the error performance of a QAM system. The results clearly indicate that QAM performance is seriously degraded when the impulsive noise is very strong.

The performance of QAM in an impulsive noise environment was further explored in [52]. An optimum receiver for combating impulsive noise in a more effective manner was proposed by considering explicitly the statistical characteristics of class-A noise. The basic structure of this receiver is shown in block diagram form in Fig. 2-19. If during one symbol duration, k samples are taken, then, the received symbol $\boldsymbol{r}$ can be represented as :

$$\boldsymbol{r} = \{r_1,\ r_2, \dots, r_k\} \tag{2.85}$$

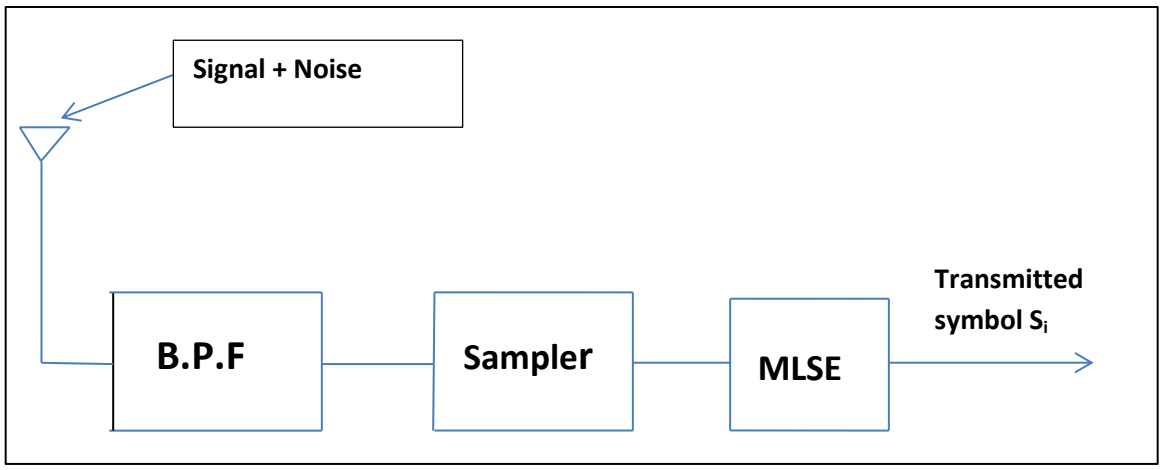

Figure 2- 19: Maximum likelihood receiver model [52]

Where B.P.F is Band Pass Filter**,** MLSE is Maximum likelihood estimator, r_k is the received symbol k^{th} sample. It is assumed here that the k samples, $r_1,\ r_2, \dots, r_k$, are statistically independent. In a similar manner, the transmitted symbol and the additive class-A noise are described by $s = \{s_1,\ s_2, \dots, s_k\}$ and $n = \{n_1,\ n_2, \dots, n_k\}$, respectively. The pdf of $r = s + n$, given that the symbol s was sent, is given by:

$$p(r|s) = p(n = r - s) = \prod_{k=1}^{K} p_A(r_k - s_k) \tag{2.86}$$

Where p_A is the probability density function of the class-A impulsive noise. Generally, the probability density given in Equation (2.86) is referred to as "likelihood". For a given r in this equation, a maximum likelihood detection receiver selects the symbol that maximizes the equation. This strategy minimizes the symbol error probability, and in this sense, a receiver that does maximum likelihood detection is known as an optimum receiver. If we make a substitution of the complex class-A impulsive noise above into Equation (2.86), the likelihood for class-A impulsive noise is computed as [15]:

$$p(r|s) = \prod_{k=1}^{K} \sum_{m=0}^{\infty} e^{-A} \frac{A^m}{m!} \frac{1}{2\pi\sigma_m^2} exp\left(-\frac{|r_k - s_k|^2}{2\sigma_m^2}\right) \tag{2.87}$$

Under class-A noise impulsive noise conditions, a receiver which performs maximum likelihood detection selects the symbol s that maximizes $p(r|s)$ as the transmitted one. However, the complexity of the receiver based on this equation would make its implementation a difficult task.

The finite sum of the equaition can be approximated by the first three terms, if the impulsive index A is sufficiently small [52]. By making use of the optimal and sub-optimal receiver here, the authors have shown that the performance of impulsive QAM systems is much better than when conventional receivers are used. More specifically, the improvement in performance achieved is around 40 dB at the error probability of 10^{-2} for A=0.1 and $\Gamma = 10^{-3}$.

2.4.2 Binary Turbo Coded Modulation (Binary TCM)

Turbo codes that are iteratively decoded have shown superb error performance, and are therefore a good choice for single-carrier digital communication systems. Turbo code working principles were first presented by Berrou *et al.* [57] and have even discussed in a clearer way by Lin and Costello [58] for Gaussian noise channels. The first investigation of how turbo codes could be used to improve the error performance in channels affected by impulsive noise was reported in [48, 53]. The application of turbo codes in the elimination of the effects of impulsive noise in channels as presented in [53] is discussed next.

Figs. 2-20 and 2-21 show examples of turbo encoder and turbo decoder respectively. The turbo encoder shown in Fig. 2-20 uses two identical recursive systematic convolutional (RSC) codes. The encoder output includes $u = \{u_1, \dots, u_N\}$, $v_1 = \{v_{11}, \dots, v_{1N}\}$ and $v_2 = \{v_{21}, \dots, v_{2N}\}$. The interleaver in this turbo encoder is a random block interleaver whose size is *N*.

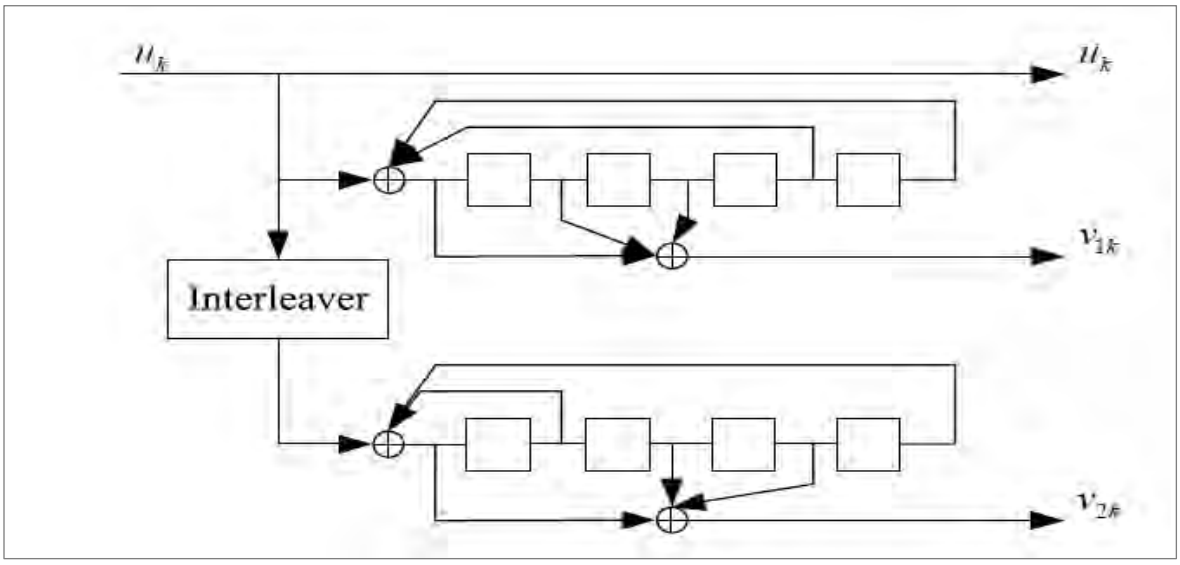

Figure 2- 20: Turbo encoder with two identical RSC encoders

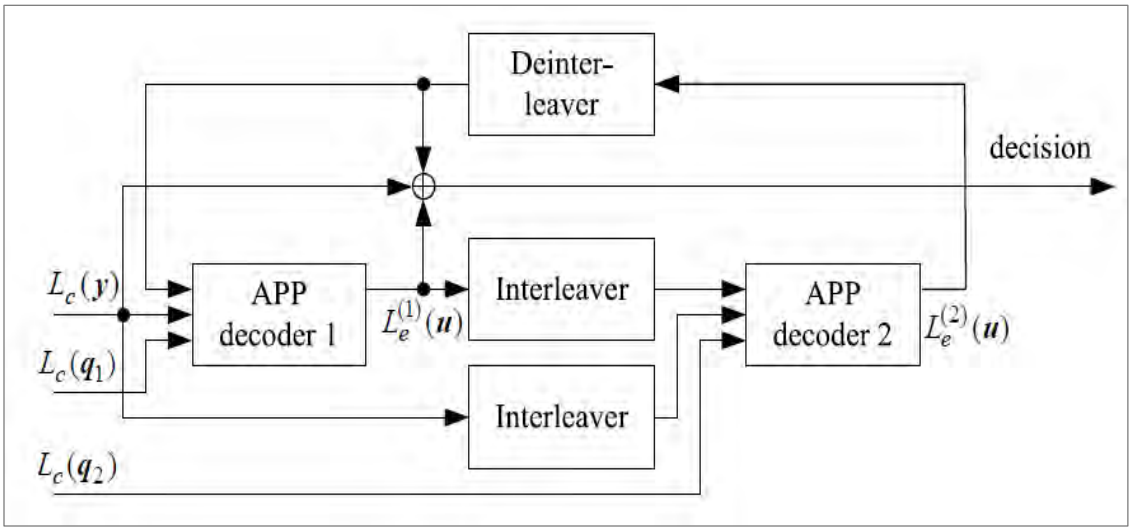

Figure 2- 21: Turbo decoder

We denote the match filter's outputs sequences as $y = \{y_1, \dots, y_N\}$, $q_1 = \{q_{11}, \dots, q_{1N}\}$ and $q_2 = \{q_{21}, \dots, q_{2N}\}$ which correspond to u, v_1, v_2 respectively. The decoder has two *a posteriori probability* (APP) decoders which correspond to the two RSC codes in the encoder. Each APP is either an optimal or suboptimal *maximum a posteriori* (MAP) decoder. Extra details concerning the MAP decoder and the computation of the log likelihood ration (LLR) of the *a posteriori probability* are available in [53, 57, 59, 60].

In [53], Umehara e*t al.* report that the conventional turbo coded system decoder differs from the one used in an impulsive noise channel in the way the channel value L_c is determined. Particularly, the channel value for an impulsive turbo coded system takes into consideration the distribution attributes of the class-A impulsive noise. The channel value is thus calculated as:

$$L_c(y_k) = In\frac{P\{y_k|u_k = +1\}}{P\{y_k|u_k = -1\}} = In\frac{p_A(y_k - 1)}{p_A(y_k + 1)} \tag{2.88}$$

Where p_A is the probability density function of the class-A impulsive noise. It is reported in [53] that the optimal or sub-optimal decoder implemented for impulsive noise channel greatly boosts the error performance of the system . For example, with A=0.1 and Γ=0.1 as the channel parameters, a coding gain of 10 dB at a bit error rate (BER) of 10^{-5} is achieved.

2.4.3 Spread spectrum modulation

Spread sprectrum modulation is a kind of modulation in which the data is spread across the total available frequency band, in excess of the minimum bandwidth required to send information. This modulation was designed for wireless digital communication systems , specifically for dealing with jamming situations in case an adversary intended to disrupt communications. This modulation therefore has its origins tied to military needs and has also been used in hostile communcations enviroments like PLC. This modulation is rather immune to selective attenuation and all manner of narrowband interference. The modulation also has a low power spectral density of the transmitted signal; which is a big advantage from an electromagnetic compatibility (EMC) perspective. As with Code-Division Multiple Access (CDMA), the total frequency band is open to each signal, and therefore , access does not have to be coordinated [27, 61].

In Fig. 2-22, an illustration of the spread spectrum principle is shown, where the information carrying signal, having a bandwidth B and duration T_s , is converted through a pseudo-noise signal into a signal with spectrum ocuupation W, with $W \gg B$. Thus, there is a multiplicative factor of bandwidth expansion that is measured in terms of a spread spectrum parameter referred to as spreading factor (SF), also known as spreading gain or processing gain, and is given by [27, 61]:

$$SF = \frac{W}{B} = W.T_s \tag{2.89}$$

For military applications for example, the SF is between 100 and 1000.

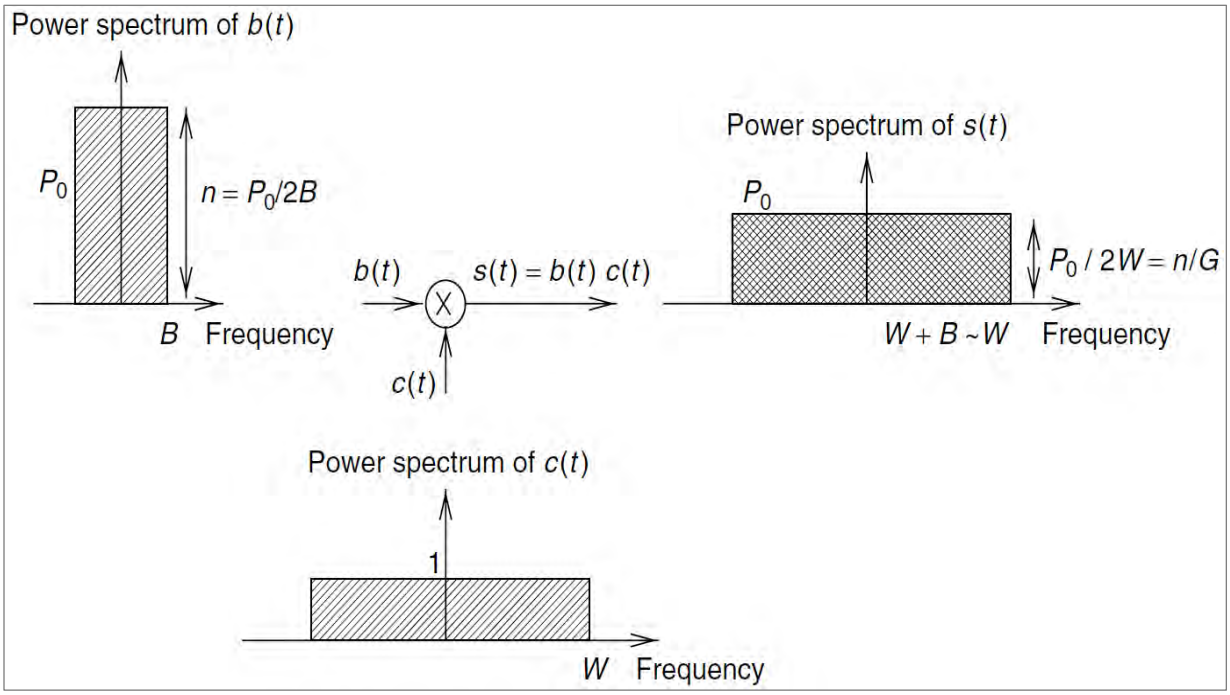

Figure 2- 22: Bandwith spreading principle in DSSS

Spread spectrum modulation has several advantages, among them resistance to multipath and fading effects, resistance to interference from other sources, inherent transmission security and redundancy. There are several spread sprectrum technologies, which include: MultiCarrier Spread Spectrum (MCSS), Time Hopping spread spectrum (THSS), Direct Sequence Spread Spectrum (DSSS) and Frequency Hopping Spread Spectrum (FHSS). It is however possible to combine a number of these spread spectrum techniques to develop hybrid ones that have the advantages of each individual technique. Interested readers are referred to [61] for more on this modulation technique.

2.4.4 Orthogonal Frequency Division Multiplexing (OFDM)

This is another commonly used modulation method for the performance enhancement in both wireless and wired (PLC) communication systems. OFDM operates on the principle of a well-chosen linear transform at the transmitter and the use of the transform's inverse at the receiver. The OFDM system draws its biggest strength from the fact that the signal, together with the noise is spread across a number of sub-channels (subcarriers). The signal that is transmitted goes through both transforms and therefore remains unaffected, but the noise signal goes through receiver's

transform only. The individual noise impulses' energy is therefore smeared or dispersed over the increased symbol duration [62, 63]. The error floor usually experienced in uncoded transmission systems plagued by impulsive noise is thus partially eliminated in this way.

The Fig. 2-23 shows a simplified block diagram of typical OFDM system. For an OFDM system with *N* subcarriers, the symbol stream after the *M*-ary modulator is passed through a serial-to-parallel converter, whose output will be a set of *N M*-ary symbols denoted by $\{S_0,\ S_1, \dots, S_{N-1}\}$ corresponding to the symbols transmitted over each carrier. For the generation of the transmitted signal, the inverse discrete Fourier transform (IDFT) is performed on the *N* symbols. Usually, *N* is chosen to be a power of 2 and the IDFT in this case is implemented using the inverse fast Fourier transform (IFFT) algorithm. The OFDM symbol that is produced by the IFFT is a sequence given by $\{s_0,\ s_1, \dots, s_{N-1}\}$, whose length is *N*, where

$$s_k = \frac{1}{\sqrt{N}} \sum_{i=0}^{N-1} S_i^{j2\pi ki/N}, \qquad 0 \le k \le N-1 \tag{2.90}$$

The symbols received after the filtering and sampling process, assuming that perfect synchronization and timing takes place, are expressed as follows:

$$r_k = s_k + n_k \qquad 0 \le k \le N-1 \tag{2.91}$$

Where n_k is the additive complex class-A impulsive noise. At the receiver's side, an *N*-point fast Fourier transform (FFT) is performed on the received *N* sequence symbols $\{r_0,\ r_1, \dots, r_{N-1}\}$ yielding:

$$R_k = \frac{1}{\sqrt{N}} \sum_{i=0}^{N-1} r_i^{-\frac{j2\pi ki}{N}}, \qquad 0 \le k \le N-1 \tag{2.92}$$

Equation (2.92) can be simplified as:

$$R_k = S_k + n'_k \qquad 0 \le k \le N-1 \tag{2.93}$$

where the noise samples $n'_k = \{n'_0, n'_1, \dots n'_{N-1}\}$ are the *N*-point FFT of the original impulsive noise samples $\{n_0,\ n_1, \dots, n_{N-1}\}$, and they are given by:

$$n'_k = \frac{1}{\sqrt{N}} \sum_{i=0}^{N-1} n_i^{-\frac{j2\pi ki}{N}}, \qquad 0 \le k \le N-1 \tag{2.94}$$

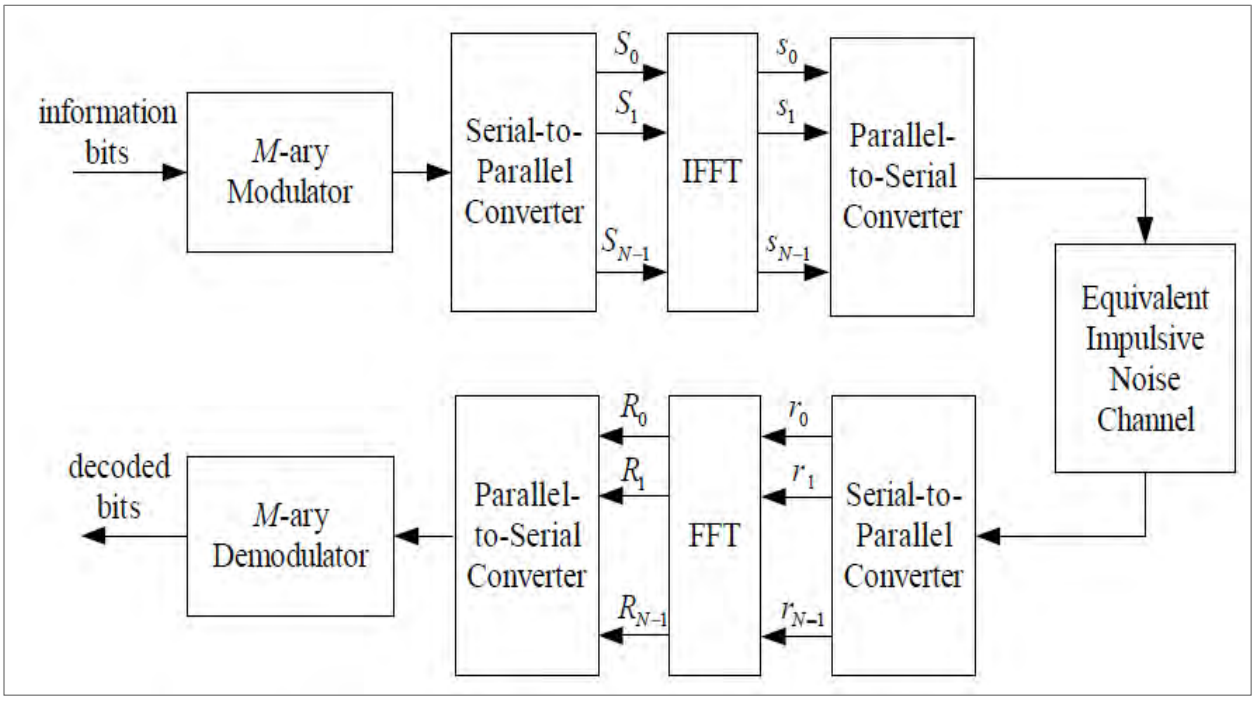

Figure 2- 23: Simplified block diagram of an OFDM system

The FFT outputs are then passed to a parallel-to-serial converter. The parallel-to-serial converter output is then passed on to a conventional *M*-ary demodulator that demodulates each of the sample r_k for $0 \leq k \leq N-1$. Conventional *M*-ary demodulator here means the demodulator designed for AWGN channels. The OFDM system's additive noise spreading is the major difference between it and a single–carrier system. This is the main reason behind OFDM's superior error performance as compared to single-carrier systems.

Of all the modulation schemes, OFDM outperforms all of them in most aspects. This can be seen in the comparative tabulation of the different modulation schemes performance for PLC applications as shown in Table 2.4 below and the reader is referred to the referenced material for further details.

Table 2. 4: A comparison of different modulation schemes for PLC [27]

Modulation scheme	Spectral efficiency in b/(s · Hz)	Max. data rate in Mb/s	Robustness against channel distortions	Robustness against impulsive noise	Flexibility and adaptive features	System costs	EMC aspects, regulation
Spread spectrum techniques	< 0.1	≈ 0.5	-	0	--	--	+
Single-carrier broadband, no equalizer	1–2	< 1	--	+	--	++	--
Single-carrier broadband with equalizer	1–2	≈ 2	+	+	0	-	-
Multicarrier broadband with equalizer	1–4	≈ 3	+	0	0	-	0
OFDM	>> 1	> 10	++	0	++	-	+

2.4.5 OFDM-based BPSK system performance evaluation in an impulsive noise environment

From the above background study on OFDM which shows that it best suited for the PLC channel, a performance study was carried out to determine the impact of impulsive noise on an OFDM-based BPSK (binary phase shift keying) system. This work is motivated by the fact that the very characteristics of the impulse noise, namely; pulse width, amplitude and interarrival time, have not been studied at an elementary level in terms of their influence on the performance of the PLC channel. Here, the mathematics behind the impulse function is utilized in an attempt to fully characterize the impulse noise for the PLC channel. The performance of the PLC system is compared in terms of the bit error rate (BER) characteristics for given signal to noise ratio (SNR) values for different impulsive noise parameters.

In the study, amplitude of the noise impulses is assumed to be constant for ease of comparison; where we consider the maximum amplitude of the impulsive noise which also translates to maximum impulse power. A constant impulse width of 50μs is used while the interarrival time is varied between 100μs and 10000μs. The channel gains are assumed to be random. The performance of the system as the interarrival time is varied is then determined in terms of the bit error rate (BER) and signal-to-noise (SNR) ratio. The results for three different values of the interarrival time considered are shown in Figure 2-24. From this graph, the performance of the system is best when

IAT=10000 µs while the worst performance is obtained when the IAT=100µs. This means that the impact of the impulsive noise on the system is least when the interarrival time is greatest at a constant pulse duration and constant pulse amplitude. The reverse is also true. For example, at a BER value of 10^{-3}, the SNR values for IAT=10000 µs, 1000 µs and 100µs are 15 dB, 19.5 dB and 21.5 dB respectively. Thus, a smaller value of interarrival time would translate to more frequent impulses and deteriorated system performance, and vice versa. It is interesting to note that a constant pulse width in a varying IAT translates to a varying impulse distance according to Equation (2.68). The impulse distance actually varies in direct proportion to the IAT at contestant pulse width.

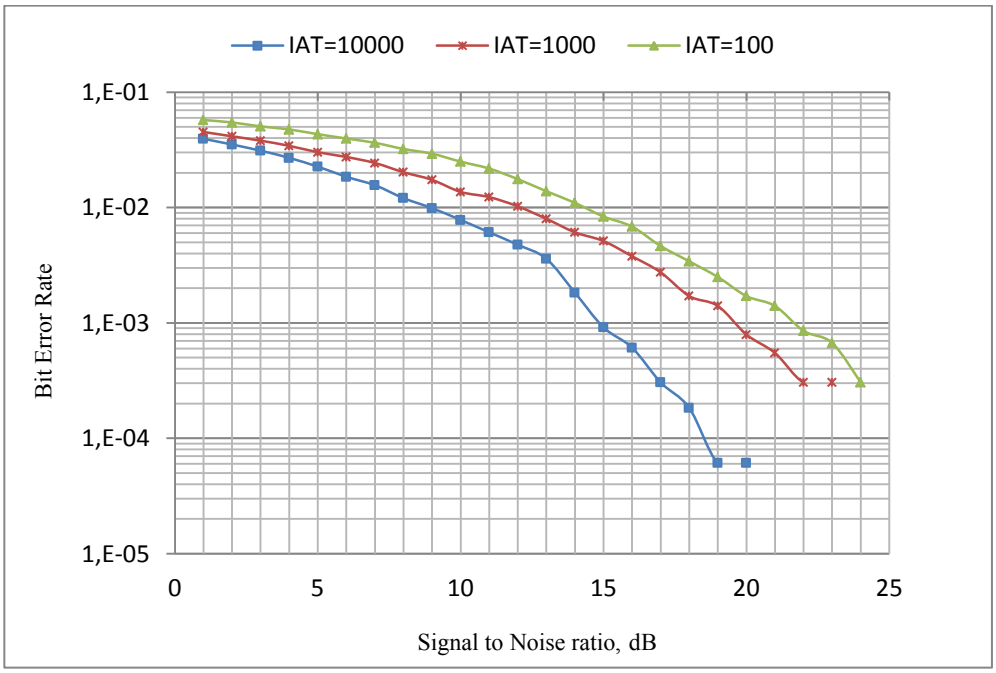

Figure 2- 24: Performance characteristics for different noise interarrival time values [C1]

The error statistics above show that the performance of the system is highly limited in the presence of impulsive noise in the channel. Thus, the SNR for example cannot improve beyond 19 dB for IAT=10000 while for IAT=1000, it cannot improve beyond 22 dB for the same BER. Thus to improve on the system performance, modern digital signal processing techniques should be implemented on the channel, although the gains achievable are limited by the associated system complexity. But, a performance-complexity trade-off is crucial for the realizations of a more reliable PLC system. These techniques, for example robust coding schemes, will be able to reduce and/or correct both bit and burst errors that occur due to the corruption of the OFDM signals by noise. An application of the models derived in later chapters in this work to such a system is of interest in future so as to benchmark the model's performance against existing ones.

2.5 Electromagnetic compatibility issues in PLC

The cables of any power supply grid have been designed to carry high-power low-frequency power signal at approximately 50Hz to 60 Hz. Therefore, from an electromagnectic point of view, the injection of a low-power high-frequency PLC carrier signal into the power lines makes them leaky resulting in an electromagnetic field being radiated into the environment. This therefore means that the power cables start behaving like linear antennas with low efficiency. This radiated field could interfere with other systems resulting in electromagnetic interference (EMI). For electromagnectic compatibility (EMC) to be realized between the PLC system and other communication systems, the EM field radiated by the PLC system should not exceed certain limits. Therefore, EMC refers to ability of the PLC system co-existing with other systems in the same environment without causing disturbance to their functionality and vice versa [61, 64-66]. Thus, for EMC requirements to be met, a sytem should be able to function satisfactorily in its environment without introducing intolerable EM disturbances in form of interference to other systems in the same environment, including itself. From this last definition, there are several notable aspects of EMC, and some are discussed next [61].

- *To function satisfactorily:* means that the device or system is tolerant of others. The device is not susceptible to EM signals that other devices emit to the environment. This EMC aspect is known as electromagnetic susceptibility (EMS).
- *Without producing intolerable EM disturbances:* meaning that the equipment or device does not bother others, which means that whatever EM signals a device produces does not cause EMI issues in other equipment present. This EMC aspect of causing disturbances is poined out as electromagnetic emission (EME).

The different areas/aspects of EMC are summarized in Fig. 2-25 below.

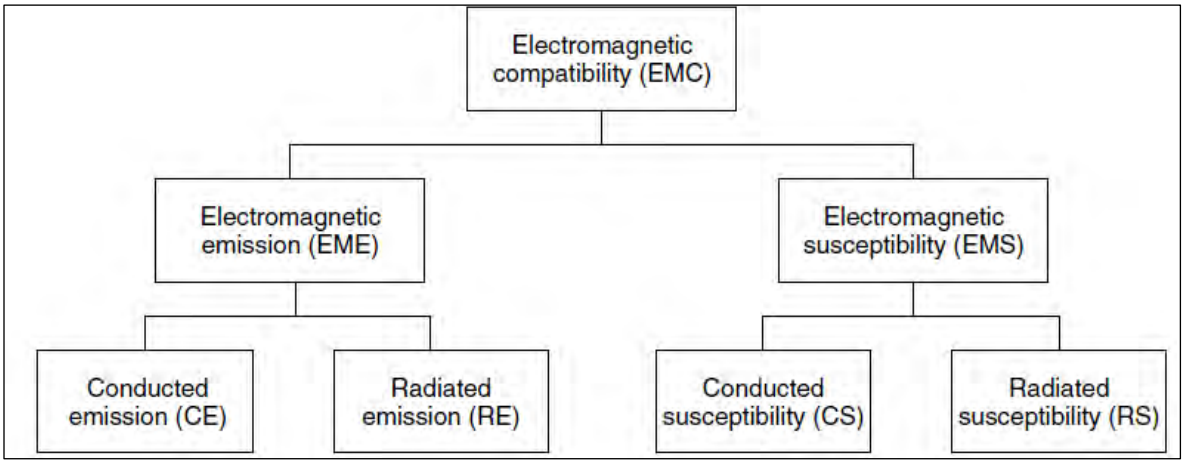

Figure 2- 25: Different areas of EMC [61]

All in all, for a PLC system to co-exist with other systems without causing EMC/EMI issues, there are things that must be addressed, most importantly the transmit power of the communication

signals for all systems, which directly impacts on the EM fields radiated or conducted by other devices in the same environment. This falls under regulatory bodies, like the Federal Communications Commission (FCC), CISPR (*Comité International Spécial des Perturbations Radioélectrique*s-international committee for radio interferences) and the IEEE, that are responsible for setting the necessary limits and standards [61, 67].

Possible systems that may be affected by PLC system EM field radiations are shown in Table 2.5, together with the frequency bands they occupy.

Table 2. 5: Possible PLC EMC victims and their frequency band occupancy [61]

Service classes	Services	Occupied bands (MHz)
Broadcasting	Medium waves (MW) and Short waves (SW) broadcasting	1.3–1.6; 3.9–4.0; 5.9–6.0, 6.0–6.2; 7.1–7.3; 7.3–7.35; 9.4–9.5; 9.5–9.9; 13.5–13.6; 13.6–13.8; 15.1–15.6; 25.6–26.1
Maritime mobile	Tactical/strategic maritime Maritime Mobile S5.90 Distress and Safety Traffic	1.6–1.8; 2.04–2.16; 2.3–2.5; 2.62–2.65; 2.65–2.8; 3.2–3.4; 4.0–4.4; 6.2–6.5; 8.1–8.8; 12.2–13.2; 16.3–17.4; 18.7–18.9; 22.0–22.8; 25.0–25.21
	Naval broadcast communications	1.6–1.8
	Maritime DGPS	1.8–2.0; 2.0–2.02
Radio Amateur	Datamode, CW, fax, phone, etc.	1.81–1.85; 3.5–3.8; 7.0–7.1; 10.1–10.15; 14.0–14.2; 14.25–14.35; 18.0–18.16; 21.0–21.4; 24.8–24.9; 28.0–29.7
Military	NATO & UK long-distance communications	2.0–2.02; 2.02–2.04; 2.3–2.5
Aeronautical	Aeronautical	2.8–3.0; 3.02–3.15; 3.4–3.5; 3.8–3.9; 4.4–4.65; 5.4–5.68; 6.6–6.7; 8.81–8.96; 10.0–10.1; 10.1–11.1; 21.0–22.0; 23.0–23.2
Radio astronomy	Radio Astronomy	13.3–13.4; 25.55–25.67

Some EMC standards that regulate the power injected by PLC systems include CENELEC EN 50561-1 [68] and CISPR 22 standard [69].

2.6 Chapter summary and conclusion

In this chapter, a comprehensive survey of PLC has been presented. The various aspects of PLC, which range from its merits and demerits, channel transfer function, channel noise, modulation as well as EMC issues have been studied. The channel modeling approaches in PLC can be widely divided into two: top-down and bottom-up techniques. On the other hand, PLC channel noise falls into three main classes which are: coloured background noise, narrowband interference/noise and impulsive noise. The noise models available in literature are all parametric, with the most popular ones being the two-term Gaussian mixture and Middleton's class A models, even though these models were not originally developed for power line noise. Also, modulation schemes in PLC can be grouped into two: single-carrier modulation like QAM, multicarrier modulation like OFDM. OFDM is quite immune to impulsive noise and outperforms single carrier systems as well as other multicarrier systems in many respects. For this reason, a preliminary investigation of the impact of impulsive noise on an OFDM-based BPSK system was done. This study differs with earlier ones in that the impulsive noise impact is considered in terms its elementary characteristics. Additionally, there are EMC/EMI issues that are associated with PLC systems. The interference into or from PLC systems can be spread through radiation or condution. PLC systems must operate in the communications environment without interfering with other communication systems and vice versa; what is referred to as EMC . There are stringent regulations in place that control the allowable interference from different communication systems and PLC is not an excepetion. All in all, PLC presents a viable and attractive technology that can supplement or even replace other communication technologies in certain areas of the communication network, for example in offering last-mile and last-inch communication access through the ubiquitous MV and LV power networks. Specifically, PLC is attractive in smart metering, power equipment monitoring, as well as in home automation and networking. This technology puts the power utility company in full control of the communication channel. And again, the synergy achieved through the use of various communication technologies for specific needs and specific reasons in the same communications network is usually unrivaled. In the next chapter, noise measurements are presented.

Chapter references

[1] J.O. Onunga and R.W Donaldson, "Personal computer communications on intra-building power line LANS using CSMA with priority acknowledgements," *IEEE Journal on Selected Areas in Communications*, vol. 7, no. 2, February 1989, pp. 180-191.

[2] L.T Berger, A. Schwager and J.J. Escudero-Garzas, "Power line communications for smart grid applications," *Journal of Electrical and Computer Engineering*, vol. 2013, Article 712376, 16 pages.

[3] H.C. Ferreira *et al.*, "Power Line Communications: An Overview," *IEEE AFRICON 1996*, 24-27 September 1996, Stellenbosch, South Africa, pp. 558-563.

[4] M. Zimmermann and K. Dostert, "A multi-path signal propagation model for the power line channel in the high frequency range," *Proceedings of the 3rd International Symposium on Power Line Communications and Applications*, Lancaster, U.K., 1999, pp. 45-51.

[5] H. Philipps, "Modeling of power line communications channels", *Proceedings of the 3rd International Symposium on Power Line Communications and Applications*, Lancaster, U.K., 1999, pp. 14-21.

[6] M. Zimmermann and K. Dostert, "A multipath model for the power line channel", *IEEE Transactions on Communications*, Vol. 50, No. 4, pp.553-559, April 2002.

[7] J. Anatory, M.M. Kissaka and N.H. Mvungi, "Channel model for broadband power line communication," *IEEE Transactions on Power Delivery*, vol. 22, no. 1, pp. 135-141, January 2007.

[8] A.M. Nyete, T. J. O. Afullo, and I.E. Davidson, "Statistical analysis and characterization of power line noise for telecommunication applications," *In Proceedings of the IEEE AFRICON 2015 Conference*, Addis Ababa, Ethiopia, 14–17 September 2015, pp. 213-217.

[9] H. Meng, S. Chen, Y.L. Guan, C. Law, P.L. So, E. Gunawan, T.T. Lie, "Modeling of Transfer Characteristics for the Broadband Power Line Communication Channel," IEEE Trans. Power Delivery, vol. 19, no. 3, pp. 1057-1064 July 2004.

[10] A.M. Nyete, T. J. O. Afullo, and I.E. Davidson, "On the application of non-parametric estimation methods for low voltage PLC network noise modelling," *In Proceedings of the Southern Africa Telecommunication Networks and Applications Conference (SATNAC)* 2015, Arabella Hotel & Spa, Western Cape, South Africa, 6-9 September 2015, pp. 59-63 .

[11] A.M. Nyete, T. J. O.Afullo, and I.E. Davidson, "Performance evaluation of an OFDM-based BPSK PLC system in an impulsive noise environment," *In PIERS Proceedings*, Guangzhou, China, August 25-28 2014, pp. 2510-2513.

[12] E. Biglieri, “coding and modulation for a horrible channel,” *IEEE Communications Magazine*, May 2003, pp. 92-98.

[13] A.J. Han Vinck and J. Haring, “Coding and modulation for power-line communications,” *ISPL2000*, pp. 265-272.

[14] A. M. Nyete, T. J. O. Afullo,, and I.E. Davidson, “Intra-building power network noise modelling in south africa,” *In Proceedings of the 23rd Southern African Universities Power Engineering Conference*, University of Johannesburg, Johannesburg, South Africa, 28-30th January 2015, pp. 468-472.

[15] T.Q Bui, *Coded Modulation Techniques with Bit Interleaving and Iterative Processing for Impulsive Channels*, MSc. Thesis, University of Saskatchewan, 2006.

[16] A. Majumder and J. Caffrey, “Power line communications,” *IEEE Potentials*, vol. 23, pp. 4-8, October 2004.

[17] T.S Pang, P.L So, K.Y See and A. Kamarul, “Common-mode current propagation in power line communication networks using multi-conductor transmission line theory,” *In Proceedings of ISPLC2007*, 26-28 March 2007, pp. 517-522.

[18] M. Bogdanovic, “ Computer based simulation model realization of OFDM communication over power lines,” *In 20th Telecommunications Forum TELFOR 2012*, Serbia Belgrade, November 20-22, 2012, pp. 249-252.

[19] E.P Guillen, J.J Lopez and C.Y Barahoma, “Throughput analysis over power line communication channel in an electric noisy scenario,” *World Academy of Science, Engineering and Technology*, vol. 19, pp. 206-212, 2012.

[20] G. Bumiller and N. Pirschel, “Airfield ground lighting automation system realized with power line communication,” *In Proceedings of the ISPLC*, 2003, pp. 16-20.

[21] G. Griepentrog, “Powerline communication on 750V DC networks,” *In Proceedings of the ISPLC*, 2001, pp. 259-265.

[22] J. Barnes, “A physical multi-path model for power distribution network propagation,” *In Proceedings of the ISPLC*, Tokyo, Japan, March 1998, pp. 76-89.

[23] A. Dalby, “Signal transmission on powerlines-analysis of powerline circuits,” *In Proceedings of the ISPLC*, Essen, Germany, 1-4, April 1997, pp. 37-44.

[24] O. Hooijen, “A channel model for the residential power circuit used as a digital communication medium,” *IEEE Transactions on Electromagnetic Compatibility*, vol. 40, pp. 331-336, 1998.

[25] J. Anatory and N. Theethayi, *Broadband power line communication systems: Theory and Applications*, WitPress 2010.

[26] T. Esmailian, F. Kschischang and G. Gulak, “An in-building power line channel simulator,” *In Proceedings of the ISPLC*, Greece, 2002, pp.1-5.

[27] M. Gotz, M. Rapp and K. Dostert, “Powerline channel characteristics and their effect on communication systems design,” *IEEE Communications Magazine*, vol. 42, no. 4, pp. 78-86, April 2004.

[28] H. Philipps, “Performance measurements of powerline channels at high frequencies,” *In Proceedings of the ISPLC, Tokyo, Japan, March 1998, pp. 229-237.*

[29] D.K. Cheng, *Fundamental of Engineering Electromagnetics*, Adison Wesley.

[30] D.M. Pozar, *Microwave Engineering*, New York: Wiley.

[31] G. Gonzalez, *Microwave Transistor Amplifiers*, Englewood Cliffs, NJ: Prentice Hall, 1997.

[32] J. Anatory *et. al.* "Broadband power-line communication channel model: Comparison between theory and experiments", Proc. IEEE Int. Symp. Power Line Communications and Its Applications, Jeju city, Jeju Island, pp.322 -324, Apr 2008.

[33] J. Anatory, N. Theethayi, R. Thottappillil, M.M. Kissaka and N.H. Mvungi, “The effects of load impedance, line length and branches in the BPLC- transmission lines analysis: a case of indoor voltage channel,” *IEEE Transactions On Power Delivery,* vol.22, no 4, pp. 2150-2155, 2007.

[34] C.T Mulangu, *Channel Characterization for Broadband Power Line Communications*, PhD Thesis, University of KwaZulu-Natal, 2014.

[35] *Mie Theory* : http://www.orc.soton.ac.uk/publications/theses/1460T_lnn/1460T_lnn_03.pdf, last accessed on 17th February 2016.

[36] F. Zwane, *Power Line Communication Channel Modelling*, Masters Dissertation, University of KwaZulu-Natal, 2014.

[37] C. Assimakopoulos and N. Pavlidou, "A enhanced powerline channel noise model," *WSEAS Transactions on Power Systems*, vol. 1, Issue 1, pp. 239-245, January 2006.

[38] H. Philipps, "Development of a statistical model for powerline communication channels," *In Proceedings of the ISPLC, 2000, pp.153-160.*

[39] M. Zimmermann and K. Dostert, "Analysis of the broadband noise scenario in powerline networks," *In Proceedings of the ISPLC, 2000, pp.131-138.*

[40] E. Yavuz, F. Kural, N. Coban, B. Ercan and M. Safak, "Modeling of power lines for digital communications," *In Proceedings of the ISPLC,* 2000, pp.161-168.

[41] R.M Vines, H.J Trussell, L. Gale and J.B O'Neal, "Noise on residential power distribution circuits," *IEEE Transactions on Electromagnetic Compatibility*, vol. 26, pp. 161-168, November 1984.

[42] J.A Cortes, L. Diez, F.J Canete and J.J Sanchez-Martinez, "Analysis of the indoor broadband power-line noise scenario," *IEEE Transactions on Electromagnetic Compatibility*, vol. 52, no. 4, pp. 849-858, November 2010.

[43] M. Zimmermann and K. Dostert, "Analysis and modeling of impulsive noise in broad-band powerline communications," *IEEE Transactions on Electromagnetic Compatibility*, vol. 44, no. 1, pp. 249-258, November 2002.

[44] Y. Ma, K. Liu, Z. Zhang, J. Yu and X. Gong, "Modeling the colored background noise of power line communication channel based on artificial neural network," in 19th Wireless and optical communications conference (WOCC), 14-15th May, 2010.

[45] S.V Vaseghi, *Advanced Digital Signal Processing and Noise Reduction,* John Wiley and Sons, 4th Edition, 2008.

[46] A. Papoulis and S.U. Pillai, *Probability, Random Variables and Stochastic Processes*, McGraw-Hill, 4th Edition, 2002.

[47] L.D. Bert, P. Caldera, D. Schwingshackl, and A.M Tonello, "On noise modeling for power line communications," *In Proceedings of the ISPLC,* 2011, pp.283-288.

[48] Y. Ma, P. So, and E. Gunawan, “Performance analysis of OFDM system for broadband power line communications under impulsive noise and multipath effects," *IEEE Transactions on Power Delivery*, Vol. 20, No.2, pp. 674-682, April 2005.

[49] T. Faber, T. Scholand, and P. Jung, “Turbo decoding in impulsive noise environments," *Electronics Letters,* vol. 39, pp. 1069-1071, July 2003.

[50] H. V. Poor and M. Tanda, “Multiuser detection in fading non-Gaussian channels," *IEEE Transactionson Communications*, vol. 50, no. 11, pp. 1769-1777, November 2002.

[51] D. Middleton, “Statistical-physical models of electromagnetic interference," *Electromagnetic Compatibility; Proceedings of the Second Symposium and Technical Exhibition*, vol. EMC-19, pp. 331-340, June 1977.

[52] S. Miyamoto, M. Katayama, and N. Morinaga, “Performance analysis of QAM systems under Class-A impulsive noise environment," *IEEE Transactions on Electromagnetic Compatibility*, vol. 37, pp. 260-267, May 1995.

[53] D. Umehara, H. Yamaguchi, and Y. Morihiro, “Turbo decoding in impulsive noise environment," *In Proceedings of IEEE Global Telecommunications Conference*, July 2004, pp. 194-198.

[54] M. Ardakani, F. R. Kschischang, and W. Yu, “Low-density parity-check coding for impulse noise correction on power line channels," *In Proceedings of the 2005 ISPLC*, pp. 90-94, March 2005.

[55] J. G. Proakis, *Digital Communication*, McGraw-Hill, 4th edition, 2000.

[56] J. Seo, S. Cho, and K. Feher, “Impact of non-Gaussian impulsive noise on the performance of high level QAM," *IEEE Transactions on Electromagnetic Compatibility*, vol. 31, no. 2, pp. 177-180, May, 1989.

[57] C. Berrou, A. Glavieux, and P. Thitimajshima, “Near Shannon limit error correction coding and decoding: Turbo codes*,” In Proceedings of IEEE International Conference on Communications*, pp. 1064-1070, May, 1993.

[58] S. Lin and D. J. Costello, *Error Control Coding,* Prentice Hall, 2nd edition, 2004.

[59] P. Robertson, E. Villebrun, and P. Hoeher, “A comparison of optimal and suboptimal MAP decoding algorithms operation in the log domain," *In Proceedings of* IEEE *International Conference on Communications*, June 1995, pp. 1009-1013.

[60] S. Benedetto, D. Divsalar, G. Montorsi, and F. Pollara, “Soft-input soft-output maximum a posteriori (MAP) module to decode parallel and serial concatenated codes," *TDA Progress Report 42-127,* November 15, 1996.

[61] H. Hrasnica, A. Haidine, R. Lehnert, *Broadband Powerline Communications Networks, Network Design,* John Wiley & Sons Ltd, 2004.

[62] G. R. Lang, “Rotational transformation of signals,” *IEEE Transactions on Information Theory*, vol.9, no.3, pp.191-198, Jul 1963.

[63] J. Bingham, “Multicarrier modulation for data transmission: An idea whose time has come," *IEEE Communications Magazine*, vol.28, no.5, pp.5-14, May 1990.

[64] A. Chubukjian, J. Benger, R. Otnes and B. Kasper, "Potential effects of broadband wireline telecommunications on the HF spectrum," *IEEE Communications Magazine*, vol.46, no.11, pp.49-54, November 2008.

[65] M. Gebhardt, F. Weinmann and K. Dostert, "Physical and regulatory constraints for communication over the power supply grid," *IEEE Communications Magazine*, vol.41, no.5, pp.84-90, May 2003.

[66] S. Galli, A. Scaglione and Z. Wang, “For the grid and through the grid: The role of power line lommunications in the smart grid,” *Proceedings of the IEEE*, vol. 99, no. 6, pp. 998-1027, June 2011.

[67] Seventh Framework Programme: Theme 3 ICT-213311, OMEGA, Deliverable *D3.3*, "*Report on Electro Magnetic Compatibility of Power Line Communications* ", 16 April 2010.

[68] *CENELEC EN 50561-1, :* http://www.hd-plc.org/modules/standards/cenelec.html.

[69] CISPR 22/IEC, *Information technology Equipment – Radio Disturbance Characteristics – Limits and methods of measurements*, Third Edition, 11-97.

Chapter Three

3. Powerline Noise Measurements

3.1 Introduction

Most of the models that have been developed for the channel transfer function as well as noise are based on measurements. This is primarily so because the PLC channel presents a very complex environment, from a communications point of view. Thus, to get a clear understanding of the power line channel transfer function as well as noise, there is need to do comprehensive measurements for both under different loading conditions and different network configurations. The conditions considered should be able to provide an average feel of the environment that the communication signal is to be sent through. Various efforts by different researchers toward this goal have been reported in Chapter two. The noise scenario in power line networks presents an interesting complex phenomenon. This is primarily so because the noise in power line networks differs from the classical AWGN found in many other communication systems. The noise in PLC channels is mainly influenced by the impulsive component which leads to a complete departure from the Gaussian behavior of the noise distribution in other systems. Thus, PLC noise needs to be studied thoroughly; especially through measurements and not just through mere analytical methods, so as to understand it properly for communication applications. The objectives of this chapter are:

1. To present a detailed description of the measurement equipment used in our noise measurement campaign.
2. To present a brief on the coupling circuitry designed
3. To describe the procedure used for the noise measurements as well as the environment where the measurements were carried out.
4. To present a brief summary of the noise measurements results (sample results) carried out in low voltage power line networks in an indoor environment.

3.2 Measurement equipment description

A Rhode and Schwarz FS300 spectrum analyzer and a four-channel Tektronix TDS 2024B digital storage oscilloscope (DSO) were used to do comprehensive noise measurements in various rooms in the two buildings at the Department of Electrical, Electronic and Computer Engineering, University of KwaZulu-Natal, Howard College in Durban, South Africa in both frequency and time

domains respectively. This section is dedicated towards the description of the two measuring devices.

3.2.1 Rhode and Schwarz FS300 spectrum analyzer

The Rhode and Schwarz FS300 (R&S®FS300) spectrum analyzer is a highly accurate spectrum analyzer that offers high quality measurements. The particular one used in our noise measurements is shown in Fig. 3-1 below, while a summary of the specific measurement characteristics of this instrument are summarized in Table 3.1 below.

Figure 3- 1: The R&S®FS300 equipment in a set up for background noise measurement in the PLC Laboratory at UKZN

Below is a more detailed description of the equipment's key features and benefits:

1. Capability to perform high quality measurements

Relatively weak signals can be reliably detected by the device given that average noise level displayed is typically -120 dBm (300 Hz). This is feature is very crucial especially for harmonics and spurious measurements. No inherent distortions occur within the R&S®FS300 intermodulation-free dynamic range, which results in interference free measurements. At times when a high dynamic range is a requirement, this becomes particularly very useful, that is, simultaneous measurements of both low and high levels are to be done. The measurement trace points are displayed with an uncertainty level of <1.5 dB. This value is a key prerequisite for high accuracy in measurements.

2. 200 Hz to 1 MHz Resolution bandwidth

The R&S®FS300 can be adapted to best suit the measurement task by making use of the sixteen (16) digitally implemented resolution bandwidths that range from 200 Hz to 1 MHz. For overall measurements, short sweep times are ensured with wide resolution bandwidths.

Table 3. 1: R&S®FS300 specifications [1]

Frequency range	9 kHz to 3 GHz
Resolution bandwidths (–3 dB)	200 Hz to 1 MHz
Video bandwidths	10 Hz to 1 MHz
Displayed average noise level	< –110 dBm, typ. –115 dBm (300 Hz)
Intermodulation-free range	< –70 dBc at –36 dBm input level
SSB phase noise, 10 kHz offset	< –90 dBc (1 Hz)
Level uncertainty	< 1.5 dB, typ. 0.7 dB
Detector	peak
Measurement functions	TOI, TDMA power, frequency counter,

On the other hand, narrow bandwidths are best suited for low noise level and high frequency resolution measurements. The R&S®FS300 fulfills every measurement requirement that lies between the two extreme cases.

3. 1 Hz resolution frequency counter

In the whole frequency range, the frequency of the signal can be comfortably measured with the help of a frequency counter of 1 Hz resolution that is a built-in feature of the R&S®FS300. Hence, there is no need for extra frequency counter, which leads to big savings in terms of laboratory bench space.

4. Maximum level of input is +33 dBm

The maximum level of input of this spectrum analyzer allows for the measurement of signals that are way beyond common limits. It is possible to even connect mobile phones with a 2 W maximum output power directly to R&S®FS300 without the use external attenuators.

5. Locating EMC weak spots

Locating weak EMC spots on shieldings, integrated circuits, cables and printed boards , among other trouble spots can easily be done with the use of the R&S®HZ-15 near-field probes. For measurement of emissions from 30 MHz to 3 GHz, the R&S®HZ-15 Near-Field probe set is very

adequate. The sensitivity of the measurements is increased with the Preamplifier R&S®HZ-16 up to 3 GHz, with a gain of approximately 20 dB and a 4.5 dB noise figure. In combination with the R&S®FS300/FS315, the near-field probe set together with the preamplifier provide a very cost-effective way of analyzing and locating interference sources during development.

6. The user interface is ergonomic

All users of the equipment, including untrained ones can quickly obtain correct measurements since all operations are menu-guided. Navigation within the menus is simplified using very clear structures. Menu items from other Rohde & Schwarz instruments are included which makes the instrument user friendly; familiarity with other spectrum analyzers from Rohde & Schwarz means that users can easily adapt this version of spectrum analyzer. A 320*240 pixel resolution that gives a very bright TFT colour display allows for the reading of traces even at odd angles or under unfavorable incidence of light.

Figure 3- 2: Illustration of EMC weak spots location kit [1]

7. USB Remote control

Another important characteristic of the R&S®FS300 spectrum analyzer is the USB remote-control interface. By simply establishing a USB connection, through a hot plug and play, a user can select external PC control even if it is during instrument operation. This is the first instrument which allows for remote-control via USB without any restrictions. Thus, with the USB cable help, the spectrum analyzer operation is possible even at positions that are difficult in terms of access, for example, in a shielded chamber. The R&S®FS300 comes with a Windows (2000/XP)-compatible driver for various development environments. For result display and recording, and remote control of the R&S®FS300, a PC software package is also available.

8. Compact housing with flexible handle

This spectrum analyzer has a very robust and compact design. Thus, it has very little space occupancy. For example, in a 19-inch rack, two series instruments can be comfortably

accommodated next to one another. Also, the adjustable handle performs several functions like carrying it around. The handle can be moved and locked in any required position for the recording of measurements. With the handle aid, the instrument can be set up in a tilted position so that the display can be viewed optimally.

9. High picture refresh rate

Smooth display of measurements is guaranteed with a refresh rate that is as high as 10 pictures per second. Parameters changes during module adjustment are thus quickly displayed which saves time in development and production.

10. Several measurement functions

For signal analysis support, this spectrum analyzer offers a number of marker and measurement functions. One normal and one delta maker or two normal markers are provided for the determination of the signal level. For instance, the normal marker can be positioned as a reference marker on the fundamental, while the delta marker is positioned on a harmonic. In this case, the difference between both levels is representative of the harmonic suppression. For measurement of the power density of noise, the delta or normal markers can be used as the noise markers. The *n* dB signal bandwidth, for example, the 4 dB or 7 dB bandwidth measurements can also be easily done with this spectrum analyzer.

11. Settings and traces internal memory

In the internal memory of this spectrum analyzer, storage of as many as five traces and ten settings is possible. Hence, it is possible to call up settings that are frequently used and therefore the same parameters do not have to be set over and over again. This also helps prevent setting errors on the spectrum analyzer. The information stored in the equipment can be called up later for other uses, for example, external storage or printing.

3.2.2 Four-channel Tektronix TDS2024B digital storage oscilloscope

The four-channel Tektronix TDS2024B digital storage oscilloscope (DSO) is the most advanced of the 2000B digital storage oscilloscopes series. Compared to its predecessors, it has much more superior performance capabilities, as shown in Table 3.2 below. The four-channel Tektronix TDS2024B digital storage oscilloscope used for our noise measurements is shown in Figure 3-3 below.

Table 3. 2: TDS2000B series digital storage oscilloscopes characteristics [3-4]

	TDS2002B	TDS2004B	TDS2012B	TDS2014B	TDS2022B	TDS2024B
Sample rate on each channel	1.0 GS/s	1.0 GS/s	1.0 GS/s	1.0 GS/s	2.0 GS/s	2.0 GS/s
Bandwidth*2	60 MHz	60 MHz	100 MHz	100 MHz	200 MHz	200 MHz
Number of Channels	2	4	2	4	2	4
Display(1/4 VGA LCD)	Colour	Colour	Colour	Colour	Colour	Colour
Time Base Range	5 ns to 50 s/div	5 ns to 50 s/div	5 ns to 50 s/div	5 ns to 50 s/div	2.5 ns to 50 s/div	2.5 ns to 50 s/div
Waveform Storage w/o USB Flash Drive	(2) 2.5K point	(4) 2.5K point	(2) 2.5K point	(4) 2.5K point	(2) 2.5K point	(4) 2.5K point
Record Length	2.5K points at all time bases on all models					
Vertical Resolution	8-Bits					
External Trigger	Included on all models					
Vertical Sensitivity	2 mV to 5 V/div on all models with calibrated fine adjustment					
DC Vertical Accuracy	±3% on all models					
Vertical Zoom	Vertically expand or compress a live or stopped waveform					
Maximum Input Voltage	300 VRMS CAT II; derated at 20 dB/decade above 100 kHz to 13 Vp-p AC at 3 MHz					
Position Range	2 mV to 200 mV/div +2 V; >200 mV to 5 V/div +50 V					
Input Coupling	AC, DC, GND on all models					
Time Base Accuracy	50 ppm					
Horizontal Zoom	Horizontally expand or compress a live or stopped waveform					
I/O Interfaces	USB Ports USB host port on front panel supports USB flash drives USB device port on back of instrument supports connection to PC and all PictBridge-compatible printers					
Reference Waveform Display	(2) 2.5K point reference waveforms					
Waveform Storage with USB Flash Drive	96 or more reference waveforms per 8 MB					
Setups with USB Flash Drive	4000 or more front-panel setups per 8 MB					
Save All with USB Flash Drive	12 or more Save All operations per 8 MB A single Save All operation creates 3 to 9 files (setup, image, plus one file for each displayed waveform)					

*2 Bandwidth is 20 MHz at 2 mV/div

Figure 3- 3: Tektronix TDS2024B DSO used for time domain measurements

3.3 Measurement environment, set up and coupling circuits

Using a Rhode and Schwarz FS300 spectrum analyzer and a four-channel Tektronix TDS 2024B digital storage oscilloscope (DSO), comprehensive low voltage noise measurements were done in various rooms in the two buildings at the Department of Electrical, Electronic and Computer Engineering, University of KwaZulu-Natal, Howard College in Durban, South Africa in both frequency and time domains respectively. Some of the rooms where the measurements were done included computer LANs, staff offices, electrical laboratories, electronic workshops, and postgraduate research offices and laboratories, among others. The noise measurements were done during busy hours, between 8 am and 5pm and also during off-peak hours when most of the rooms had little or no activity going on. This was to enable the capturing of different noise scenarios and to be able to have a grasp of the different noise components especially the distinction between background noise and impulsive noise components. The measurements were done in a random manner from day to day, and hundreds of thousands of noise samples in both time and frequency domains were collected from thousands of measurements. Figs 3-4 to 3-7 are pictures of some of the rooms where the measurements were done.

Figure 3- 4: An electronic workshop

Figure 3- 5: Second year laboratory

Figure 3- 6: Machinery workshop

Figure 3- 7: RF communications laboratory

With no ready-made coupling circuit available for the noise measurements, we designed suitable couplers for our measurements. The schematic of the couplers that were designed for the measurements is shown in Fig. 3-8. The coupling circuit acts as an interface between the power line network and the measuring device. It provides a galvanic isolation between the ac mains and the measuring device.

The coupler is comprised of a broadband 1:1 transformer and a series capacitor. The leakage inductance of the transformer together with the series capacitance essentially creates a series resonant coupling circuit. Transient voltage surge suppressors (TVSSs) are placed on either side of the transformer; with a back-to-back zeners placed on the secondary side and a metal oxide varistor placed on the primary side. The function of the TVSSs is the suppression of voltage spikes that may be large enough to cause damage to the measuring device. Two fully fabricated couplers are shown in Fig. 3-9 below.

The coupler transfer characteristic is shown in Fig. 3-10. From Fig. 3-10, we see that the transfer characteristic is fairly flat between 1MHz to 30MHz, with about 1.60 dB loss as the worst case.

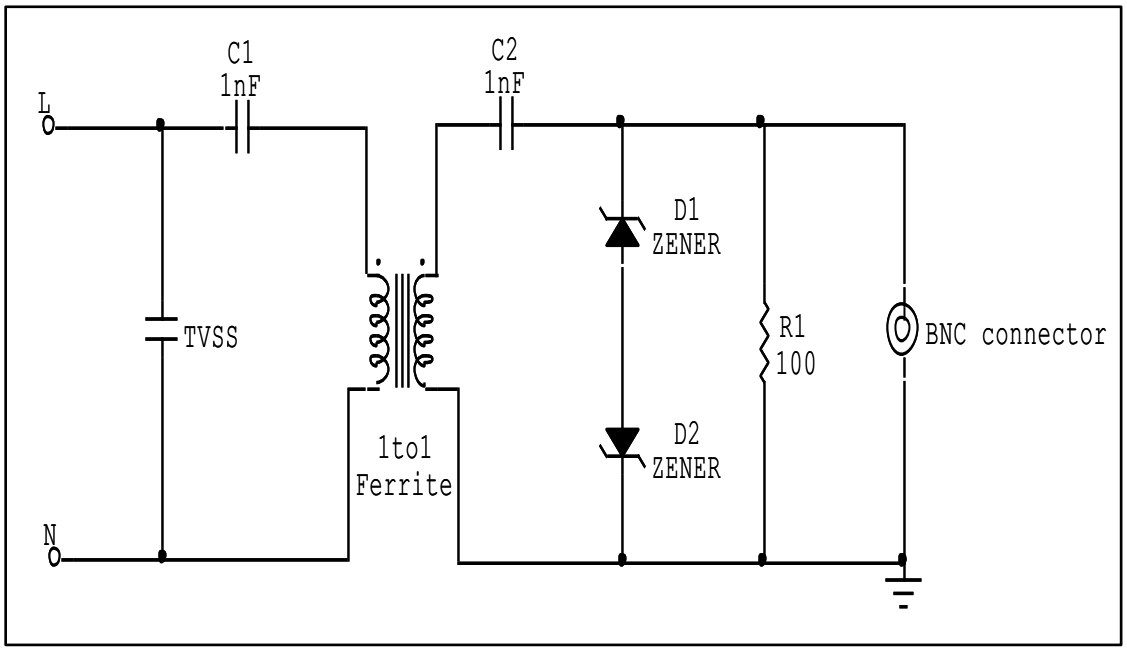

Figure 3- 8: Coupling circuitry schematic

Figure 3- 9: Assembled couplers

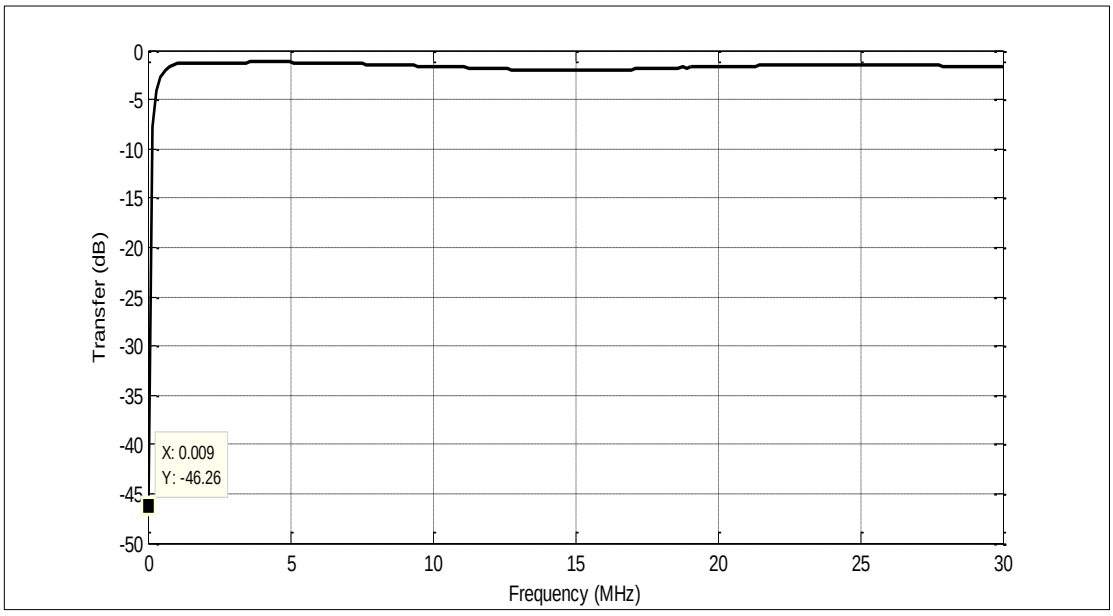

Figure 3- 10: Coupler transfer function

The overall noise measurement set up schematic is shown in Fig. 3-11 below while some actual noise measurement set ups are shown in Figs. 3-12 and 3-13.

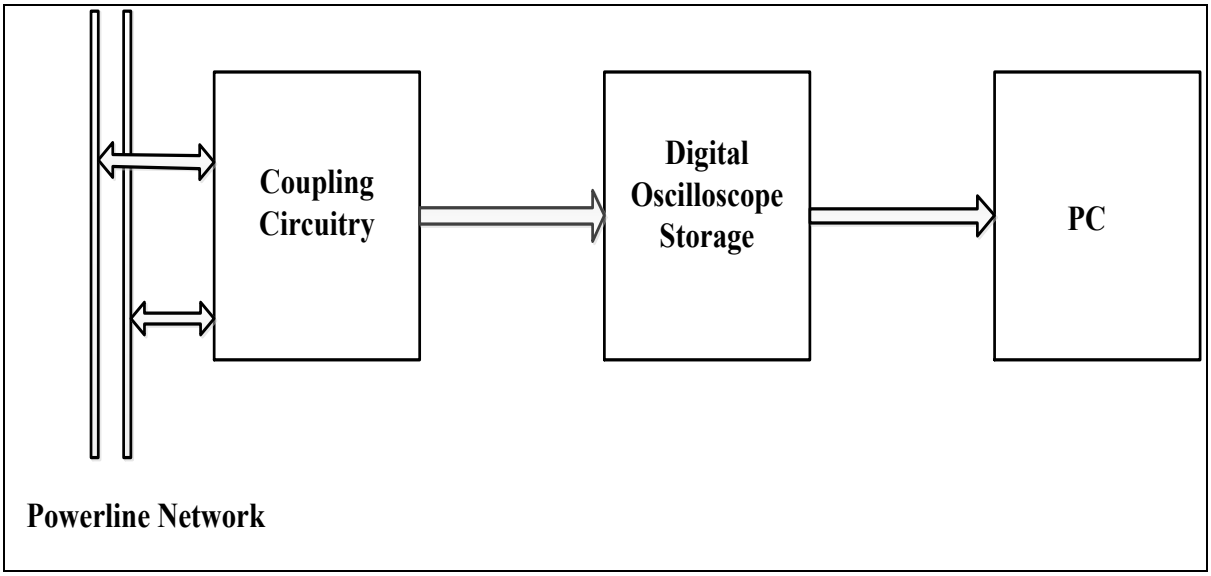

Figure 3- 11: Measurement set up schematic

Figure 3- 12: Frequency domain noise measurement set up in the PLC laboratory

Figure 3- 13: Time domain noise measurement set up in an electronic workshop

3.4 Noise measurement results and discussion

Due to space considerations, only a few measurements are shown. Some of the measured noise in the frequency domain for different rooms are shown in Fig. 3-14 to Fig. 3-16 while Fig. 3-17 to Fig. 3-19 show sample noise measured in the time domain.

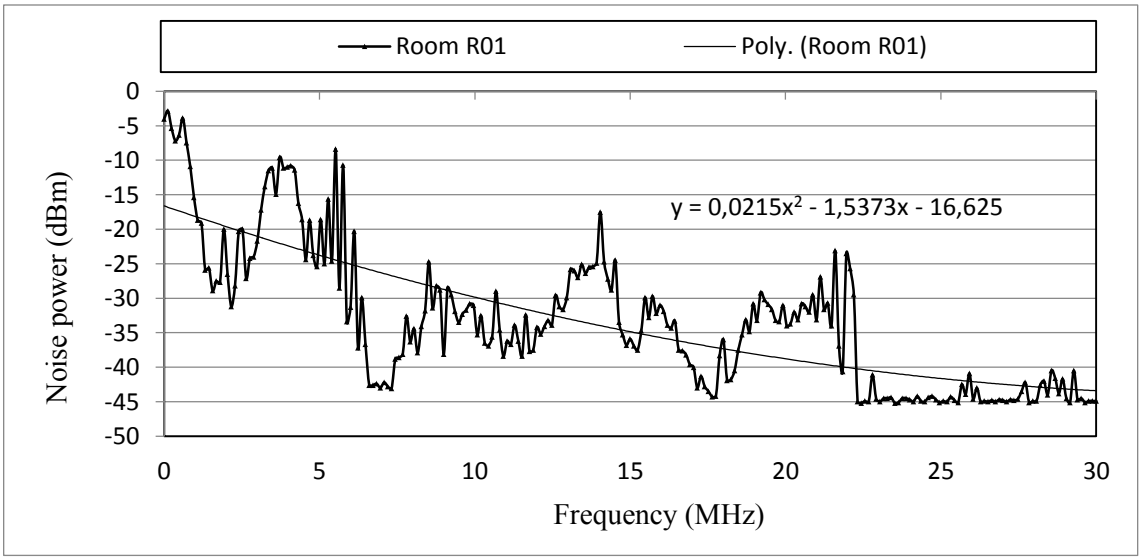

Figure 3- 14: Radio Frequency laboratory (R01) frequency domain noise

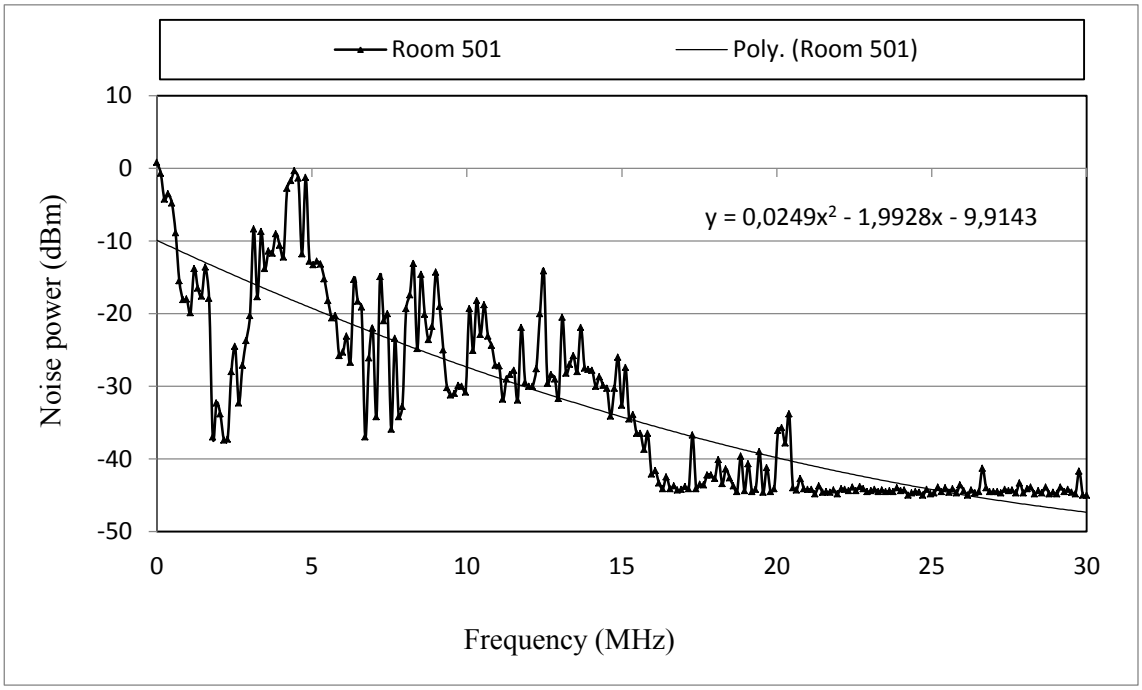

Figure 3- 15: Electromagnetic laboratory (Room 501) frequency domain noise

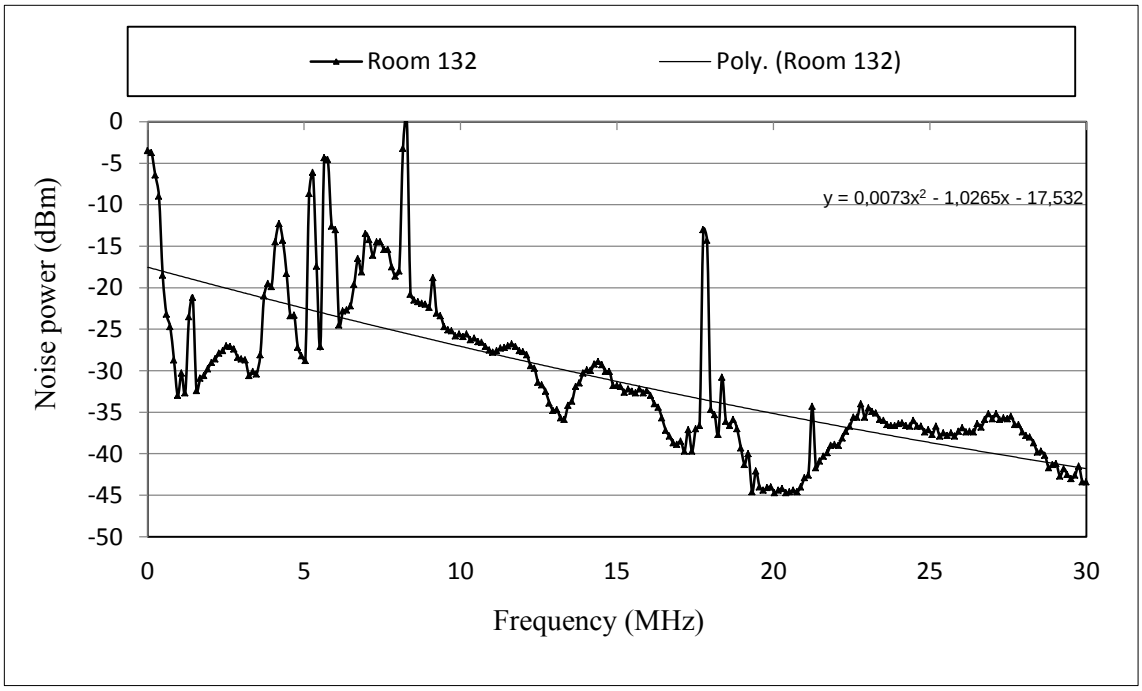

Figure 3- 16: Postgraduates office (Room 132) frequency domain noise

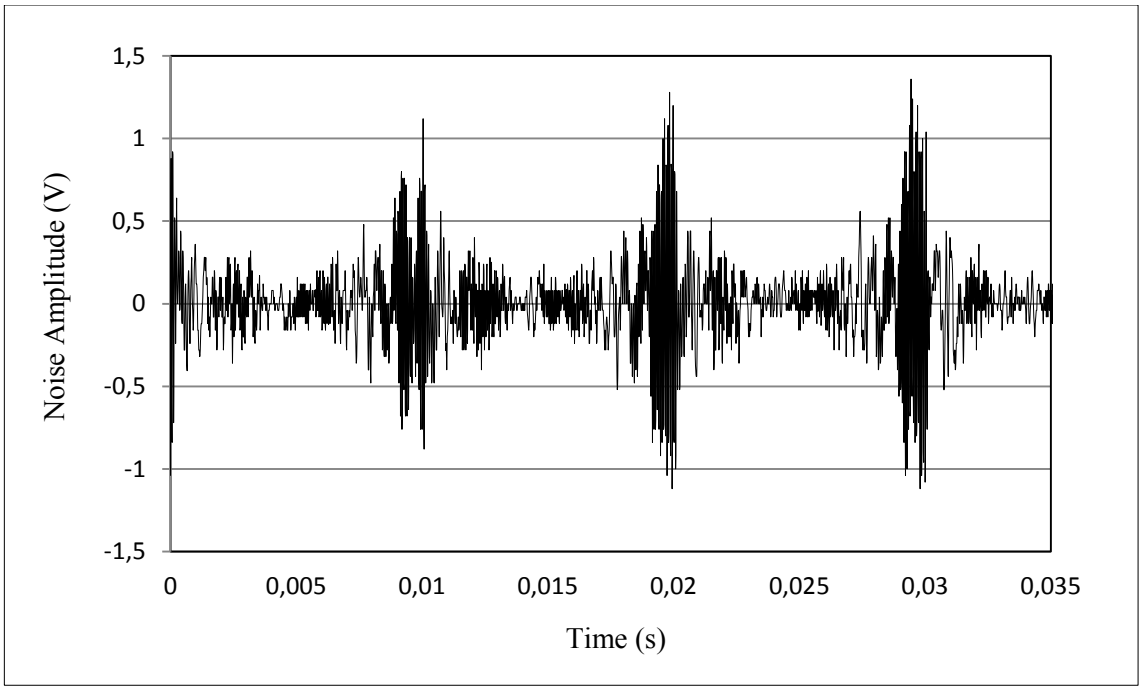

Figure 3- 17: Radio Frequency laboratory (Room R01) time domain noise

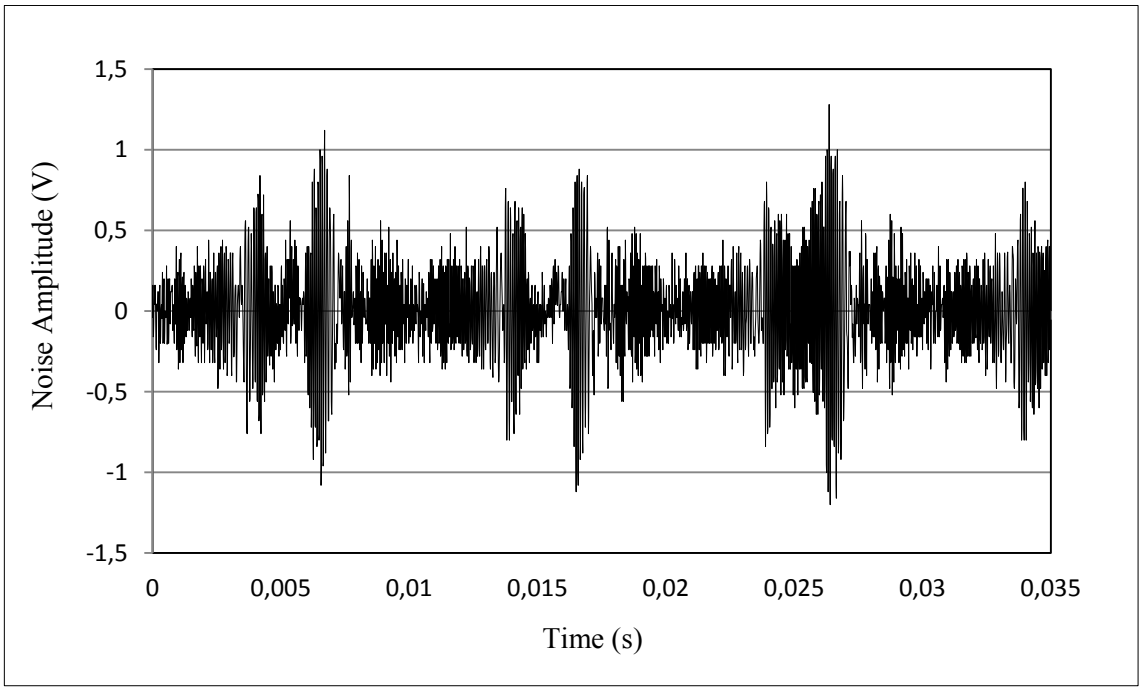

Figure 3- 18: Electromagnetic laboratory time domain noise

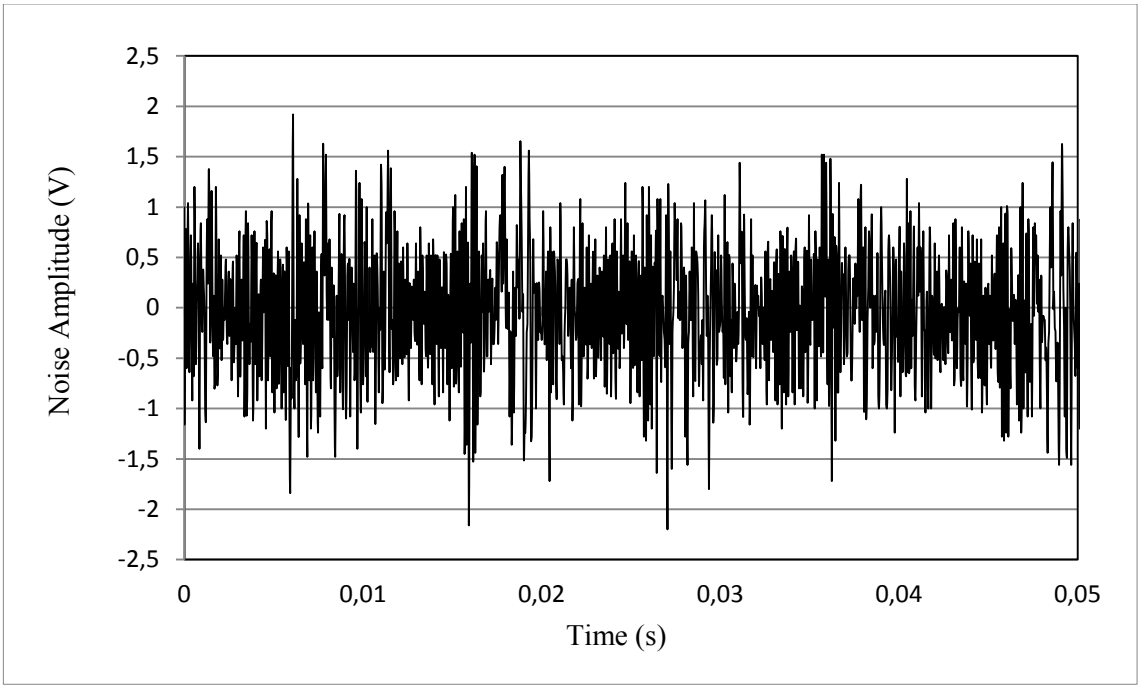

Figure 3- 19: Postgraduates office time domain noise

For the frequency noise, we see that much of the noise is concentrated in the frequencies between 0 MHz and 15 MHz. A possible explanation for this observation could be the fact that most of the narrowband noise tends to be prevalent in the same band, as well as noise from switched mode power supplies, especially below 10 MHz. A simple trend analysis using polynomial fits show that, on average, as we go from 0 MHz towards 30 MHz, the noise decays. Also, the time domain noise measurements show that there are periodic features in the noise, as well as some aspects of randomness. The periodic nature of the time domain noise in some cases is such that its frequency is two times that of the mains power. Additionally, in other cases, the noise components remained periodic only for a few seconds to minutes, while others remained cyclic and stationary for long periods of observation.

From the sample noise measurements shown above, we observe that noise in power lines is complex and cannot be modelled and characterized using pure mathematical derivations. This is the reason why almost all existing noise models are derived from empirical measurements. In order to capture the random concentration of the noise distribution across different frequency bands in the frequency domain or the voltage level variation concentration (which is an indicator of the impulse power), statistical tools need to be employed to model and characterize the noise into certain probability density functions (pdfs) and cumulative frequency distributions (cdfs). This is crucial because, with the corresponding parameters derived from the noise measurements for the pdf or cdf plot, for example, the mean, variance and standard deviation as well as the associated errors, we can then give a full statistical description of the overall noise characteristics, as seen in the models discussed in Chapter two above. All the models presented in Chapter two are rigid and therefore we

introduce a flexible modelling tool for the noise measured in this study, based on nonparametric kernel density estimators in the next chapter.

3.5 Chapter summary and conclusion

In this chapter, a detailed description of the measurement equipment used in our noise measurement campaign has been presented. An outline of the procedures used for the measurements in this thesis has also been presented. Measurements form a big part of the study in this thesis and in many other research works in PLC. This is because, it is only through measurements that the actual channel characteristics can be properly understood, from which analysis, modelling and characterization, as well as the synthesis of the results obtained can be done. This is necessary for the derivation of the overall phenomena trends, and to enable the researcher to come up with a conclusive deduction regarding the variables studied; which is the focus of the next three chapters in this thesis. The coupling scheme used for the noise measurements has also been described. A pictorial representation of some of the rooms where the measurements were done has also been presented. It is important to note that the pictures are for demonstration only and do not represent the actual settings under which the noise measurements were done. A decay of the noise in the frequency domain has been observed as we go from 0 MHz towards 30MHz. Also, periodicity and as well as randomness is observed in the time domain noise measurements. It is important to mention here that only a few noise measurements are presented in the results due to space constraints. Overall, we observe that noise in power lines is complex and cannot therefore be studied through mere analytical derivations; hence the need for actual noise measurements in live power networks. In the next chapter, nonparametric modelling of the noise measurements obtained in this chapter is presented.

Chapter references

[1] http://www.rohde-schwarz.co.za/en/product/fs300_fs315-productstartpage_63493-9010.html, last accessed on 2nd November, 2015.

[2]https://physics.ucsd.edu/neurophysics/Manuals/Tektronix/TDS%201000B%20and%20TDS%202000B%20Manual.pdf, last accessed on 2nd November, 2015.

[3] http://www.testequipmentdepot.com/tektronix/oscilloscope, last accessed on 2nd November, 2015.

[4] ww.upc.edu/sct/documents_equipament/d_109_id-533.pdf, last accessed on 2nd November, 2015.

Chapter Four

4. Nonparametric Modelling and Characterization of Indoor Low Voltage Power Line Noise for PLC Applications

4.1 Introduction

Most of the published work on impulsive noise and its models is based on parametric modelling techniques. Even though these techniques are good in that they represent the noise using some parameters like the variance and mean, they have a big shortcoming in that their mathematical expressions that determine the underlying distribution are fixed. The fixed form of many parametric distributions therefore introduces rigidity in the form that the noise probability density function and cumulative distribution function may take. Thus, fitting measured noise data using parametric distributions may result in an overestimation of the actual data structure that may lead to some of the salient features of the noise distribution being missed. To overcome the rigidity associated with parametric estimators, the use of nonparametric techniques is necessary. In this chapter, a novel application of nonparametric kernel density estimators to develop reference models of the power line noise measured in low voltage indoor power networks in both time and frequency domain is presented. Nonparametric kernel density techniques estimate the underlying distribution of the noise directly from the measured data, without imposing any restrictions or making any assumptions as to the particular form of the data structure. As such, no fixed parameters are used to model the data, and therefore the data is modelled as it is. The kernel density method is the most efficient and popular nonparametric estimator. In fact almost all nonparametric algorithms are asymptotically kernel methods. It is continuous and overcomes the challenges of the other popular but primitive nonparametric estimator; the histogram. This estimator is very good going by the models developed and the validation results obtained. The objectives of this chapter are:

1. To present the definitions and features of nonparametric kernel density estimators as a stochastic and probabilistic modeling tool.
2. To proof that the said estimator is actually very suitable for modeling of power line noise, more so as a reference (baseline) modeling technique.

3. To introduce this wonderful technique to the PLC research community and therefore stimulate further research in line with the findings in this chapter as well as exploration of other nonparametric estimators.

4.2 PLC impulsive noise models

This subsection revisits PLC impulsive noise models briefly. As earlier highlighted in Chapter two , noise in PLC systems falls into three main categories: impulsive noise, coloured background noise and narrowband interference. Asynchronous impulsive noise that is periodic to the frequency of the mains power, as well as narrowband and coloured background noises usually tend to remain stationary for periods that range between seconds and minutes or even hours, and therefore are generally classified as background noise. However, impulsive noise that is asynchronous with the mains frequency, and synchronous impulsive noise that is periodic with the mains frequency are time variant from microseconds to milliseconds. The spectral density of the noise power rises significantly during impulsive events and may result in bit or burst errors during transmission of data [1-6].

Since narrowband interference is mainly ingressed into the network, its effect on the system performance is not as severe as compared to the other two. On the other hand, background noise is stationary and can be modelled as a classical Gaussian process. Additionally, impulsive noise; in all its three sub-classes poses the greatest threat to the performance of the PLC channel. This type of noise has been modelled using different parametric models; but, the most commonly used ones are the two-term mixture Gaussian model and the Middleton's class-A impulsive noise model [5-13]. In two recent publications by Shongwe *et al.* [14, 15], a comprehensive study/survey of impulsive noise and its models was presented.

Even though the two-term mixture Gaussian model is simple and is used frequently in the analysis of PLC systems [16-18], it is deficient in that it does not provide a very accurate representation of the true impulse noise. Another parametric model, the Middleton's class-A impulsive noise model, which is also widely used and counters the shortcomings of this model, is discussed next.

This is a rather simple model based on a Poisson-Gaussian process and incorporates both background and impulsive noise, and was first suggested in [19]. Due to its slightly higher accuracy in the modelling and characterization of the real impulsive noise, this model has been employed by several authors in their analysis of the performance of impulsive systems [20-22]. However, this

model was not deisgned for PLC systems and also does not tell us whether or not the noise is impulsive in the time domain.

Another very flexible model that has recently featured in the study of impulsive inference/noise is the alpha stable distribution. This distribution is characterized by tails that are much fatter/longer than those of the Gaussian distribution, a characteristic synonymous with impulsive processes, like PLC noise. It is also more flexible than the other two parametric noise models described in Chapter two. This distribution is able to capture the impulsive nature of the noise and can model very extreme cases; ranging from very impulsive noise cases to pure background noise since the Gaussian distribution is one of the limiting cases [4, 13, 23, 24]. This distribution is defined by its characteristic function $\emptyset(t)$, given by [4, 13, 23, 24]:

$$\emptyset(t) = exp\{j\delta t - \gamma^{\alpha}|t|^{\alpha}[1 + j\beta sign(t)\omega(t,\alpha)]\} \tag{4.1}$$

Where,

$$\omega\,(t,\alpha) = \begin{cases} tan\dfrac{\pi\alpha}{2}, & \alpha \neq 1 \\ \dfrac{2}{\pi}\log|t|\,, & \alpha = 1 \end{cases} \tag{4.2}$$

$$sign(t) = \begin{cases} 1 & for\ t > 0 \\ 0 & for\ \ t = 0 \\ -1 & for\ t < 0 \end{cases} \tag{4.3}$$

And;

$$-\infty < \delta < \infty, \gamma > 0, 0 < \alpha \leq 2, -1 \leq \beta \leq 1 \tag{4.4}$$

α is the characteristic index or exponent, δ is the location parameter, γ is the dispersion or scale parameter and β is the symmetry parameter.

The impulsive noise models discussed above, and virtually all literature on noise modelling in PLC systems is based on parametric methods. A few parameters, expressed in fixed parametric mathematical equations are used in all the cases to describe the noise distribution. These parametric

methods therefore introduce rigidity in the particular structure that the noise distribution may take. Thus, if these models are fitted straight to some measured noise data, as seen in [10] for example, the resultant models are just approximations to the measurements and may actually miss out on some of the salient features of the measured data distribution in most cases. Nonparametric density estimators are able to overcome the rigidity associated with parametric methods. To this end, in this chapter, we introduce an alternative reference power line noise modelling framework that is based on nonparametric kernel density estimation techniques. The density estimate is obtained straight from the data itself and therefore "hugs" the measured data almost 100%. Thus, these models are seen as reference models of the measured noise distribution, and give an actual feel of any data distribution. Also, kernel density methods are the most accurate and widely used nonparametric estimators. This modelling framework is applied to measured noise characteristics and found to produce very good baseline results.

4.3 Nonparametric density estimation

Existing PLC noise models, including the ones discussed in Subsection 4.2 are based on parametric statistical distributions. This is to say that the estimation of the probability density function (pdf) that defines a set of noise data is done via a fixed set of parameters, which introduces rigidity in the particular shape that a data structure can take. As such, these fixed parameters mean that a data set structure can only take an approximate parametric distribution fit. The function $f(x)$ is assumed to belong to some distributions that are parametric like Gamma, Rayleigh, Lognormal, Erlang, Gaussian and Exponential, among others. With the parametric data modelling technique, the estimation of the parameters that relate the data to a particular distribution is usually the main task. Some error analysis to validate the assumption is then done. For instance, if the Gaussian distribution is used to model some data set, then the estimator would be given by:

$$f(x) = \frac{1}{\sqrt{2\pi\sigma^2}} e^{(x-\mu)\hat{}2/2\sigma^2} \quad , \quad x \epsilon R \tag{4.5}$$

where, $\mu = \frac{1}{n}\sum_{i=1}^{n} x_i$ and $\sigma^2 = \frac{1}{n}\sum_{i=1}^{n}(x_i - \mu)^2$. Parametric data modelling is fine as long as the distribution that is assumed to fit the data is correct or not seriously wrong at the very least. This method is quite easy to apply in many cases, and gives rise to relatively stable estimates. But, the fixed forms of the parametric distributions render them rigid, and this comes across as the biggest disadvantage of this data modelling technique. The data can only be trained to take on a particular structure whose final outcome is fixed. This would imply that in most of the cases, key aspects of

the data structure like skewness, actual tail probabilities, peakiness and bimodality may be missed out and therefore a misinterpretation of the underlying data distribution occurs. For instance, the Gaussian estimator above gives rise to models that are symmetrical and dome-shaped, and therefore this renders it inappropriate for modelling data that is bimodal, heavily tailed, and/or skewed [8, 25].

To address the rigidity concerns associated with parametric distributions, nonparametric methods are used. These methods estimate the probability density straight from the raw data without any prior assumptions as to the characteristic structure for the underlying distribution. As such, no fixed parameters are used to model the data, and therefore the data is modelled as it is. The histogram was the only known nonparametric density estimation technique until the 1950s, when meaningful progress was made in both spectral density estimation and density estimation. However, the histogram suffers from serious shortcomings that include the sharp transitions (discontinuities) between the bins, which results in a step-like data structure that is usually difficult to interpret, as well as an exponential growth in bin numbers with the number of dimensions, and that the data structure also depends on the bins' start and end points. For many practical cases, these shortcomings render histograms useless, and they are therefore only useful in quick visualizations of data in both one and two dimensions.

On the other hand, smooth nonparametric density estimation methods like kernel density estimators overcome the drawbacks associated with the histogram. One of the earliest papers on kernel density estimators is by Rosenblatt in 1956 [26]. The kernel density estimator is motivated as an averaged shifted histogram limiting case. Some of the techniques that can be applied in demonstrating its superior qualities, as well as providing a deeper understanding of it include numerical analysis and finite differences, smoothing by convolution and orthogonal series approximations. In fact almost all nonparametric algorithms are asymptotically kernel methods, a fact that was clearly demonstrated by Walter and Blum [27] and later proven in a rigorous way by Terrell and Scott [28]. The kernel density estimator for a random variable n is given as [28-30]:

$$f(n) = \frac{1}{kh}\sum_{i=1}^{k} K\left(\frac{n - X_i}{h}\right) = \frac{1}{k}\sum_{i=1}^{k} K_h(n - X_i) \tag{4.6}$$

where k is the number of data points, h is the smoothing parameter, also referred to as the bandwidth or window width, X_i is the i^{th} data point and $K(\cdot)$ is the kernel function. The kernel

function is symmetric in most cases which means that $K(u) = K(-u)$. A second order kernel function is defined by the following properties [28-30]:

$$\int_{-\infty}^{+\infty} K(u)du = 1 \tag{4.7}$$

$$\int_{-\infty}^{+\infty} uK(u)du = 0 \tag{4.8}$$

$$\int_{-\infty}^{+\infty} u^2K(u)du > 0 \tag{4.9}$$

From Equations (4.8) and (4.9), we conclude that the kernel function has a zero first order moment and a finite second one respectively. Equation (4.7) on the hand shows that the kernel function is a true pdf. The kernel density estimate, as seen in Equation (4.6) is controlled by two main factors, the kernel function and the smoothing parameter. Optimal selection of the bandwidth is the most important aspect of modelling using kernel density estimators. A very small value of the smoothing parameter results in a very peaky (spiky) and spurious under-smoothed density estimate that is hard to interpret while a very large value of the same parameter results in over-smoothed densities that would mask the data structure. A simple illustration on how the density estimation is carried out in the kernel technique is shown in Fig. 4-1 below. From this figure, as well as from Equation (4.6), we conclude that the density estimate is a summation of "bumps" centred on every data point in the neighbourhood of the point of estimation. The bump's shape is determined by the kernel function while the value of the bandwidth determines how spread (wide) they are.

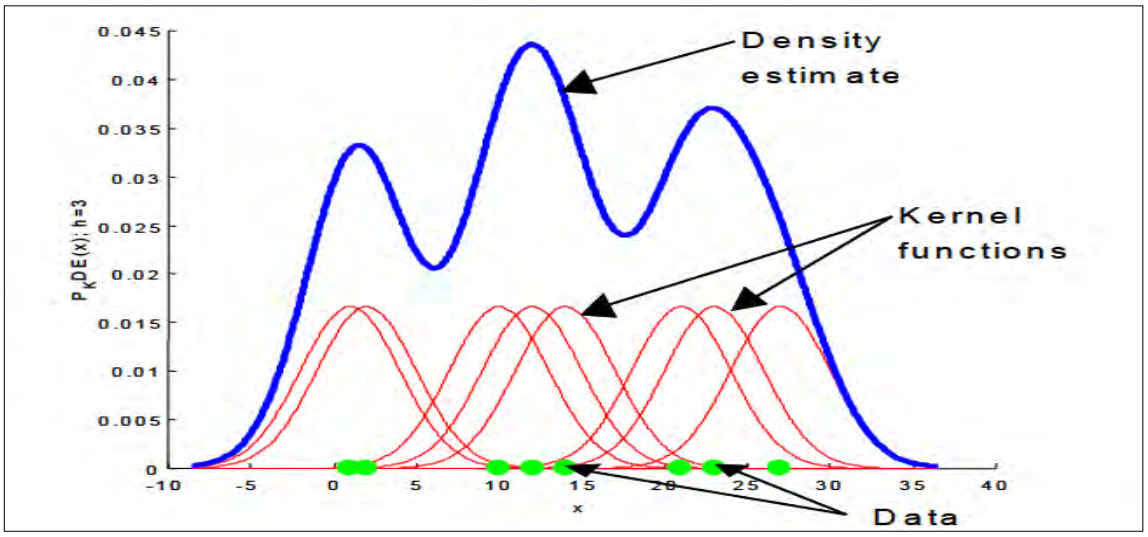

Figure 4- 1: Kernel density estimation illustration

There are several techniques that are used in the determination of the optimal value of the smoothing parameter. These include automatic techniques like plug-in and classical methods, and the reference to a distribution methodology. Plug-in methods refers to those ones that find a pilot estimate of the density using a pilot value of the smoothing parameter then use the estimated density to determine the error. Classical methods are basically extensions of methods used in parametric estimations and they include: least squares cross-validation, biased cross-validation, likelihood cross-validation and indirect cross-validation. Even though these optimal smoothing parameter selection methods have been explored by many authors, none is considered the best in every situation [29]. There are many second order and higher order kernels available in literature but some of the common second order kernels are shown in Table 4.1 below.

4.3.1 Bandwidth selection for kernel density estimators

Kernel density estimation effectiveness as a modelling tool is dependent on the choice of the smoothing parameter more than even the choice of the kernel function itself. The value of the smoothing parameter determines the biasness and the variance of the estimated model.

Table 4. 1: Common kernel functions

Kernel function	**Mathematical expression, $K(u)$**
Epanechnikov	$K(u) = \begin{cases} \frac{3}{4\sqrt{5}}\left(1 - \frac{1}{5}u^2\right), -\sqrt{5} \leq u \leq \sqrt{5} \\ 0, elsewhere \end{cases}$
Triangular	$K(u) = \begin{cases} (1 - \lvert u \rvert), -1 \leq u \leq 1 \\ 0, elsewhere \end{cases}$
Gaussian	$K(u) = \frac{1}{\sqrt{2\pi}} e^{-\left(\frac{u^2}{2}\right)}, -\infty < u < \infty$
Rectangular	$K(u) = \begin{cases} \frac{1}{2}, -1 \leq u \leq 1 \\ 0, elsewhere \end{cases}$

If the value of the chosen smoothing parameter is very small compared to the optimal one, the resulting model is usually under-smoothed and very spiky, and therefore difficult to interpret. On

the other hand, high values of the smoothing parameter results in density estimates that are over-smoothed, and therefore obscure the data structure. In practical applications, an optimal choice of the smoothing parameter is done based on the kernel function, number of data samples, as well as their variance. The common method used to determine a "rough estimate" of the optimal smoothing parameter is Silverman's rule of thumb [31, 32] which assumes that the function *f (n)* is one of the standard distributions. For the Normal distribution with mean μ and variance σ^2, the roughness of the kernel function *K(u)*, $R(f'')$, is given by [33]:

$$R(f'') = \frac{3}{8\sigma^5\sqrt{\pi}} \tag{4.10}$$

If the kernel density estimator and the form of *f (n)* are known, the optimal bandwidth can be chosen. For the Gaussian kernel case, the respective values of *R(K)* and $\mu_2^2(K)$ are calculated to be $\left(2\sqrt{\pi}\right)^{-1}$ and 1 respectively, and the optimal bandwidth is given by [25, 31]:

$$h_{opt} = \sigma(4/3k)^{\frac{1}{5}} \tag{4.11}$$

where σ is the standard deviation. The value of h_{opt} is quickly calculated by estimating σ from the observed data.

If the size of the sample data is small and the data density is close to the normal distribution, another bandwidth expression is used [34]:

$$h_{opt} = 0.79(\hat{q}_3 - \hat{q}_1)k^{\frac{-1}{5}} \tag{4.12}$$

where $\hat{q}_3$ and $\hat{q}_1$ are respectively the third quartile and the first quartile of the sample data. When the data density is not close to the normal distribution, the following expression is used:

$$h_{opt} = 0.9\min\left(\hat{\sigma}, \frac{\hat{q}_3 - \hat{q}_1}{1.349}\right)k^{\frac{-1}{5}} \tag{4.13}$$

where $\hat{\sigma}$ is the standard deviation of the sample data.

All in all, extensive modelling with kernel density estimators shows that there is no single plug-in formula that is applicable in all situations. Usually, simple plug-in formulas are available for the "first rough estimate" of the smoothing parameter from the data set, from which other validation and goodness of fit tests can be applied to obtain the optimal model. To this end, the error between the kernel model and the measured data can be minimized with respect to the kernel under

consideration. Silverman showed that the optimal kernel is Epanechnikov kernel. Thus, the efficiency of any kernel is estimated by comparing it to that of the Epanechnikov kernel. But, in our modeling with kernel density estimators, we found out that the results obtained are almost the same as long as the optimization of all the models is carried out appropriately. The optimal bandwidths and efficiencies of some common kernel functions are given in Table 4.2. The value of sample variance σ is estimated from the sample data with k observations.

Table 4. 2: Common kernel efficiencies and bandwiths plug-in formulae

Kernel	**Efficiency (%)**	**Optimal bandwidth**
Epanechnikov	100	$\frac{2.34\sigma}{k^{\frac{1}{5}}}$
Triangular	98.6	$\frac{2.58\sigma}{k^{\frac{1}{5}}}$
Gaussian	95.1	$\frac{1.06\sigma}{k^{\frac{1}{5}}}$
Rectangular	93	$\frac{1.84\sigma}{k^{\frac{1}{5}}}$

4.4 Nonparametric low voltage power line noise modeling

As can be seen in noise results presented in Chapter Three, noise in power lines is complex and cannot be modelled and characterized using pure mathematical derivations. This is the reason why almost all existing noise models are derived from measurements. In order to capture the random concentration of the noise distribution across different frequency bands in the frequency domain or the voltage level variation concentration (which is an indicator of the impulse power), statistical tools need to be employed to model and characterize the noise into certain probability density functions (pdfs) and cumulative frequency distributions (cdfs). This is crucial because, with the corresponding parameters derived from the noise measurements for the pdf or cdf plot, we can then give a full statistical description of the overall noise characteristics. As pointed out earlier, the models presented in Subsection 4.2 are rigid and hence are unsuitable for the reference modelling (initial fitting) of power line noise. In this research work therefore, we introduce a flexible

modelling tool for the power line noise measured in this study, based on the novel application of nonparametric kernel density estimators for the modelling of PLC noise.

The four kernels shown in Table 4.1 above are used in the derivation of simple nonparametric models that expresses the noise characteristics in form of some tractable mathematical forms. These models are optimized through an error-based optimization procedure. The determination of the optimum kernel models is based on the optimal choice of the bandwidth. The model optimization procedure developed in this study follows an iterative methodology that is described below:

1. From the bandwidth plug-in formula for each kernel as shown in Table 1, determine the first rough estimate of the bandwidth.
2. Derive the kernel models for each kernel and compute the error between the measured and modelled pdf.
3. Choose a slightly larger or smaller value of the bandwidth and repeat step 2.
4. Compare the errors calculated in step 2 and 3, and choose a smaller or larger value of the bandwidth.
5. Repeat step 2 to 4 until the error computed is minimum, determined when the otherwise diminishing error starts increasing.
6. The bandwidth that gives the minimum error is the optimal value.

Different global measures of accuracy can be used in the optimization of the kernel density estimates, but in this study we chose the mean integral square error (MISE), which is by far the most popular error criteria used in ensuring accurate results with kernel modelling.

From the basic definition of the MISE, we have:

$$MISE = E[\int_{-\infty}^{\infty} [f(n) - f^*(n)]^2 \, dk] \tag{4.14}$$

Where $f(n)$ is the measured pdf values and $f^*(n)$ is the kernel model values. The asymptotic MISE (AMISE) is given by:

$$MISE(f) = \frac{R(K)}{kh} + \frac{1}{4} h^4 \mu_2^2 \, R(f'') \tag{4.15}$$

where k is the size of the sample data, $R(K) = \int K^2(u)\,du$ is the roughness of *K(u)*, $\mu_2^2(K) = \int\left(u^2K(u)\right)^2\,du$ is the second moment squared of the pdf defined by the kernel *K(u)*, and $R(f'') = \int (f''(n))^2\,dn$ is a roughness measure. A bias-variance trade-off ensures that the MISE obtained is minimum. Assuming the second derivative of the density is square integrable and absolutely continuous, then by a Taylor series expansion of $f(n - yh)$ about n we obtain:

$$f(n - yh) = f(n) - hyf'(n) + \frac{1}{2}h^2y^2f''(n) + o(h^2) \tag{4.16}$$

From which, the bias of the density estimate is:

$$Bias\left(f(n)\right) = \frac{h^2}{2}f''(n)\mu_2(K) + O(h^2) \tag{4.17}$$

Also, the estimated function variance is given by:

$$Var\left(f(n)\right) = \frac{1}{kh}\int K^2(y)\,f(n - yh)dy - \frac{1}{k}\left(E\left(f(n)\right)\right)^2 \tag{4.18a}$$

$$= \frac{1}{kh}\int K^2(y)\,\{f(n) + O(1)\}dy = \frac{1}{k}\{f(n) + O(1)\}^2 \tag{4.18b}$$

$$= \frac{1}{kh}K^2(y)dyf(n) + O\left(\frac{1}{kh}\right) \tag{4.18c}$$

$$= \frac{1}{kh}R(K)f(n) + O\left(\frac{1}{kh}\right) \tag{4.18d}$$

Decreasing the bias leads to a very noisy estimate (large variance) while decreasing the variance leads to over-smoothed estimates (large bias). The variance-bias trade-off ensures consistency in the density estimation.

The time domain and frequency domain results obtained for the four kernels from the above procedure are shown in Table 4.3. In this table, we demonstrate the three special classes in power line noise modelling using kernel density estimation, namely: under-smoothing, optimal smoothing and over-smoothing. The first value of the bandwidth for each kernel is an under-smoothed case while the second is the optimal value, with last one representing an over-smoothed one. The errors

for each value of the smoothing parameter are shown; where we observe that the optimal bandwidth value gives the minimum error.

Table 4. 3: Power line noise kernel modelling errors

Kernel	**Time domain**		**Frequency domain**	
	h	MISE	h	MISE
Triangular	0.03	0.0083	0.02	0.0014
	0.21	0.0058	0.481	0.0002
	0.9	0.0077	1.4	0.0008
Gaussian	0.05	0.0079	0.04	0.0013
	0.163	0.0056	0.423	0.0001
	1.0	0.0078	2.0	0.0011
Epanechnikov	0.03	0.0081	0.06	0.0012
	0.1841	0.0052	0.445	0.0002
	1.3	0.0078	1.7	0.0010
Rectangular	0.05	0.0084	0.10	0.0008
	0.189	0.0057	0.512	0.0001
	1.0	0.0076	1.2	0.0015

The minimum error for the optimal time domain models is obtained for the Epanechnikov kernel while the same is obtained for both the Gaussian and Rectangular kernels respectively for the frequency domain. This means that the kernels are equally efficient as long as the optimization is done right. Also we see that the error values are quite close across the four kernel used in the modelling, from which we conclude that the choice of the optimal value of the bandwidth has more weight on the resulting density estimate than the kernel function itself.

The time domain noise kernel model plots are shown in Figs. 4-2 to 4-5, while the frequency domain noise kernel models are shown in Figs. 4-6 to 4-9. From these noise models, we see that the time domain models are quite symmetrical (bell-shaped) while the frequency domain ones are clearly not. The frequency domain models actually exhibit long tails, with the tail probabilities representing the probability of occurrence of the impulsive noise. We see that much of the noise spectrum density is concentrated between -49.7 dBm and -45.5 dBm. This noise density band essentially represents the background noise density in this study. It also points to the fact that the background noise has a much higher probability of occurrence than impulsive noise, by comparing this noise band with the tails of the models. We note here that the measured noise is modelled as it is, which means that no effort has been made to separate the noise components.

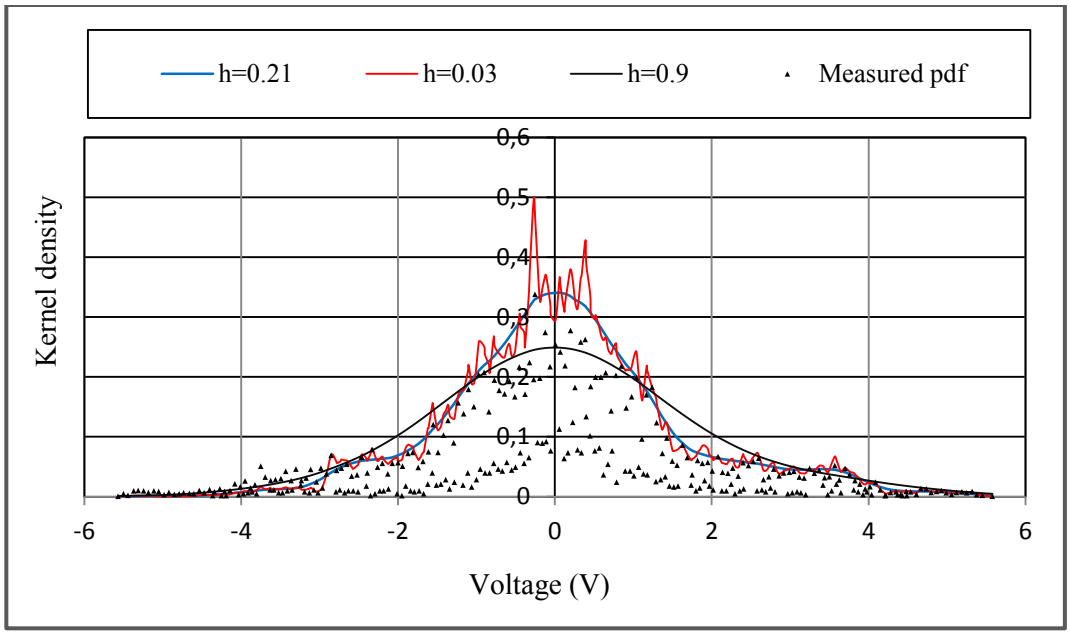

Figure 4- 2: Triangular kernel time domain models

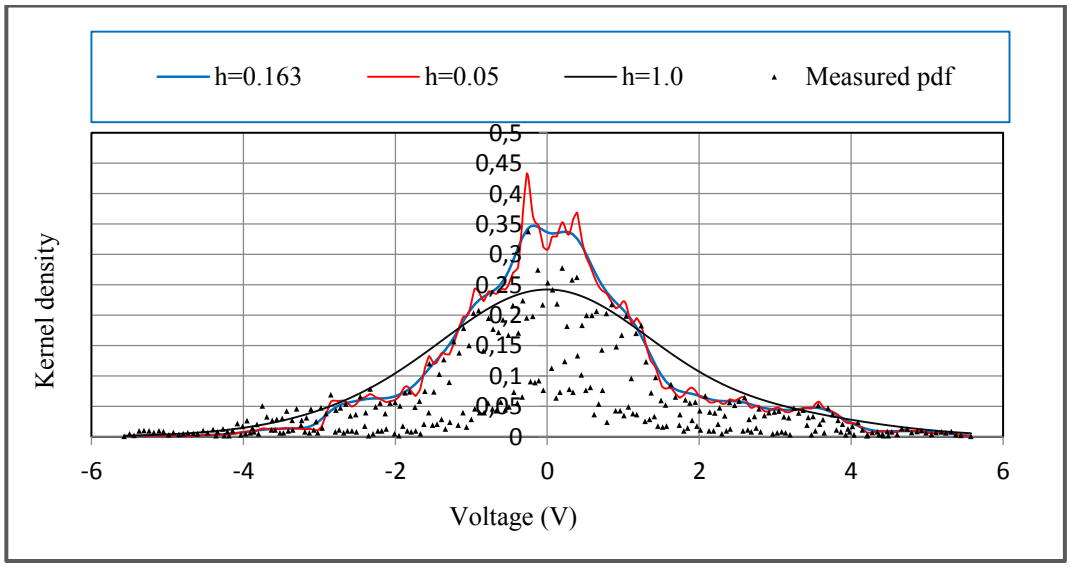

Figure 4- 3: Gaussian kernel time domain models

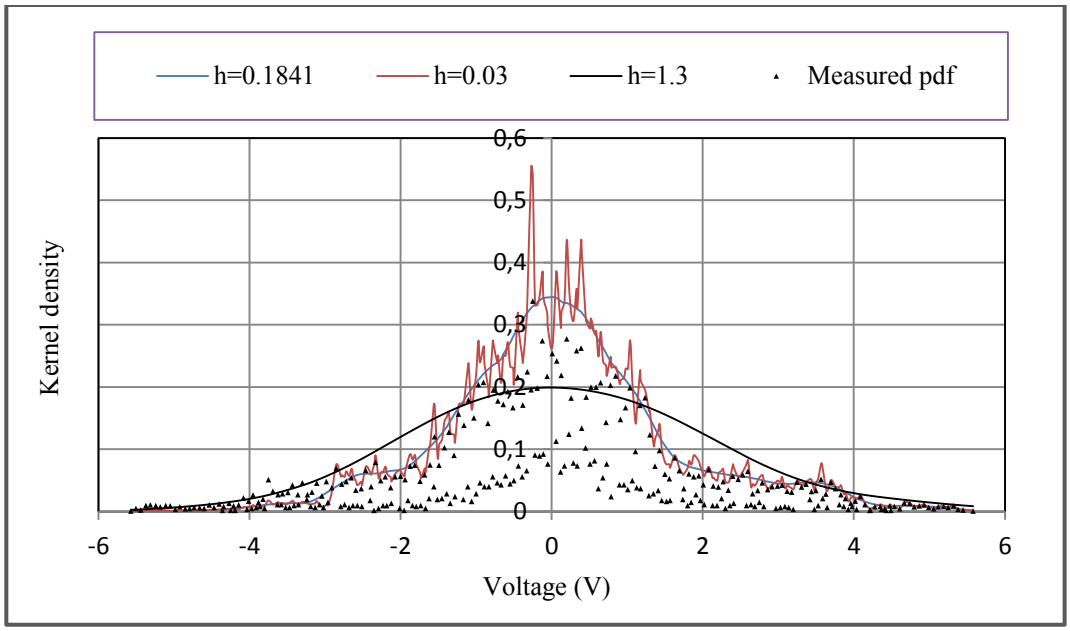

Figure 4- 4: Epanechnikov kernel time domain noise models

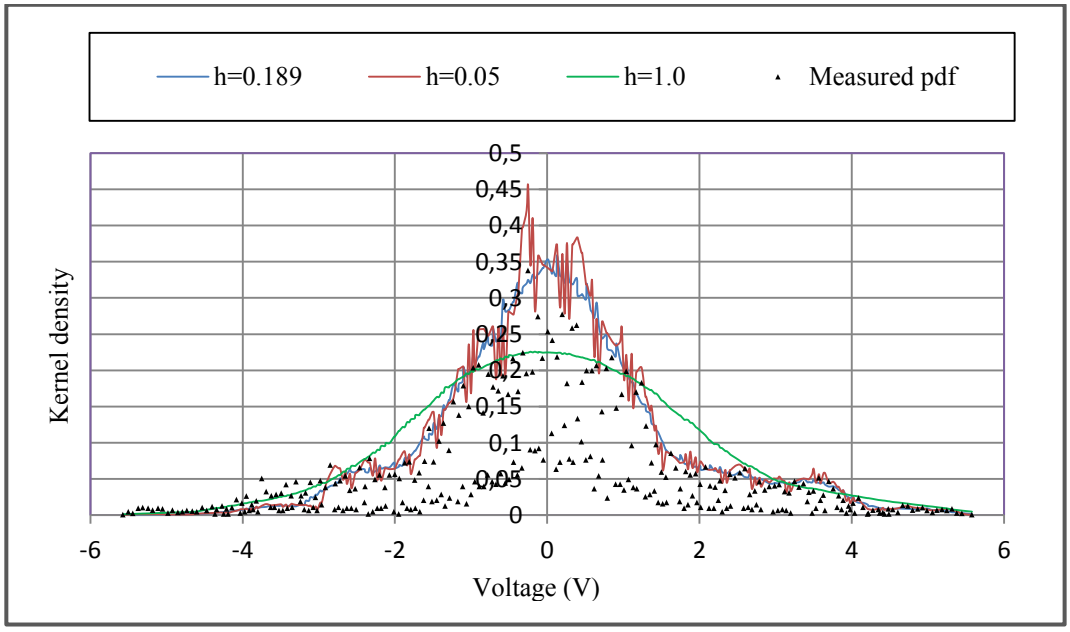

Figure 4- 5: Rectangular kernel time domain noise models

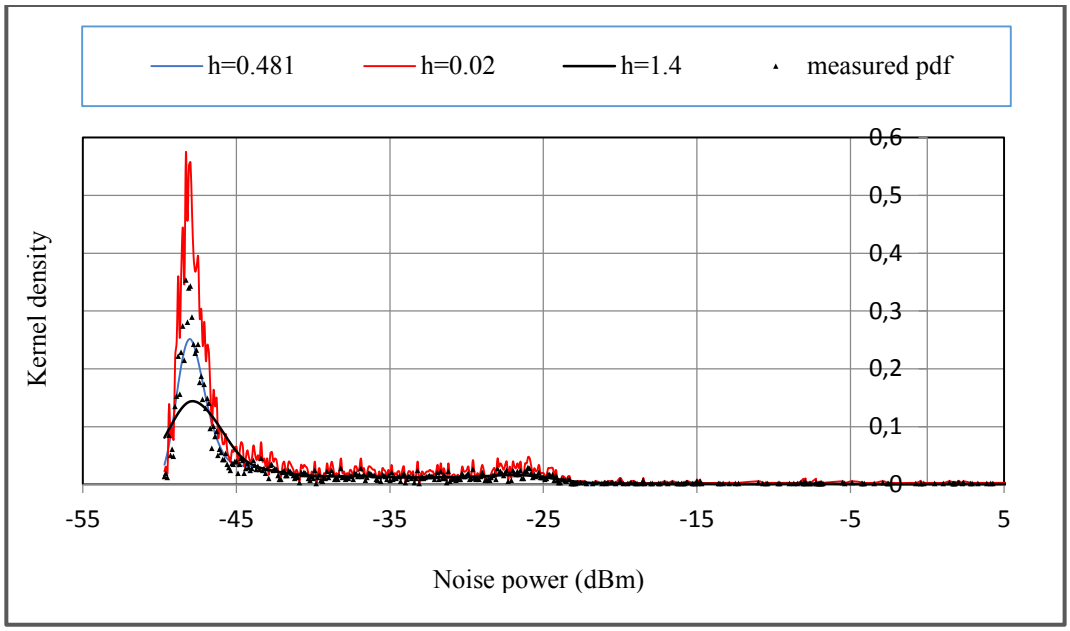

Figure 4- 6: Triangular kernel frequency domain noise models

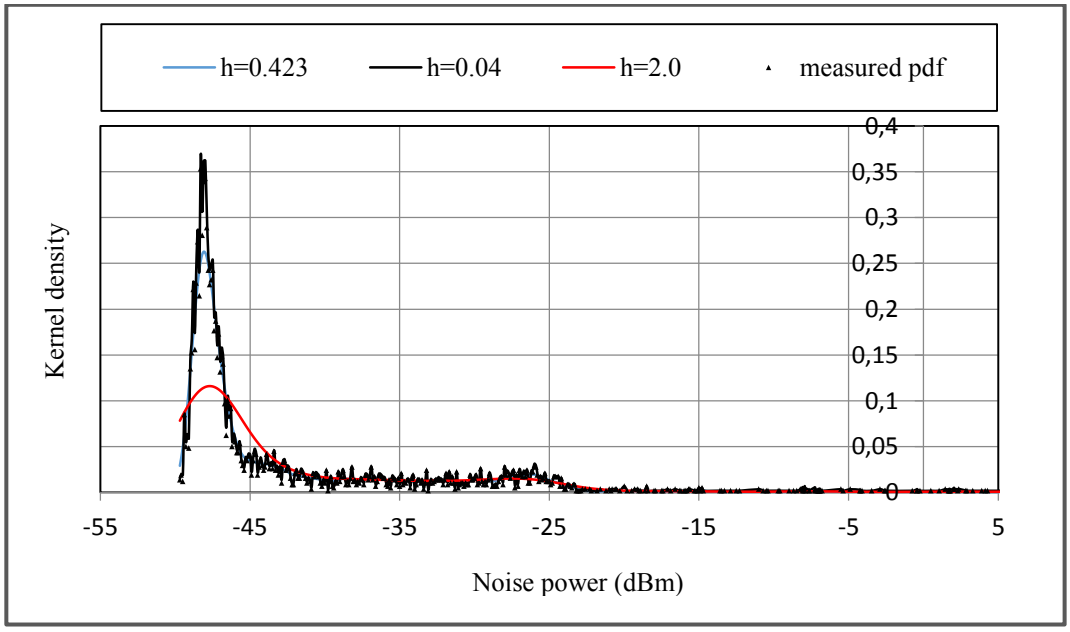

Figure 4- 7: Gaussian kernel frequency domain noise models

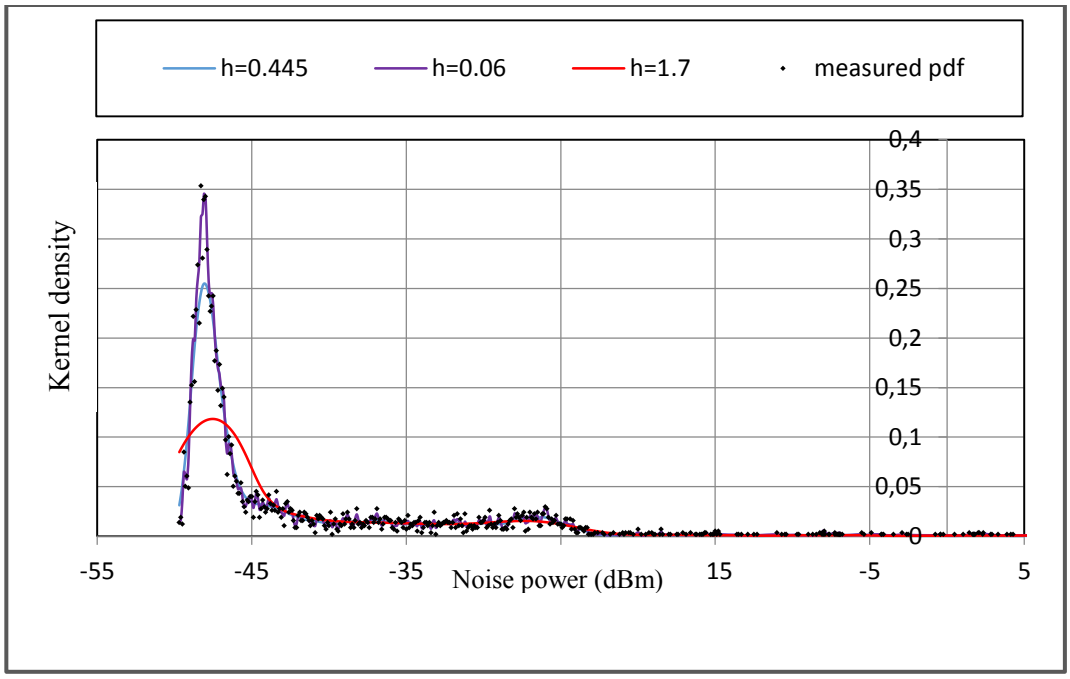

Figure 4- 8: Epanechnikov kernel frequency domain noise models

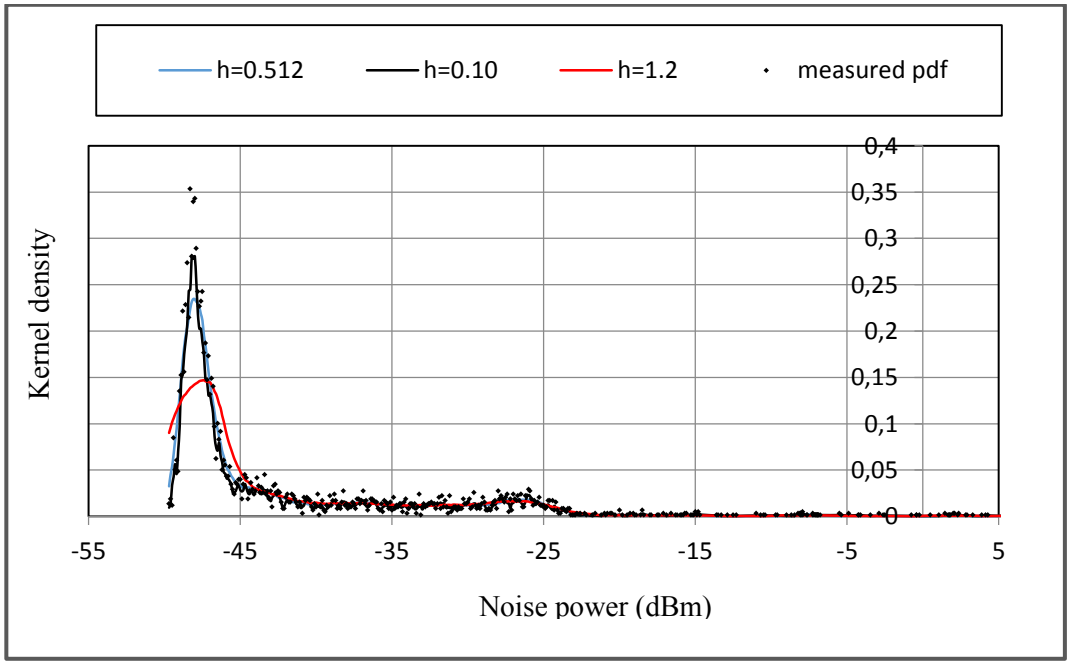

Figure 4- 9: Rectangular kernel frequency domain noise models

Even though previously the performance of kernel models has traditionally only been evaluated via the MISE, in this research work, we go an extra mile to ascertain the stability and consistency of the optimal kernel noise models obtained in both time and frequency domains, by applying the Chi-square (χ^2) statistics test. The χ^2 statistics are computed as:

$$\chi^2 = \sum_{i=1}^{N} \frac{[f(x) - g(x)]^2}{g(x)} \tag{4.19}$$

where $f(x)$ is the measured data values, $g(x)$ is the optimal kernel data values, and N is the sample data length. A tabulation of the different Chi-square test parameters is given in Table 4.4 below.

Table 4. 4: Chi-square test parameters

Kernel	Time domain			
	χ^2	DF	CV	SL
Triangular	11.74	250	287.88	0.05
Gaussian	11.75	250	287.88	0.05
Epanechnikov	11.77	250	287.88	0.05
Rectangular	11.62	250	287.88	0.05
Kernel	Frequency domain			
	χ^2	DF	CV	SL
Triangular	0.871	300	341.44	0.05
Gaussian	0.812	300	341.44	0.05
Epanechnikov	0.862	300	341.44	0.05
Rectangular	1.01	300	341.44	0.05

From the results in Table 4.4, we see that the computed χ^2 values for both the time and frequency domains are very close to each other for all the four kernels, for the same degrees of freedom (DF) and significance level (SL). The χ^2 values are also very small compared to the critical values (CV). Given that none of the χ^2 values exceeds the CVs, we therefore accept the null hypothesis H_0 and reject the alternative hypothesis H_1 for all the cases. Thus, all the models are consistent with the measured data and, with a 95% confidence, we can say that there is no significance difference between the kernel models obtained with the optimum smoothing parameter and the models obtained from the measured data. This confirms that kernel models "hug" the measured data as close as possible, which means that they can even be used as an excellent approximation (reference models) of the measured data density, given the small errors and χ^2 values obtained in Tables 4.3

and 4.4 above. This therefore implies that the optimal kernel models can be used as a reference for parametric modeling of power line noise.

4.5 Chapter summary and conclusion

In this chapter, we have presented an alternative technique (new approach) for the modeling and characterization of power line noise in low voltage indoor power networks. The nonparametric kernel density estimator applied models the data as it is, and therefore the resultant models can be used as a reference/benchmark in the application of parametric techniques to model similar noise. An error-based optimization procedure has been developed and applied to derive optimal kernel models, as can be seen in the errors in Table 4.3. We also observe that the optimal value of the smoothing parameter has more weight on the resulting estimate than the choice of a particular kernel function, going by the errors obtained for the various optimal kernel models. Also, the models have been tested for consistency using the Chi square fitness test. This fitness test results further confirm the suitability of kernel techniques in the modeling of power line noise. As such there is no significant difference between the χ^2 values for the four kernels for both time and frequency domain cases. The computed χ^2 values are very small compared to their corresponding CVs for the same SL and DF. This is a further demonstration of the suitability of this technique for nonparametric modeling of low voltage indoor power line noise, as long as the correct values of the optimal smoothing parameters for the various kernels are used. The time domain noise models are dome-shaped and rather symmetrical, while the frequency domain ones are clearly skewed with long tails (heavy tails), which points to the impulsive nature of the measured power line noise. Overall, we have studied noise characteristics in an indoor environment and proposed simple and tractable models that can be benchmarked upon for parametric modeling of indoor power line noise. In the next chapter, we will develop parametric models of the measured noise characteristics based on a very flexible stochastic modeling tool; the stable distributions, that are benchmarked on the kernel models developed in this chapter, and validate them appropriately.

Chapter References

[1] M. Zimmermann and K. Dostert, "Analysis and modeling of impulsive noise in broadband powerline communications," *IEEE Transactions on Electromagnetic Compatibility*, vol. 44, no. 1, pp. 249-258, November 2002.

[2] M. Zimmermann and K. Dostert, "Analysis of the broadband noise scenario in powerline networks," *in proceedings of the ISPLC Conference*, 2000, pp.131-138.

[3] J.A. Cortes, L. Diez, F.J. Canete and J.J. Sanchez-Martinez, "Analysis of the indoor broadband power-line noise scenario," *IEEE Transactions on Electromagnetic Compatibility*, vol. 52, no. 4, pp. 849-858, November 2010.

[4] A.M. Nyete, T. J. O. Afullo, and I.E. Davidson, "Statistical analysis and characterization of power line noise for telecommunication applications," *IEEE AFRICON 2015 Conference Proceedings*, Addis Ababa, Ethiopia, 14–17 September 2015, pp. 213-217.

[5] A. M. Nyete, T. J. O. Afullo, and I.E. Davidson, "Power line noise measurements and statistical modelling in the time domain," *Proceedings of PIERS 2015 in Prague*, July 6-9 2015, Prague, Czech Republic, pp. 1569-1574.

[6] R.M. Vines, H.J. Trussell, L. Gale and J.B. O'Neal, "Noise on residential power distribution circuits," *IEEE Transactions on Electromagnetic Compatibility*, vol. 26, pp. 161-168, November 1984.

[7] T.Q Bui, *Coded modulation techniques with bit interleaving and iterative processing for impulsive channels*, MSc. Thesis, University of Saskatchewan, 2006.

[8] A.M. Nyete, T. J. O. Afullo, and I.E. Davidson, "On the application of non-parametric estimation methods for low voltage PLC network noise modelling," *Southern Africa Telecommunication Networks and Applications Conference (SATNAC) 2015*, pp. 59-63.

[9] L.D. Bert, P. Caldera, D. Schwingshackl, and A.M. Tonello, "On noise modeling for power line communications," *in Proc. Int. Symp. Power Line Communication and its Applications,* 2011, pp. 283-288.

[10] C. Assimakopoulos and N. Pavlidou, "A enhanced powerline channel noise model," *WSEAS Transactions on Power Systems*, Issue 1, vol. 1, pp. 239-245, January 2006.

[11] T. Esmailian, F.R. Kschischang, P.G. Gulak "In-building power lines as high-speed communication channels: channel characterization and a test channel ensemble," *International Journal of Communication Systems 2003*; vol. 16, pp. 381–400.

[12] H.C. Ferreira et al., "Power line communications: An overview," *IEEE AFRICON 1996*, 24-27 September 1996, Stellenbosch, South Africa, pp. 558-563.

[13] A. M. Nyete, T.J.O. Afullo, I.E. Davidson, “Statistical models of noise distribution in broadband plc networks,” *In Proceedings of PIERS 2015 Conference*, July 6-9 2015, Prague, Czech Republic, 423-429.

[14] T. Shongwe, A. J. Han Vinck, H. C. Ferreira, “On impulse noise and its models,” *In proceedings of the18th ISPLC Conference*, Glasgow, Scotland, March 30th 2014-April 2nd 2014, pp. 12-17.

[15] T. Shongwe, A. J. Han Vinck, H. C. Ferreira, “A study on impulse noise and its models,” *SAIEE Africa Research Journal*, vol. 106, no.3, pp. 119-131, September 2015.

[16] Y. Ma, P. So, and E. Gunawan, “Performance analysis of OFDM system for broadband power line communications under impulsive noise and multipath effects," *IEEE Transactions on Power Delivery*, Vol. 20, pp. 674-682, April 2005.

[17] T. Faber, T. Scholand, and P. Jung, “Turbo decoding in impulsive noise environments," *Electronics Letters,* vol. 39, pp. 1069-1071, July 2003.

[18] H. V. Poor and M. Tanda, “Multiuser detection in flat fading non-Gaussian channels," *IEEE Transactions on Communications*, vol. 50, no. 11, pp. 1769-1777, November 2002.

[19] D. Middleton, “Statistical-physical models of electromagnetic interference," *Electromagnetic Compatibility; Proceedings of the Second Symposium and Technical Exhibition*, vol. EMC-19, pp. 331-340, June 1977.

[20] S. Miyamoto, M. Katayama, and N. Morinaga, “Performance analysis of QAM systems under Class-A impulsive noise environment," *IEEE Transactions on Electromagnetic Compatibility*, vol. 37, no. 2, pp. 260-267, May 1995.

[21] D. Umehara, H. Yamaguchi, and Y. Morihiro, “Turbo decoding in impulsive noise environment," *in Proceedings of the IEEE Global Telecommunications Conference*, 29 Nov.-3 Dec. 2004, pp. 194-198.

[22] M. Ardakani, F. R. Kschischang, and W. Yu, “Low-density parity-check coding for impulse noise correction on power line channels," *in Proceedings of the 2005 ISPLC Conference*, March 2005, pp. 90-94.

[23] G. A. Tsihrintzis, and C. L. Nikias, “Fast estimation of the parameters of alpha-stable impulsive interference,” *IEEE Transactions on Signal Processing*, vol. 44, no. 6, 1996.

[24] R. Weron, *Performance of the estimators of stable law parameters*, Research report HSC/95/1, Hugo Steinhaus Center for Stochastic Methods, Institute of Mathematics, Wroclaw university; Available online: http://prac.im.pwr.wroc.pl/~hugo/publ/RWeron_HSC_95_1.pdf -last accessed on 3/4/2015.

[25] W. Zucchini, *Applied smoothing techniques, part 1: Kernel Density Estimation*, Available: http://staff.ustc.edu.cn/~zwp/teach/Math-Stat/kernel.pdf.

[26] M. Rosenblatt, "Remarks on some nonparametric estimates of a density function," *The Annals of Mathematical Statistics*, vol. 27, no. 3, pp. 832-837, 1956.

[27] G. Walter and J. Blum, "Probability density estimation using delta sequences," *The Annals of Statistics*, vol. 7, no. 2, pp. 328-340, 1979.

[28] G.R. Terrell and D.W. Scott, "Variable kernel density estimation," *The Annals of Statistics*, vol. 20, no. 3, pp. 1236-1265, 1992.

[29] A. Z. Zambom and R. Dias, *A Review of Kernel Density Estimation with Applications to Econometrics*, Cornell University library, December 2012, Available : http://arxiv.org/abs/1212.2812.

[30] S. Hovda, "Using pseudometrics in kernel density estimation," *Journal of Nonparametric Statistics*, vol. 26, no. 4, pp. 669-696, 2014.

[31] D. F. Froelich and M. Rahman, "A note on the choice of the smoothing parameter in the kernel density estimate'', *BRAC University Journal*, vol. VI, no.1, pp. 59-68, 2009.

[32] B. W. Silverman, *Density estimation for statistics and data analysis*, Chapman and Hall, London, 1986.

[33] V. C. Raykar and R. Duraiswami, "Very fast optimal bandwidth selection for univariate kernel density estimation", *Perceptual Interfaces and Reality Laboratory of Maryland University*, June 28, 2006.

[34] S. J. Sheather, "Density estimation," *Institute of Mathematical statistics*, Australia, vol. 19, No.4, pp. 588-597, 2004.

5. Parametric Modelling and Characterization of Indoor Low Voltage Power Line Noise for PLC Applications

5.1 Introduction

In this chapter, the suitability of the alpha stable distribution in the modelling of indoor power line noise is explored. Stable distributions have been shown to excellently capture long tailed behaviour of different phenomena (associated with impulsiveness) in other systems and therefore an investigation as to their suitability in modelling indoor low voltage power line noise is necessary. The greatest strength that this distribution has is its flexibility; an aspect that is brought about by the four parameters that define it. The distribution has the Gaussian distribution as one of the limiting cases, and therefore it can be applied to model non-impulsive phenomena as well. In this chapter, stable distribution is first studied, and then it is applied in the modelling of power line noise measured in indoor power networks. The models obtained are referenced on the kernel density estimator models obtained in Chapter four. The validity of the kernel models to act as reference models is proven through Chi-squared test and root mean square error analysis for the same dimensions. From the results obtained, the noise distribution models developed in Chapter four and this chapter for both time and frequency domain data match very well, a fact cemented by the validation statistics obtained. From a general perspective, the objectives of this chapter are:

1. To present the necessary properties, definitions and applications of alpha stable distributions to the PLC signal processing community and to help PLC researchers in understanding and utilizing stable laws to characterize, model and analyse power line noise/interference.
2. To illustrate the gains that can be obtained by modelling power line noise under the assumption that it is alpha stable.
3. To motivate further research in this area in line with the approach adopted in this chapter, for the development of robust and efficient signal processing algorithms relevant to the power line channel.

5.2 Parametric noise modelling and characterization

The main reason for the poor performance of PLC systems can be attributed to the fact that conventional and relatively old-fashioned signal processing algorithms that were developed for environments very different from PLC enviroment, like wireless systems, have been introduced into PLC. Therefore, the introduction of modern communication schemes that are adapted to suit the PLC environment is very necessary if superior performance is to be realized. For the development and introduction of such schemes, the PLC environment needs to be properly known, viz a viz the noise characteristics, channel frequency response, impedance variations and attenuation characteristics. The most critical of these characteristics in the design of coding and modulation schemes suitable for PLC systems is the non-white non-Gaussian noise. In the analysis and design of many digital systems, the noise model that is widely used is the stationary additive white Gaussian noise (AWGN). In PLC however, the noise features are totally non-Gaussian and are believed to be the cause of many poorly performing PLC systems. Actually, given that Gaussian noise has the highest entropy, this would imply that a communication system affected by non-Gaussian noise achieves a much higher performance than one affected by AWGN, if and only if the system is designed to adapt to the noise characteristics. Hence PLC systems still have the capacity to attain more superior performance than many other systems, if the noise is properly characterized and modelled and then the results taken into consideration in the PLC system design [1-9].

In order to fully understand communication systems in both man-made and natural noise environments, a simple model that expresses the noise characteristics in form of some tractable mathematical equation is necessary. One of the common models that define non-Gaussian noise is the Middleton's class A model for electromagnetic interference. In this model, the noise probability density function is expressed as a sum of Gaussian functions. Using this model, different classes of impulsive noise can be expressed by a simple function with a small number of parameters. However, this model does not define the time domain features of the noise. The model also does not describe whether or not the noise is spiky or smooth in the time domain [7, 10].

The noise in power lines has a power spectral density (PSD) that is complicated. In [11], Voglgsang *et al.* define the probability density function (pdf) of the noise by dividing the bandwidth into several sub-bands, and then sampling the noise voltages at each sub-band. The different pdf sets for each sub-band are then used to generate the overall noise pdf. In [2], Meng *et al*. use a similar approach where the pdf of each sub-band is approximated using Nakagami-m distribution. In [8], Zimmerman and Dostert study the time domain features of the noise using partitioned Markov

chains with multiple states. Also in [12], Cortes *et al.* have reported on noise measurements and classification in terms of the stationarity and impulsiveness of the noise components. In the recent past, Shongwe et al. have also presented a study of impulsive noise models [13, 14].

From all these previous studies, it goes without saying that, in order to capture the random behaviour of the noise at each individual frequency as well as the noise amplitude voltage variations in the time domain, statistical analysis methods should be used to model the noise distribution, that is: the pdf and the cumulative distribution function (cdf). This is necessary because, from the results of such modelling, and deductions and inferences thereof, we can then fully describe the statistical behaviour of the noise.

In this chapter, we first present a review of stable distribution, followed by a modelling framework for the measured indoor noise characteristics as summarized in Chapter three. This statistical tool is very flexible and captures impulsiveness very well through the characteristic exponent. We develop simple, accurate and realistic noise models that confirm that the noise in indoor PLC systems can actually be fully described by an alpha stable distribution stochastic process.

5.3 Stable distributions

An increasingly wide class of phenomena that are not Gaussian are encountered in practice like telephone accidental hits, atmospheric lightning, underwater signals in the case of ice cracking and seabed reflections, as well as power line noise. Most of these phenomena are characterized by impulsiveness. Noise and signals of this nature exhibit sharp spikes and random bursts that one would not expect from signals that are Gaussian distributed. As a consequence of their impulsiveness, the tails of their marginal distributions tend to decay less rapidly than those of their Gaussian counterpart. The tails for the density functions of such signals/noise are therefore heavy or long. As a well-known fact, noise in PLC has impulsive characteristics and is therefore not Gaussian distributed. Stable distributions have tails that decay at a slower rate than those of the Gaussian distribution and therefore are very suitable for modelling impulsive signals and noise. As a matter of fact, the stable law is obtained as a direct generalization of the Gaussian distribution, and therefore the Gaussian distribution is one of the limiting cases of stable distributions. Stable distributions share some of their defining characteristics like the central limit theorem and stability property with the Gaussian distribution [14-23]. It is for this reason, and the fact that results of a noise measurement campaign at the University of KwaZulu-Natal confirm the impulsive characteristics of the PLC noise, with heavier tails than those of the Gaussian distribution, that we have chosen the alpha stable distribution to model the noise [15-20]. In fact, the idea of using

alpha-stable distribution in the characterization and modelling of general impulsive interference is not new; see the paper by Kogon and Williams [22] and that of Tsihrintzis, and Nikias [21]. However the use of alpha stable distribution of the characterization and modelling of power line noise appeared only recently, with the authors in [24] applying the distribution to study power line noise in an industrial environment, although their results are not validated through any criteria, and also the details of the suitability of such a method are very scanty from the work. Also, the authors applied the Maximum likelihood technique to study their noise. The purpose of this chapter is therefore to first give a comprehensive study of alpha stable distributions, followed by its application in the modelling of the noise measured in Chapter three; where a Fourier technique based on the empirical characteristic function and a quantile-based technique are used in the extraction/estimation of the alpha stable noise parameters. The two methods apply totally different approaches for the estimation of the noise parameters, something that brings diversity in the approach adopted in the current research work. Also, a numerical computation of integrals is applied in the calculation of the pdfs and the cdfs. The results obtained demonstrate that alpha stable distribution is appropriate in modelling the noise marginal distribution in indoor PLC networks and provides evidence that actually noise in indoor PLC networks is alpha stable. All the results obtained are validated, with the optimal kernel models in Chapter four acting as reference models.

An alpha stable (α-stable) distribution is a stable distribution that has the characteristic exponent α. α determines the tail thickness and is actually regarded as the distribution shape parameter. Its value would therefore be an indicator of how impulsive a process is. A smaller value of this exponent points to a very impulsive process and vice versa. If $\alpha = 2$, the distribution is Gaussian. If $\alpha = 1$ and $\beta = 1$, the distribution is a Cauchy distribution. Also, if $\delta = 0$ and $\gamma = 1$, the stable distribution is referred to as standard stable distribution. We can see that if a random variable is stable, then $(X - \delta)/\gamma^{\frac{1}{\alpha}}$ is standard with skewness parameter β and characterictic exponent α. A standard stable density function is defined by [23]:

$$f(x;\alpha,\beta) = \frac{1}{\pi}\int_0^{\infty} exp(-t^{\alpha})\cos[xt + \beta t^{\alpha}\omega(t,\alpha)]dt \qquad (5.1)$$

For $\alpha \neq 1$, $\beta > 0$ and $\beta < 0$ represent left and right skewness respectively. Figure 5-1 below is a simulated result of showing how the different values of the characteristic exponent have an influence on the tail probabilities, for a symmetric alpha stable distribution ($\beta = 0$), with parameters $\gamma = 1$ and $\delta = 0$.

Figure 5-2 is a simulated result for a close-up examination of how the tails of the pdfs shown in Figure 5-1 decay as the characteristic exponent changes. We see that the tail of $\alpha = 2$ decay fastest while that of $\alpha = 0.6$ decay slowest. A simulated result of the effect of the skew parameter is also shown in Figure 5-3.

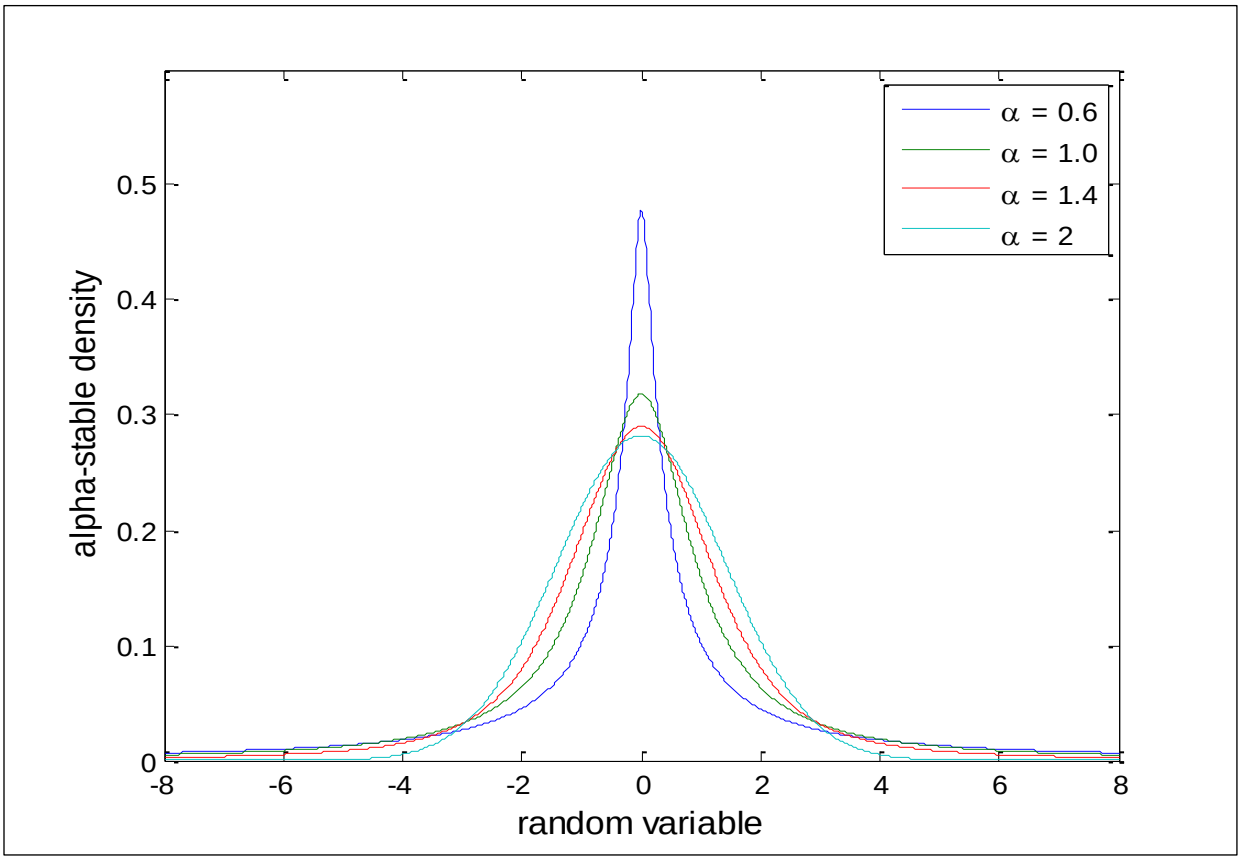

Figure 5- 1: Alpha-stable densities, $\beta = 0,\ \gamma = 1, \delta = 0$

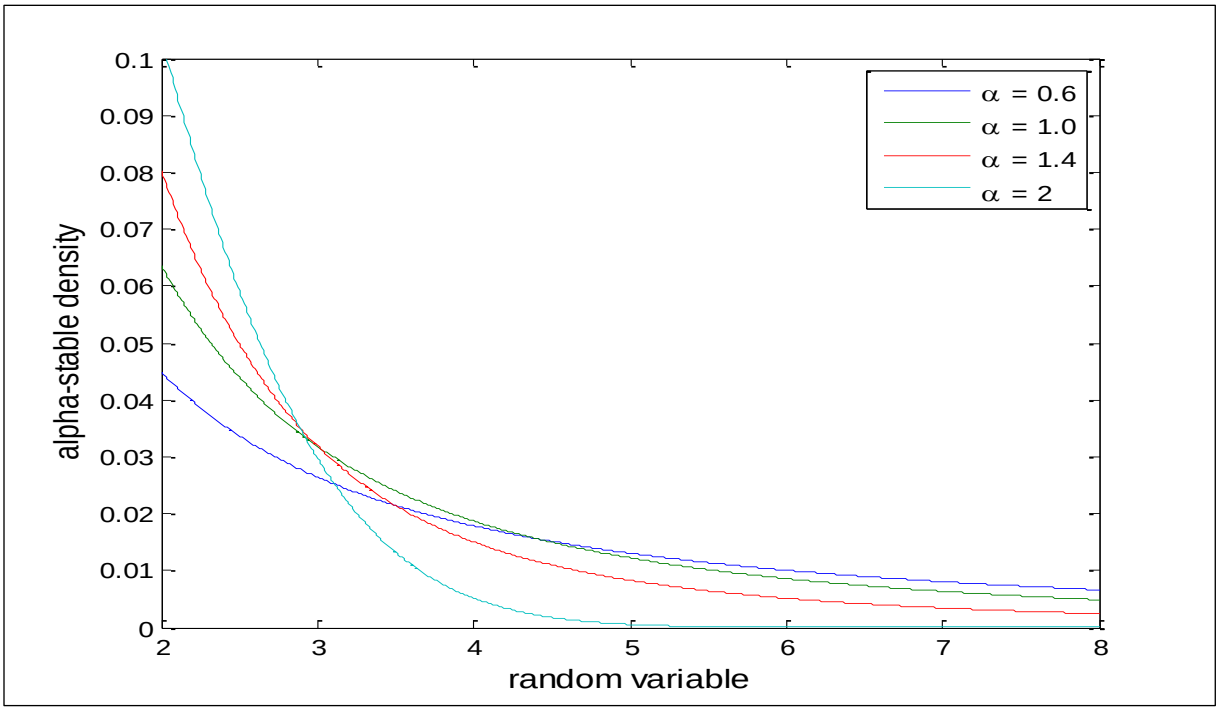

Figure 5- 2: Closer look at the tail densities for Fig. 5-1

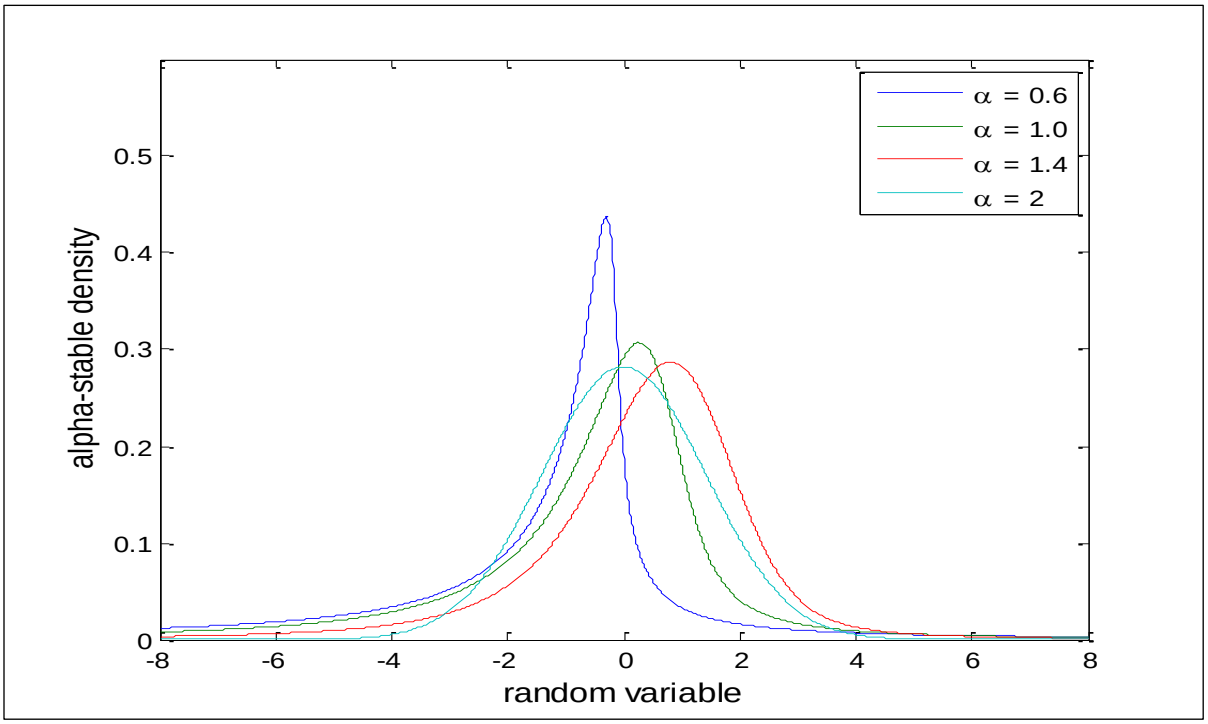

Figure 5- 3: Alpha-stable densities, $\beta = -0.5,\ \gamma = 1, \delta = 0$

5.3.1 Parameterization of stable distributions

Multiple parameterizations of the one-dimensional stable distribution exist. But in all the parameterizations, one common feature is that stable distribution is a four-parameter distribution. The four parameters that define the stable distribution, as earlier stated in Chapter four are the characteristic exponent α, symmetry parameter β, scale parameter γ and the location parameter δ. For instance, there are different parameterizations that were proposed by Zolotarev [25], all of which are applicable to different problems. Since the closed form formula for most stable densities does not exist, except for a few known ones, the stable distributions are usually specified in terms of their characteristic functions. The characteristic function, according to Zolotarev can be formulated as:

$$\emptyset_0(t) = \begin{cases} exp\left\{j\delta_0 t - \gamma^\alpha |t|^\alpha \left[1 + j\beta \tan\frac{\pi\alpha}{2} sgn(t)(|\gamma t|^{1-\alpha} - 1)\right]\right\} & if\ \alpha \neq 1 \\ exp\left\{j\delta_0 t - \gamma|t|\left[1 + j\beta\frac{2}{\pi} sgn(t) In(\gamma|t|)\right]\right\} & if\ \alpha = 1 \end{cases} \quad (5.2)$$

Where the parameters in Equation (5.2) are as defined in Equations (4.1)-(4.4) except for δ_0 which is translated to conform with the form given in Equation (4.1) as:

$$\delta_0 = \begin{cases} \delta_1 + \beta\gamma \tan\frac{\pi\alpha}{2} & if\ \alpha \neq 1 \\ \delta_1 + \beta\frac{2}{\pi}\gamma In\gamma & if\ \alpha = 1 \end{cases} \quad (5.3)$$

On the basis of Equations (5.2) and (5.3), a $S_1(\alpha, \beta, 1, 0)$ distribution corresponds to a $S_0(\alpha, \beta, 1, \beta\gamma \tan\frac{\pi\alpha}{2})$ distribution provided that $\alpha \neq 1$.

In some other cases, another parameterization is sometimes used [25]:

$$\emptyset_2(t) = \begin{cases} exp\left\{j\delta_1 t - \gamma_2^\alpha |t|^\alpha exp\left[-j\frac{\pi\beta_2}{2} sgn(t) min(\alpha, 2-\alpha)\right]\right\} & if\ \alpha \neq 1 \\ exp\left\{j\delta_1 t - \gamma_2|t|\left[1 + j\beta\frac{2}{\pi} sgn(t) In(\gamma_2|t|)\right]\right\} & if\ \alpha = 1 \end{cases} \quad (5.4)$$

Where again the following translations are applicable in conformity to Equation (4.1):

$$\beta = \cot\frac{\pi\alpha}{2}\tan\left(\frac{\pi\beta_2}{2}min(\alpha, 2-\alpha)\right) \tag{5.5}$$

And

$$\gamma = \gamma_2\left[cos\left(\frac{\pi\beta_2}{2}min(\alpha, 2-\alpha)\right)\right]^{\frac{1}{\alpha}} \tag{5.6}$$

On the other hand, Nolan [26, 27] defines a $S_\alpha^0(\gamma, \beta, \mu^0)$ parameterization, by taking a standardized stable distribution in Zolotarev's (M) parameterization given in Equation (5.2) as the basic quantity. By fixing α and β, and letting $Z = Z_{\alpha,\beta}$ be a random variable, then, the characteristic function in Equation (5.1) reduces to [26, 27]:

$$E\ exp(jtZ) = \begin{cases} exp\left\{-|t|^\alpha\left[1 + j\beta\tan\frac{\pi\alpha}{2}sgn(t)(|t|^{1-\alpha} - 1)\right]\right\} & \alpha \neq 1 \\ exp\left\{-\gamma|t|\left[1 + j\beta\frac{2}{\pi}sgn(t)In(|t|)\right]\right\} & \alpha = 1 \end{cases} \tag{5.7}$$

Next, a variation of Equation (5.2) is defined as a simple scale and location change of Z: by taking $X^0 = S_\alpha^0(\gamma, \beta, \mu^0)$ if X^0 has the same distribution as $\gamma Z + \mu^0$. Then the characteristic function of X^0 in this case is given by:

$$E\ exp(jtX^0) = \begin{cases} exp\left\{-\gamma^\alpha|t|^\alpha\left[1 + j\beta\tan\frac{\pi\alpha}{2}sgn(t)((\gamma|t|)^{1-\alpha} - 1)\right] + j\mu^0 t\right\} & \alpha \neq 1 \\ exp\left\{-\gamma|t|\left[1 + j\beta\frac{2}{\pi}sgn(t)In(\gamma|t|)\right] + j\mu^0 t\right\} & \alpha = 1 \end{cases} \tag{5.8}$$

$$= \begin{cases} exp\left\{-\gamma^\alpha|t|^\alpha\left[1 - j\beta\tan\frac{\pi\alpha}{2}sgn(t)\right] + j\left[\mu^0 - \beta\,\gamma\tan\frac{\pi\alpha}{2}\right]t\right\} & \alpha \neq 1 \\ exp\left\{-\gamma|t|\left[1 + j\beta\frac{2}{\pi}sgn(t)In(\gamma|t|)\right] + j\left[\mu^0 - \beta\frac{2}{\pi}\gamma In\gamma\right]t\right\} & \alpha = 1 \end{cases}$$

Also, a random variable random variable $X \sim S_\alpha(\gamma, \beta, \mu)$ in the form of (4.1) can be expressed as:

$$X = \begin{cases} \gamma\left(Z + \beta\tan\frac{\pi\alpha}{2}\right) + \mu & \alpha \neq 1 \\ \gamma\left(Z + \beta\frac{2}{\pi}In\gamma\right) + \mu & \alpha = 1 \end{cases} \tag{5.9}$$

Where α, β, and γ have the same meaning as defined in all earlier Equations, while the location parameters of the two representations are related by the following equation:

$$\mu = \begin{cases} \mu^0 - \beta\gamma\tan\frac{\pi\alpha}{2} & \alpha \neq 1 \\ \mu^0 - \beta\frac{2}{\pi}\gamma In\gamma & \alpha = 1 \end{cases} \tag{5.10}$$

We note here that when the mean exists (iff $\alpha > 1$), it is μ, not μ^0, and then the density $f(x|\alpha, \beta, \gamma, \mu^0)$ has support :

$$f(x|\alpha,\beta,\gamma,\mu^0) = \begin{cases} \left(\mu^0 - \gamma\tan\frac{\pi\alpha}{2}, \infty\right) & \alpha < 1\,, \beta = 1 \\ \left(-\infty, \mu^0 + \gamma\tan\frac{\pi\alpha}{2}\right) & \alpha < 1\,, \beta = -1 \\ -\infty, +\infty & otherwise \end{cases} \tag{5.11}$$

Of all the different parameterization defined by different authors, the most commonly used one is the one defined by Equations (4.1)-(4.4) [22, 23, 25, 28, 29], and this is the parameterization that is used in the current study.

5.3.2 Properties of stable distributions

Stable distribution as a statistical tool that can model phenomena that is impulsive is a generalization of the Gaussian distribution. This distribution is particularly appealing because it satisfies the generalized central limit theorem and is the only distribution that satisfies the stability property. The applicability of the stable distribution in modeling PLC noise is therefore based on the fact that the total noise is a summation of many noise terms that originate from sources that are independent of each other.

5.3.2.1 Stability Property

A random variable is stable iff for any independent random variables X_1, X_2 with the same distribution as X , and for arbitrary constants a_1, a_2, there exist constants a and b such that [23, 28, 29]:

$$a_1X_1 + a_2X_2 = aX + b \tag{5.12}$$

Where "=" denotes that both sides of the equation have the same distribution. By making use of the stable distribution characteristic function, one can easily show a more general statement: if X_1, X_2,…, X_n are independent and follow stable laws with the same (α, β), then all linear combinations

of the form $\sum_{j=1}^{n} a_j X_j$ are stable with the same parameters α and β. From the stability property consequence, it can be shown that stable distributions are the only possible limit distributions for sums of independent and identically distributed (i.i.d) random variables. This is known as the generalized central limit theorem and is discussed below.

5.3.2.2 Generalized central limit theorem

The generalized central limit theorem states that: X is stable iff it is the limit distribution of the sum [29-32]:

$$S_n = \frac{X_1 + X_2 + \cdots + X_n}{a_n} - b_n \tag{5.13}$$

Where X_1, X_2,…, X_n are i.i.d random variables and $n \to \infty$. Parameter b_n is real while a_n is real and positive. In particular, if the X_i's are i.i.d and have finite variance, then the limit distribution is Gaussian. Of course, this is the result of the well-known central limit theorem.

The main cause of the difference in behaviors of the (non-Gaussian) stable and the Gaussian distributions is their tails. It can be shown that for an alpha stable random variable X with zero location parameter and dispersion parameter (location parameter) [33]:

$$\lim_{t \to \infty} t^{\alpha} P(|X| > t) = \gamma C(\alpha) \tag{5.14}$$

Where $C(\alpha)$ is a positive constant that depends on α. Hence, stable distributions have inverse power, that is, algebraic tails, while in contrast the tails of the Gaussian distribution are exponential. This serves as proof that the tails of stable distributions are much heavier (thicker) than those of the Gaussian distribution. The smaller the value of α, the heavier the tails and vice versa.

5.4. Statistical noise modelling and characterization with alpha stable distributions

Noise in power lines is complex and cannot be modelled and characterized using pure mathematical derivations. This is the reason why almost all existing power line noise modelling attempts are based on empirical measurements, although some are mere approximations of models that were developed for interference/noise in other communication systems, like the Middleton's models. In order to capture the random concentration of the noise distribution across different frequency bands in the frequency domain or the voltage level variation concentration/variations (which is an indicator of the impulse power), statistical tools need to be employed to model and characterize the noise into certain pdfs and cdfs. This is essential because, with the corresponding parameters

derived from the noise measurements for the pdf as well as the cumulative distribution function (cdf), we can then give a full statistical description of the overall noise characteristics, as well as determine an appropriate noise synthesis process for the noise found in any network.

In this chapter, we seek to parametrically model the measured noise power in the frequency domain and the noise voltage amplitudes in the time domain. We model the noise characteristics using the alpha stable distribution, which has been shown to model impulsive phenomena in other systems as earlier mentioned. This flexible and simple statistical tool has drawn a lot of interest among mathematicians/statisticians and the digital signal processing (DSP) community in the recent past; see for example [21-39].

The pdf of a stable random variable exists and is continuous, but, except for a few known cases, the closed form expression is non-existent. The closed form expression for the pdf is only known for the three special classes below [23, 26, 36]:

- The Gaussian distribution, $S_2(\gamma, 0, \delta) = N(\mu, 2\sigma^2)$,
- The Levy distribution, $S_{1/2}(\gamma, 1, \delta)$, $S_{1/2}(\gamma, -1, \delta)$
- The Cauchy distribution, $S_1(\gamma, 0, \delta)$

Where, $S_\alpha(\gamma, \beta, \delta)$ denotes an alpha stable distribution, whose characteristic function is defined by Equation (4.1).

Thus, modelling with stable distributions is greatly hampered by the lack of closed form expressions for the density functions for all but the few cases listed above. Additionally, most of the traditional techniques in mathematical statistics, including maximum likelihood estimation procedure, cannot be directly utilized in this case since they depend on an explicit form for the density. However, several mathematical methods have been proposed in different literatures that are applicable in estimating the four parameters that define stable distributions.

5.4.1 Parameter estimation for stable laws

Different parameter estimation techniques for alpha stable distributions have been proposed. Some of them include the maximum likelihood (ML) method [36-38], sample quantile methods [35, 36, 39] and sample characteristic function methods [34, 36]. DuMouchel [37, 38] was the first person to obtain approximate ML estimates of α and γ, with the condition that δ=0. In his approach, he performed a multinomial approximation to the likelihood function. However, this method is computationally too intensive. On the other hand, Fama and Roll [39] were the first to propose a

quantile based solution for the estimation of the stable parameters. They provided estimates for the parameters of a symmetric stable distribution ($\beta = 0, \delta = 0$) for $1 < \alpha \leq 2$. They gave the following estimate for γ:

$$\gamma = \frac{x_{0.72} - x_{0.28}}{1.654} \tag{5.15}$$

However, the above estimator of γ is based on the fortuitous observation that $\frac{(x_{0.72} - x_{0.28})}{\gamma}$ lies within 0.4% of 1.654 for all $1 < \alpha \leq 2$, when $\beta = 0$, which enables one to obtain an estimate of γ using Equation (5.15) with less than 0.4% asymptotic bias without first knowing α. But, when $\beta \neq 0$, searching for an invariant change such as the one they found turns out to be futile. In their method, the characteristic exponent α is estimated from the tail behaviour by using:

$$S_\alpha = \frac{x_f - x_{1-f}}{1.654} = f \tag{5.16}$$

They find that f =0.95, 0.96, 0.97 works best for obtaining estimates of α. Further details of this method can be found in [39]. This method is simple but is limited in that it suffers from a small asymptotic bias in α and γ. McCulloch [35] improved on this method and developed a more generalized quantile method. He provided consistent estimators for all the four parameters for $0.6 < \alpha \leq 2$, while at the same time maintaining the same level of computational simplicity as Fama and Roll. After him, we define,

$$\upsilon_\alpha = \frac{x_{0.95} - x_{0.05}}{x_{0.75} - x_{0.25}} \tag{5.17}$$

Which happens to be independent of γ and δ. Also we define:

$$\upsilon_\beta = \frac{x_{0.95} + x_{0.05} - 2x_{0.25}}{x_{0.95} - x_{0.05}} \tag{5.18}$$

Which is also independent of both γ and δ. υ_α and υ_β are functions of α and β. Thus, we can write:

$$\upsilon_\alpha = \phi_1(\alpha, \beta), \ \upsilon_\beta = \phi_1(\alpha, \beta) \tag{5.19}$$

The kind of relationship in Equation (5.19) may be inverted to obtain:

$$\alpha = \psi_1(\upsilon_\alpha, \upsilon_\beta), \qquad \beta = \psi_2(\upsilon_\alpha, \upsilon_\beta) \tag{5.20}$$

And similarly,

$$\psi_1(\upsilon_\alpha, \upsilon_\beta) = \psi_1(\upsilon_\alpha, -\upsilon_\beta) \tag{5.21}$$

Table 5.1 shows the variation of α as a function of υ_α and υ_β, while Table 5.2 shows the variation of β as a function of υ_α and υ_β.

Table 5. 1: $\alpha = \psi_1(\upsilon_\alpha, \upsilon_\beta) = \psi_1(\upsilon_\alpha, -\upsilon_\beta)$

υ_α	υ_β						
	0.0	0.1	0.2	0.3	0.5	0.7	1.0
2.439	2.000	2.000	2.000	2.000	2.000	2.000	2.000
2.5	1.916	1.924	1.924	1.924	1.924	1.924	1.924
2.6	1.808	1.813	1.829	1.829	1.829	1.829	1.829
2.7	1.729	1.730	1.737	1.745	1.745	1.745	1.745
2.8	1.664	1.663	1.663	1.668	1.676	1.676	1.676
3.0	1.563	1.560	1.553	1.548	1.547	1.547	1.547
3.2	1.484	1.480	1.471	1.460	1.448	1.438	1.438
3.5	1.391	1.386	1.378	1.364	1.337	1.318	1.318
4.0	1.279	1.273	1.266	1.250	1.210	1.184	1.150
5.0	1.128	1.121	1.114	1.101	1.067	1.027	0.973
6.0	1.029	1.021	1.014	1.004	0.974	0.935	0.874
8.0	0.896	0.892	0.887	0.883	0.855	0.823	0.769
10.0	0.818	0.812	0.806	0.801	0.780	0.756	0.691
15.0	0.698	0.695	0.692	0.689	0.676	0.656	0.595
25	0.593	0.590	0.588	0.586	0.579	0.563	0.513

Table 5. 2: $\beta = \psi_2(\upsilon_\alpha, \upsilon_\beta) = -\psi_2(\upsilon_\alpha, -\upsilon_\beta)$

υ_α	υ_β						
	0.0	0.1	0.2	0.3	0.5	0.7	1.0
2.439	0.000	2.160	1.000	1.000	1.000	1.000	1.000
2.5	0.000	1.592	3.390	1.000	1.000	1.000	1.000
2.6	0.000	0.759	1.800	1.000	1.000	1.000	1.000
2.7	0.000	0.482	1.048	1.694	1.000	1.000	1.000
2.8	0.000	0.360	0.760	1.232	2.229	1.000	1.000
3.0	0.000	0.253	0.518	0.823	1.575	1.000	1.000
3.2	0.000	0.203	0.410	0.632	1.244	1.906	1.000
3.5	0.000	0.165	0.332	0.499	0.943	1.560	1.000
4.0	0.000	0.136	0.271	0.404	0.689	1.230	2.195
5.0	0.000	0.109	0.216	0.323	0.539	0.827	1.917
6.0	0.000	0.096	0.190	0.284	0.472	0.693	1.759
8.0	0.000	0.082	0.163	0.243	0.412	0.601	1.596
10.0	0.000	0.074	0.147	0.220	0.377	0.546	1.482
15.0	0.000	0.064	0.128	0.191	0.330	0.478	1.362
25.0	0.000	0.056	0.112	0.167	0.285	0.428	1.274

From these tables, bi-linear interpolation to estimate α and β is then carried out. Similarly, the location parameter δ and the dispersion parameter γ are estimated using the corresponding tabulated functions and the previous estimates for α and β. The method by McCulloch [35] is therefore the quantile based technique we use in this research work, given its obvious advantages compared to its predecessors. We refer the reader to the paper by McCulloch for more details on this method.

Different methods based on the sample characteristic function have been proposed including the method of moments (MoM), minimum distance method, and regression methods [36]. Among these three, the regression method proposed by Koutrouvelis [34] is the most efficient and is also simpler to implement. For these reasons, this is the characteristic function based method employed in this work, and going forward, this is method we shall dwell on here. The parameter estimation technique is described next. This regression type estimation method is based on the following observation concerning the characteristic function:

$$\log(-\log|\emptyset(t)|^2) = \log(c^\alpha) + \alpha \log|t| \tag{5.22}$$

where $c^\alpha = \gamma$, is the scale parameter, and the real and imaginary parts of $\emptyset(t)$, $\mathrm{Re}\emptyset(t)$ and $\mathrm{Im}\emptyset(t)$, respectively, for $\alpha \neq 1$, are:

$$\mathrm{Re}\emptyset(t) = \exp(-|ct|^\alpha) . \cos\left[\delta t - |ct|^\alpha \beta \mathrm{sgn}(t) \tan\left(\frac{\pi\alpha}{2}\right)\right] \tag{5.23}$$

$$\mathrm{Im}\emptyset(t) = \exp(-|ct|^\alpha) . \sin\left[\delta t - |ct|^\alpha \beta \mathrm{sgn}(t) \tan\left(\frac{\pi\alpha}{2}\right)\right] \tag{5.24}$$

Apart from principal values, from Equations (5.23) and (5.24), we deduce the following:

$$\arctan\left(\mathrm{Im}\emptyset(t) \Big/ \mathrm{Re}\emptyset(t)\right) = \delta t - \beta c^\alpha \tan\left(\frac{\pi\alpha}{2}\right) \mathrm{sgn}(t)|t|^\alpha \tag{5.25}$$

Parameters c and α, which control Equation (5.22), are obtained by regressing $\mathrm{y} = \log(-\log|\emptyset_n(t)|^2)$ on $\omega = \log|t|$ in the model given below:

$$y_k = \mu + \alpha\omega_k + \varepsilon_k, \quad k = 1,2 \ldots, K, \tag{5.26}$$

Where $(t_k; k = 1,2 \ldots, K)$ is an appropriate set of real numbers, $\mu = \log(2c^\alpha)$, and ε_k denotes an error term. After determining the fixed values of c and α, $\beta$and δ are obtained from (5.25), by regressing $z = g_n(u) + \pi k_n(u)$ on u and $\mathrm{sgn}(u)|u|^\alpha$ in the model:

$$z_l = \delta u_l - \beta c^\alpha \, tan\left(\frac{\pi\alpha}{2}\right) \mathrm{sgn}(u_l)|u_l|^\alpha + \eta_l \,, \quad l = 1, 2, \ldots, L \tag{5.27}$$

Where η_l denotes the error term and $(\mu_l; l = 1,2 \ldots, L)$ is an appropriate set of real numbers, integer $k_n(u)$ is introduced to take care of any possible nonprincipal branches of the arctan function, and

$$g_n(u) = \arctan\left(\mathrm{Im}\emptyset(t) \Big/ \mathrm{Re}\emptyset(t)\right) \tag{5.28}$$

The reader is referred to [34] for more details on this method. Several other methods have been proposed in literature as can be seen in the reference section of this chapter. Interested readers are referred to the publications listed in the reference list at the end of this chapter for more.

5.4.2 Evaluation of the pdf of alpha stable distributions

The pdf of stable random variables exists and is continuous but except for the three special classes listed earlier, they are not known in closed form. Therefore, without a closed form analytical expression of the pdf, practical applications of stable distributions is a nontrivial task. However, there a few useful numerical techniques that have been fronted in literature to deal with this challenge and are discussed below.

5.4.2.1 Direct numerical integration techniques

In [37], DuMouchel developed a procedure for approximating the cdf of the stable distribution using Bergstrom's [40] series expansion and Zolotarev's representation. In [41], four alternative procedures were developed by Holt and Crow for the approximation of an inversion integral for calculating the pdf values form the characteristics function. However, the algorithms presented by the Holt and Crow and DuMouchel methods are highly computationally intensive and time consuming as well, which renders the use of maximum likelihood for the estimation of parameters a very difficult task. Nolan on the other hand, using a variant of Zolotarev's (M) parameterization proposed a formula for computing the stable density by carrying out a numerical evaluation of the following integral [26, 42]:

$$p(x,\alpha,\beta) = \frac{1}{\pi}\int_0^{\infty} \cos[h(x,t;\alpha,\beta)]exp(-t^{\alpha})dt \tag{5.29}$$

where

$$h(x,t;\alpha,\beta) = \begin{cases} xt + \beta\tan\dfrac{\pi\alpha}{2}(t - t^{\alpha}), & \alpha \neq 1 \\ \mu + \beta\gamma\dfrac{2}{\pi}In\gamma & \alpha = 1 \end{cases} \tag{5.30}$$

For a more direct numerical integration for the case when $\alpha > 1$, the pdf integral is replaced with the following approximation:

$$p(x,\alpha,\beta) \approx \int_0^{\Delta} f(x,t;\alpha,\beta)dt \tag{5.31}$$

Where $\Delta = \Delta(\alpha,\varepsilon)$ is the root of $\Gamma\left(\frac{1}{\alpha},\Delta^{\alpha}\right)$ and ε is the error term of Equation (5.31).

5.4.2.2 Fast Fourier Transform (FFT) method

An algorithm for computing the pdf of stable random variables that employs the FFT was presented in [43] by Mittnik *et al.* . In terms of the characteristic function, the pdf can be calculated as:

$$p(x,\alpha,\beta) = \frac{1}{2\pi}\int_{-\infty}^{\infty} e^{-ixt}\varphi(t)\,dt \tag{5.32}$$

The integral is computed for N points that are equally spaced by distance h, namely $x_k = \left(k-1-\frac{N}{2}\right)h,\ \ k=1,\dots,N$. If we let $t = 2\pi\omega$, (5.32) then becomes:

$$p\left(k-1-\frac{N}{2}\right)h = \int_{-\infty}^{\infty} \varphi(2\pi\omega)e^{-i2\pi\omega\left(k-1-\frac{N}{2}\right)h}d\varphi \tag{5.33}$$

This integral can be approximated using the rectangle rule with spacing s as follows:

$$p\left(k-1-\frac{N}{2}\right)h \approx s\sum_{n=1}^{N}\varphi\left(2\pi s\left(n-1-\frac{N}{2}\right)\right)e^{-i2\pi\left(n-1-\frac{N}{2}\right)\left(k-1-\frac{N}{2}\right)hs} \tag{5.34}$$

5.4.2.3 Two quadratures method

In [44], a more "natural way" of evaluating the pdf integral over the interval (0, ∞) would be a 96-points Laguerre quadrature given by:

$$p(x,\alpha,\beta) \approx \frac{1}{\pi}\sum_{n=1}^{96}\omega_n exp(t-t^{\alpha})\cos\left(xt_n+\beta\tan\frac{\pi\alpha}{2}(t_n-t_n^{\alpha})\right) \tag{5.35}$$

Where the abscissas t_n are given by the roots of the Laguerre polynomial $L_{96}(t)$, and the weights $\omega_n = t_n\left(97L_{97}(t_n)\right)^{-2}$. If a direct implementation of (5.35) does not yield pdf values that possess sufficient accuracy, then the oscillations in the pdf tails can be suppressed by decreasing the power of the exponent in the integrand. Greater precision is achieved using numerical integration methods at the cost of speed; which is not a problem given the supercomputing capabilities available in today's computers.

5.4.3 Time and frequency domain alpha stable noise modelling

As stated in the above presentation on parameter estimation techniques for stable laws, we have chosen two techniques to estimate the alpha stable parameters of the total measured noise power spectra and noise amplitudes in frequency and time domains respectively. These methods are the McCulloch's quantile method and Koutrovelis' method. These two parameter estimation methods are chosen because of the differences in their estimation procedures, which present diversity in our approach, and also their merits compared to earlier similar methods as well as others that were developed much later. The choice of the alpha stable method for modelling the noise is informed by the long tailed characteristic observed in the measured noise pdfs shown in Chapter four as well its flexibility as a modeling tool. The alpha stable noise parameters determination procedures are described in subsection 5.4.1 above.

The time domain alpha stable distribution noise model parameters obtained are shown in Table 5.3 while the frequency domain ones are shown in Table 5.4. The results in Tables 5.3 and 5.4 show that regardless of the parameter determination technique, the parameters obtained are the same. This confirms the robustness of the techniques used.

Table 5. 3: Time domain noise alpha stable parameters

Time domain noise stable parameters				
Method	α	β	γ	δ
McCulloch	1.469	0.238	0.844	0.231
Koutrouvelis	1.469	0.238	0.844	0.231

Table 5. 4: Frequency domain noise alpha stable parameters

Frequency domain noise stable parameters				
Method	α	β	γ	δ
McCulloch	1.72	1	4.29	-45.69
Koutrouvelis	1.72	1	4.29	-45.69

The pdfs and cdfs for the alpha stable noise parameters are then evaluated using a similar method to the direct numerical integration method proposed by Nolan in [26, 42] (refer to Subsection 5.4.2

above). The pdfs are shown in Figures 5-4 and 5-5 below, while the cdfs are shown in Figures 5-6 and 5-7. As observed in the kernel density models, the time domain model is bell-shaped, but not Gaussian; for a Gaussian stable distribution, $\alpha = 2$. The near symmetrical aspect of the pdf is well captured as well as location and tail probabilities. Also, the frequency domain model is visibly long tailed and non-Gaussian as well, with a characteristic exponent of 1.72. Also, in the frequency domain noise model, other important features like skewness and the location of the pdf are well captured. We note from Tables 5.3 and 5.4 that none of the two models is Gaussian. This confirms that noise in PLC channels in non-Gaussian and differs from the additive white Gaussian noise (AWGN) present in many other communication systems. Also, we see that the frequency domain model fails to capture the peaky nature of the data well, and this confirms that kernel models are the best for initial modeling of the power line noise data.

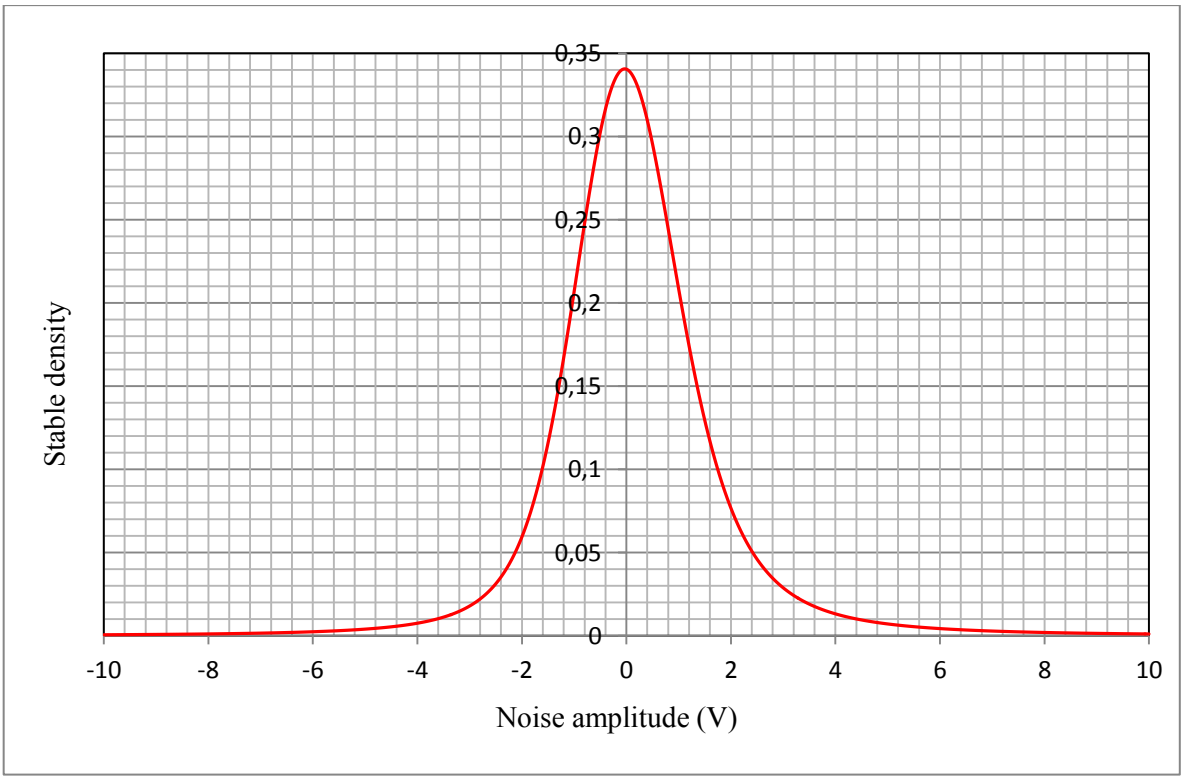

Figure 5- 4: Alpha stable time domain noise model

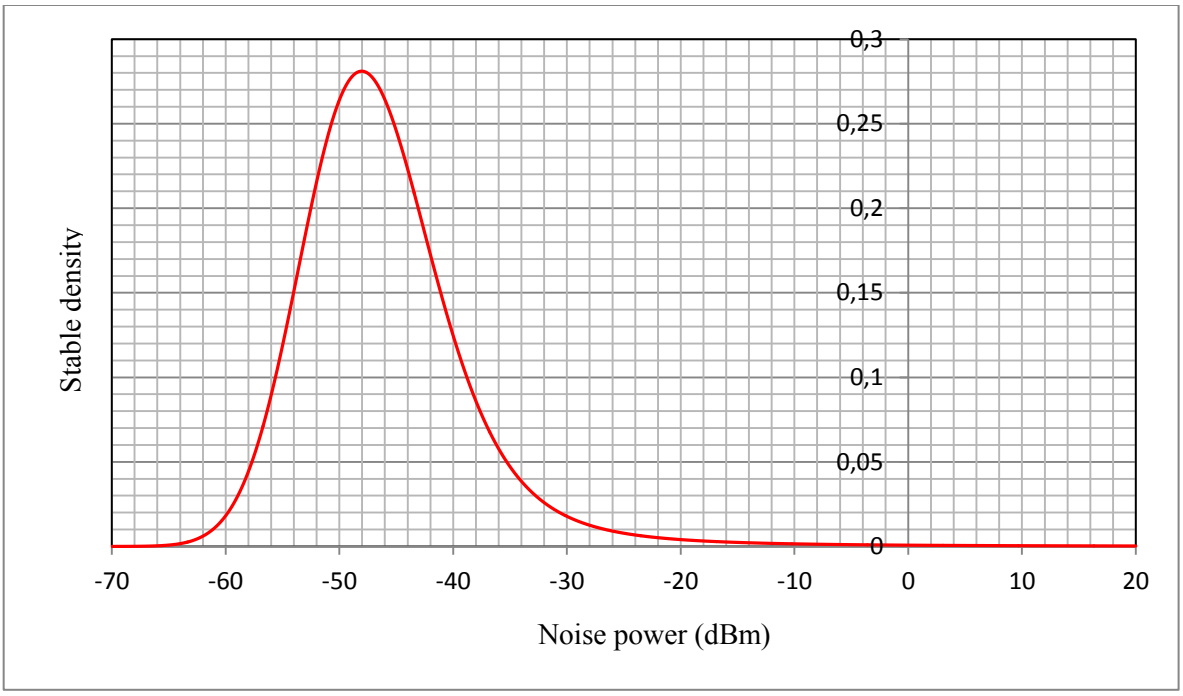

Figure 5- 5: Alpha stable frequency domain noise model

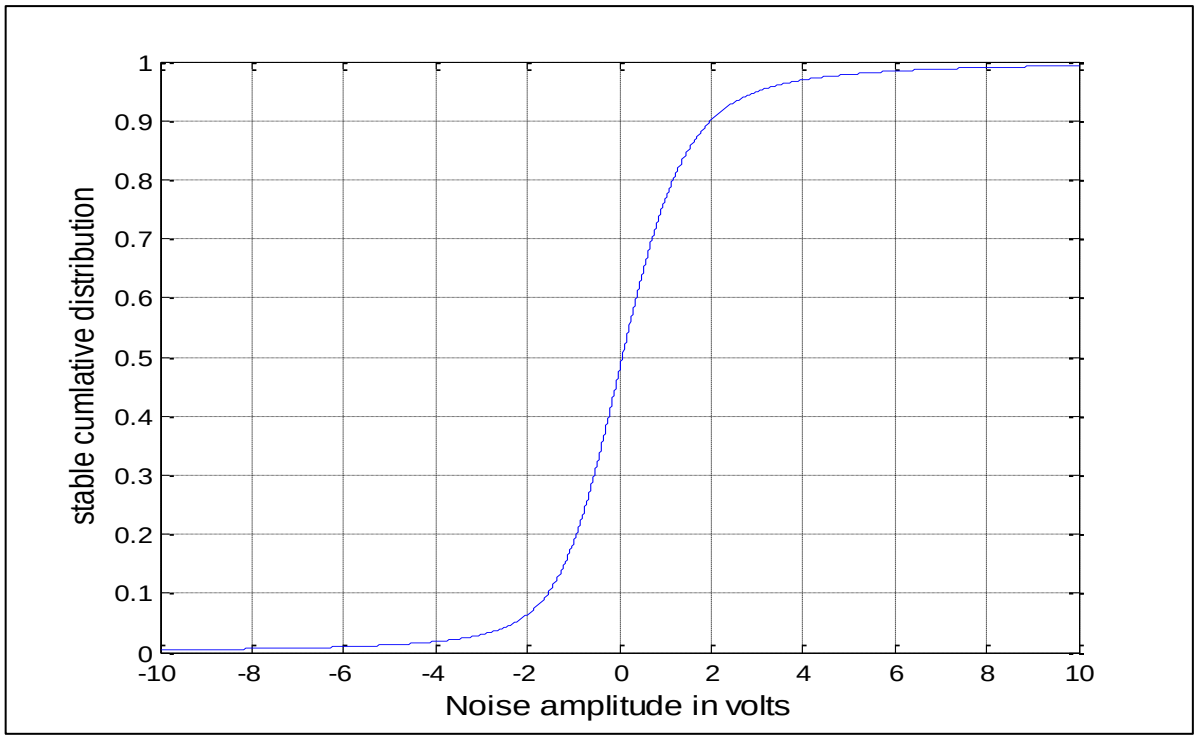

Figure 5- 6: Alpha stable time domain cdf plot

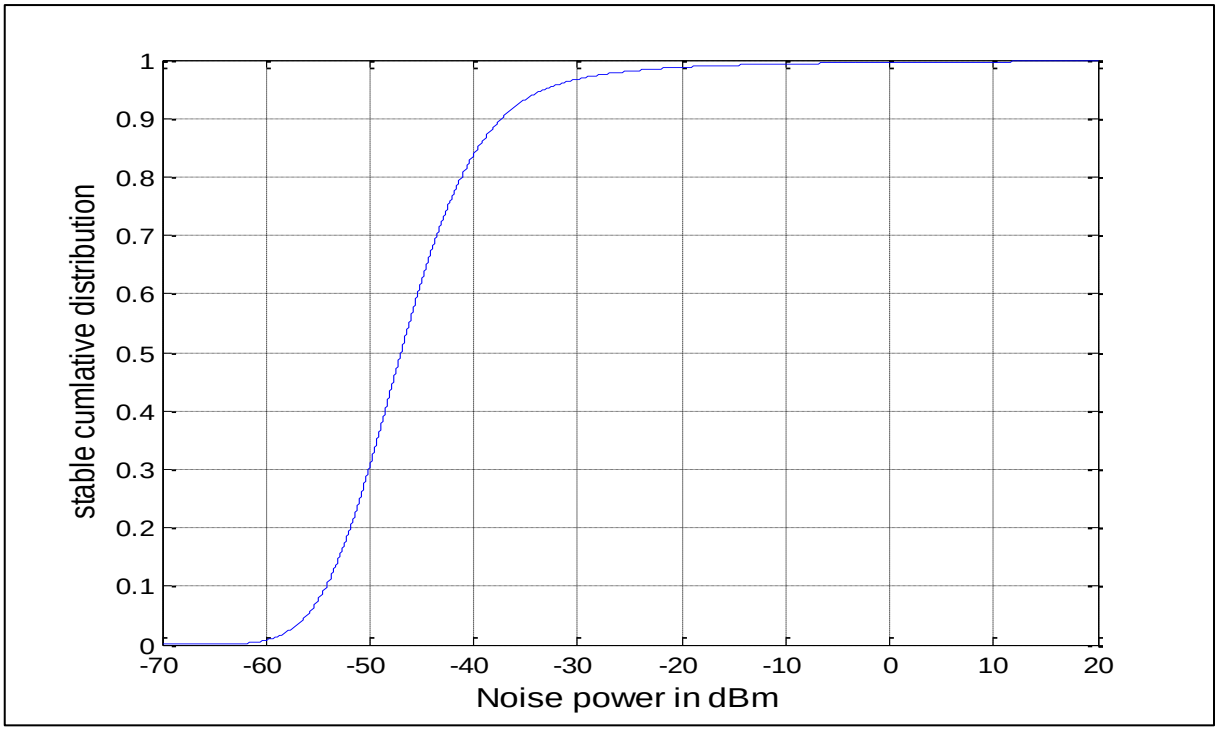

Figure 5- 7: Alpha stable frequency domain cdf plot

Thus, both the kernel and alpha stable modelling approaches are a good fit to one another as well as the measured noise characteristics, and since the kernels model the data as it is, this proves that the stable distribution is an appropriate choice for modelling the indoor power line noise. The same non-Gaussianity noise features are evident in the cdf plots. Additionally, to test for the goodness of fit between the optimal kernel models in Chapter four and the alpha stable models developed here, we apply the root mean square error (RMSE) criteria as well as the Chi-square (χ^2) test, with the kernel models acting as a reference models. The same data range (dimensions) is used in both cases in the computation of these statistics, in conformity with the results in Chapter four. These statistics are computed as follows:

$$RMSE = \sqrt{\frac{1}{N}\sum_{i=1}^{N}[f(x) - g(x)]^2} \tag{5.36}$$

$$\chi^2 = \sum_{i=1}^{N}\frac{[f(x) - g(x)]^2}{g(x)} \tag{5.37}$$

where $f(x)$ is the optimal kernel data, $g(x)$ is the alpha stable data, and N is the sample data length. These computed statistics are shown in Table 5.5. The significance level used for the Chi-square (χ^2) test is 0.05.

Table 5. 5: Error and Chi-square statistics

(a) Time domain

Kernel	**Time domain**			
	RMSE	χ^2	DF	CV
Triangular	0.0126	1.47	300	341.40
Gaussian	0.0138	1.59	300	341.40
Epanechnikov	0.0129	1.52	300	341.40
Rectangular	0.0139	1.59	300	341.40

(b) Frequency domain

Kernel	**Frequency domain**			
	RMSE	χ^2	DF	CV
Triangular	0.0843	15.06	350	394.63
Gaussian	0.0846	15.16	350	394.63
Epanechnikov	0.0845	15.12	350	394.63
Rectangular	0.0853	15.36	350	394.63

From Table 5.5, we see that none of the calculated χ^2 values exceeds the critical values (CV) of 341.40 and 394.63 for 300 and 350 degrees of freedom (DF) for the time and frequency domain models respectively. The χ^2 values are actually very small compared to their critical values, an indication of how well the testing hypothesis is satisfied. Thus, the null hypothesis is accepted for both models, with at least 95% confidence that there is no significant difference between the kernel and alpha stable models. Also, the computed RMSEs are small, a further confirmation that the fitted models are in good agreement with each other and the measured pdfs as well. The Triangular kernel however outperforms all the others and is therefore the closest match to the alpha stable models for both time and frequency domains. But, a closer look at the results in Table 5.5 show that the values obtained are very close, which points to the fact that the optimal value of the smoothing parameter for the kernel models is much more important than the choice of the kernel function itself.

5.5 Chapter summary and conclusion

In this chapter, the salient features of the alpha stable distribution have been presented, as well as a demonstration of its suitability as a modelling tool for power line noise. The alpha stable distribution has been employed in the development of suitable models for noise measured in indoor power line channels. These models have been validated against the optimal kernel models obtained in Chapter four. The models are found to satisfactorily fit the data, going by

the goodness of fit test results obtained. The models obtained here are therefore a confirmation of the suitability of the alpha stable distribution in the characterization and modelling of indoor low voltage power line noise. As such, we propose the use of this method for modelling power line noise in low voltage, medium voltage as well as high voltage power networks due to its flexibility. This flexibility renders this distribution very applicable in modelling both impulsive (heavy tailed) and Gaussian phenomena. These models are therefore suitable for the optimization of communication through the power line network. As a future work, their performance against some of the other earlier proposed parametric noise models should be tested. In the next chapter, a PLC noise synthesis framework will be developed that makes use of the alpha stable noise parameters derived in this chapter. The developed framework is generalized for all admissible values of alpha stable noise parameters, from very impulsive to background cases.

Chapter references

[1] S. Galli, A. Scaglione and Z. Wang, "For the grid and through the grid: The role of power line lommunications in the smart grid," *Proceedings of the IEEE*, vol. 99, no. 6, pp. 998-1027, June 2011.

[2] H. Meng, Y.L Guan and S. Chen, "Modeling and analysis of noise effects on broadband power-line communications," *IEEE Transactions on Power Delivery*, vol. 20, no. 2, pp. 630-637**,** April 2005.

[3] H.C. Ferreira et al., "Power line communications: An overview," *IEEE AFRICON 1996*, Stellenbosch, South Africa, September 1996, pp. 558-563.

[4] J. Anatory, N. Theethayi, R. Thottappillil, M.M. Kissaka and N.H. Mvungi, "An experimental validation for broadband power-line communication (BPLC) model," *IEEE Transactions on Power Delivery*, vol. 23, no. 3, pp. 1380-1383, July 2008.

[5] A. M. Nyete, T.J.O. Afullo and I. Davidson, "Performance evaluation of an OFDM-based BPSK PLC system in an impulsive noise environment", *PIERS Conference Proceedings*, Guangzhou, China, 25-28 August 2014, pp. 2510-2513.

[6] A. M. Nyete, T.J.O. Afullo and I. Davidson, "On Rayleigh approximation of the multipath PLC channel: Broadband through the PLC channel ", *In 2014 SATNAC Proceedings*, Port Elizabeth, South Africa, 31 August-3 September 2014, pp. 265-270.

[7] M. Katayama and T. Yamazato, “A mathematical model of noise in narrowband power line communication systems,” *IEEE Journal on Selected Areas in Communications*, vol. 24, no. 7, pp. 1267-1276**,** July 2006.

[8] M. Zimmermann and K. Dostert, “Analysis and modeling of impulsive noise in broadband powerline communications,” *IEEE Transactions on Electromagnetic Compatibility*, vol. 44, no. 1, pp. 249-258, November 2002.

[9] A. D. Spaulding and D. Middleton, “Optimum reception in an impulsive interference environment-Part I: Coherent detection,” *IEEE Transactions on Communications*, vol. COM-25, no. 9, pp. 910–923, September 1977.

[10] D. Middleton, “Statistical-physical models of electro-magnetic interference,” *IEEE Transactions on Electromagnetic Compatibility*, vol. EMC-19, no. 3, pp. 106–126, August 1977.

[11] A. Voglgsang, T. Langguth, G. Koerner, H. Steckenbiller, and R. Knorr, “Measurement, characterization and simulation of noise on powerline channels,” in *Proc. of the 4th ISPLC*, pp. 139–146, April 2000.

[12] J.A Cortes, L. Diez, F.J Canete and J.J Sanchez-Martinez, “Analysis of the indoor broadband power-line noise scenario,” *IEEE Transactions on Electromagnetic Compatibility*, vol. 52, no. 4, pp. 849-858, November 2010.

[13] T. Shongwe, A. J. Han Vinck and H. C. Ferreira, “On impulse noise and its models,” *In proceedings of the18th ISPLC Conference,* Glasgow, Scotland, March 30th 2014-April 2nd 2014, pp. 12-17.

[14] T. Shongwe, A. J. Han Vinck, H. C. Ferreira, “A study on impulse noise and its models,” *SAIEE Africa Research Journal*, vol. 106, no.3, pp. 119-131, September 2015.

[15] A. M. Nyete, T.J.O. Afullo and I.E. Davidson, “Intra-building power network noise modelling in South Africa,” *Proceedings of the 2015 South African Universities Power Engineering Conference*, University of Johannesburg, 28-30th January 2015, pp. 468-472.

[16] A. M. Nyete, T. J. O. Afullo, and I.E. Davidson, “Statistical models of noise distribution in broadband plc networks,” *In Proceedings of PIERS 2015 in Prague*, Prague, Czech Republic, July 6-9 2015, pp. 423-429.

[17] A. M. Nyete, T. J. O. Afullo, and I.E. Davidson, "Power line noise measurements and statistical modelling in the time domain," *In Proceedings of PIERS 2015 in Prague*, Prague, Czech Republic, July 6-9 2015, pp. 1569-1574.

[18] A.M. Nyete, T. J. O. Afullo, and I.E. Davidson, "Statistical analysis and characterization of power line noise for telecommunication applications," *In Proceedings of the IEEE AFRICON 2015 Conference*, Addis Ababa, Ethiopia, 14–17 September 2015, pp. 213-217.

[19] M. Mosalaosi and T.J.O. Afullo, "Broadband analysis and characterization of noise for in-door power-line communication channels," *PIERS Proceedings,* 719 - 723, August 25-28, Guangzhou, 2014.

[20] A.M. Nyete, T. J. O.Afullo, and Davidson, I. E., "Stochastic modelling of low voltage power line noise for power line communications," *PIER Journal*, (*under review*)..

[21] G. A**.** Tsihrintzis, and C. L. Nikias, "Fast estimation of the parameters of alpha-stable impulsive interference," *IEEE Transactions on Signal Processing*, vol. 44, no. 6, pp. 1492-1503, 1996.

[22] S.M. Kogon and D.B. Williams, "On the characterization of impulsive noise with α-stable distributions using Fourier techniques", *Proceedings of the ASILOMAR-29*, pp. 787-791, 1996.

[23] M. Shao and C. L. Nikias, "Signal processing with fractional lower order moments: Stable processes and their applications," *Proceedings of the IEEE,* vol. 81, pp. 986-1010, 1993.

[24] T. H. Tran, D. D. Do, and T. H. Huynh, "PLC impulsive noise in industrial zone: measurement and characterization," *International Journal of Computer and Electrical Engineering*, vol. 5, no. 1, February 2013, pp. 48-51, 2013.

[25] V. M. Zolotarev, "One-dimensional stable distributions," *Translations of Mathematical Monographs, American Mathematical Society,* vol. 65, pp. 270-277*,* 1986.

[26] J.P. Nolan, "An Algorithm for evaluating stable densities in Zolotarev's *(M)* parameterization," *Mathematical and Computer Modelling*, vol. 29, pp. 229-223, 1999.

[27] J.P. Nolan, "Parameterizations and modes of stable distributions," *Statistics and Probability Letters*, vol. 38, pp. 187-195, 1998.

[28] P.G. Georgiou, P. Tsakalides, and C. Kyriakakis, "Alpha-stable modelling of noise and robust time-delay estimation in the presence of impulsive noise," *IEEE Transactions on Multimedia*, vol. 1, no. 3, pp. 291-301, September 1999.

[29] G. Samorodnitsky and M.S. Taqqu, *Stable non-Gaussian random processes: Stochastic models infinite variance*. New York/London: Chapman and Hall, 1994.

[30] C. L. Nikias and M. Shao, *Signal processing with alpha-stable distributions and applications.* New York: Wiley, 1995.

[31] H. Stark and J. W. Woods, *Probability, random processes and estimation theory for engineers,* 2nd edition, Englewood Cliffs, NJ: Prentice Hall, 1994.

[32] L. Breiman, *Probability,* Classic edition, University of California, Berkeley: Siam, Philadelphia, 1992.

[33] A. Weron, "Stable processes and measures: A survey," *in Probability Theory on Vector Spaces III,* S**.** Cambanis, Ed. Berlin: Springer, 1983, pp. 306-364.

[34] I. A. Koutrouvelis., "Regression-type estimation of the parameters of stable laws", *Journal of the American Statistical Association*, vol. 75, no. 372, pp. 918-928, December 1980.

[35] J.H. McCulloch, "Simple consistent estimators of stable distributions parameters," *Communications in Statistics - Simulation and Computation*, vol. 15, no. 4, pp. 1109-1136, 1986.

[36] R. Weron, *Performance of the estimators of stable law parameters*, Research report HSC/95/1, Hugo Steinhaus Center for Stochastic Methods, Institute of Mathematics, Wroclaw university; Available online at: http://prac.im.pwr.wroc.pl/~hugo/publ/RWeron_HSC_95_1.pdf -last accessed on 3/4/2015.

[37] W. H. DuMouchel, "Stable distributions in statistical inference," *PhD. thesis,* Department of Statistics, Yale University*,* 1971 .

[38] W. H. DuMouchel, "On the asymptotic normality of the maximum–likelihood estimate when sampling from a stable distribution," *Annals of Statistics.* vol. 1(5), pp. 948–957, 1973.

[39] E. F Fama, and R. Roll, "Parameter estimates for symmetric stable distributions," *Journal of the American Statistical Association,* vol. 66: pp. 331-338, 1971.

[40] H. Bergstrom, "On some expansions of stable distributions," *Arkiv for Mathematik*, vol. 2, pp. 463 – 474, 1952.

[41] D.R. Holt and E.L. Crow, "Tables and graphs of the stable probability density functions," *Journal of research of the National Bureau of Standards. B. Mathematical Sciences*, 77 B(3 – 4), pp. 143 – 198, July-December, 1973.

[42] J.P. Nolan, “Numerical calculation of stable densities and distribution functions,” *Communications in Statistics - Stochastic Models*, vol.13, no. 4, pp. 759 – 774, 1997.

[43] S. Mittnik, T. Doganoglu and D. Chenyao, “Computing the probability density function of the stable paretian distribution,” *Mathematical and Computer Modelling*, vol. 29, pp. 235 – 240, 1999.

[44] I.A. Belov, “On the computation of the probability density function of α-stable distributions,”. *Proceedings of the 10th International Conference on mathematical modelling and analysis MMA2005&CMAM2*, Technika, 2005, pp. 333-441.

Chapter Six

6. Low Voltage Power Line Noise Synthesis

6.1 Introduction

In Chapters four and five, the nonparametric and parametric modelling of measured noise characteristics in both time and frequency domains was carried out. A long tailed characteristic of the measured noise was observed in the nonparametric noise models developed in Chapter four; something that was proven through alpha stable modeling in Chapter five. Thus the noise process in PLC systems can be considered a Levy (alpha) stable stochastic process that is clearly non-Gaussian. From the alpha stable noise models parameters and the models developed thereof, in this chapter, a noise synthesis stochastic framework is then developed. This is necessary because the outcome of such a synthesis process will eliminate the need to perform noise measurements in practical PLC systems in future. The objectives of this chapter are:

1. To develop a mathematical framework that is applicable in the synthesis of the noise process in practical PLC systems as a Levy stable process.
2. To develop an appropriate algorithm for PLC noise synthesis as a Levy stable process.
3. To synthesize the noise process for a PLC system using the alpha stable noise parameters obtained in Chapter five using the proposed algorithm for a random number of noise samples.
4. To validate the noise synthesis results appropriately using error analysis and Chi-square tests.
5. To stimulate further research in line with the concepts developed here amongst the PLC research community.

6.2 Background mathematical concepts for noise synthesis

The importance of stable distributions, otherwise known as Levy stable distributions cannot be overemphasized. They are fundamentally justified by the central limit theorem, as an approximation for normality. Actually, these distributions are the only limiting laws of normalized independent, identically distributed variables. These distributions are excellent for modelling phenomena that are characterized by high variability, like the one witnessed in powerline noise, where the impulsive noise can be as high as 50 dB above the background noise. With the confirmation that power line noise in indoor low voltage networks is actually alpha stable, there is need for an urgent development of a synthesizer of such noise. However, except for a few special classes of limiting distributions that include the Gaussian, Cauchy and

Levy distributions, the closed form expressions for the cumulative distribution inverse do not exist, and the inverse transform method cannot be used as well. A major breakthrough towards the development of a generator of stable random variables was proposed by Chambers *et al* [1], even though the journey towards the same was started by Kanter in 1975 [2]. The proposals in both papers have proven to be very useful and have also been applied in the generation of discrete stable and Linnik's random variables, see for example [3, 4]. More recently, this method was revisited in [5, 6], where the equality in law of a skewed stable variable was proven together with a nonlinear transformation of an independent exponential variable and an independent uniform variable. The Chamber *et al.* method is based on the proofs. The power line noise synthesis framework developed is based on the equality in law of a skewed stable variable and the nonlinear transformation of an independent exponential variable and an independent uniform variable. This is because, the method proposed in [2] has been proven to be the most accurate and the fastest as well, even though other proposals have been found in literature [7]. It has also been widely studied with applications to other fields; see for example [8-13]. The mathematical basis/background for the algorithm proposed is described below.

From Zolotarev [14], through the transformation of both β and σ, a standard random variable N is stable if and only if its log characteristic function is given as:

$$\log \phi\,(t) = \begin{cases} -{\sigma_2}^{\alpha}|t|^{\alpha} exp\left[-j\beta_2 sgn(t)\frac{\pi}{2}K(\alpha)\right] + j\mu t & \alpha \neq 1 \\ -\sigma_2|t|\left[\frac{\pi}{2} + j\beta_2 sgn(t)\log|t|\right] + j\mu t & \alpha = 1 \end{cases} \tag{6.1}$$

Where σ is another notation for dispersion parameter while μ is the location parameter, and:

$$K(\alpha) = \alpha - 1 + sgn(1-\alpha) = \begin{cases} \alpha & \alpha < 1 \\ \alpha - 2 & \alpha > 1 \end{cases} \tag{6.2}$$

The new dispersion and symmetry parameters are related to those of Equation (4.1) by:

$$\tan\left(\beta_2 \frac{\pi K(\alpha)}{2}\right) = \beta\tan\left(\frac{\pi\alpha}{2}\right), \quad \sigma_2 = \sigma\left(1 + \beta^2\tan^2\frac{\pi\alpha}{2}\right)^{\frac{1}{2\alpha}}, \qquad \text{for} \qquad \alpha \neq 1 \tag{6.3}$$

And for $\alpha = 1$,

$$\beta_2 = \beta, \quad \sigma_2 = \frac{2}{\pi}\sigma \tag{6.4}$$

Corollary: Any two admissible quadruples of parameters $(\alpha, \beta, \sigma, \mu)$ and $(\alpha, \beta, \sigma', \mu')$ uniquely determine real numbers $a > 0$ and b such that:

$$N((\alpha, \beta, \sigma, \mu)) = aN\left(\alpha, \beta, \sigma', \mu'\right) + b \tag{6.5}$$

Where

$$a = \frac{\sigma}{\sigma'}, \quad b = \begin{cases} \mu - \mu' \frac{\sigma}{\sigma'} & \alpha \neq 1 \\ \mu - \mu' \frac{\sigma}{\sigma'} + \gamma\beta \frac{2}{\pi} \ln \frac{\sigma}{\sigma'} & \alpha = 1 \end{cases} \tag{6.6}$$

If we then consider the standard stable distribution case, we can also transform it to the general case as:

$$N((\alpha, \beta, \sigma, \mu)) = aN(\alpha, \beta, 1, 0) + b \tag{6.7}$$

With

$$a = \sigma, \; b = \begin{cases} \mu & \alpha \neq 1 \\ \mu - +\sigma\beta \frac{2}{\pi} \ln \sigma & \alpha = 1 \end{cases} \tag{6.8}$$

Next the integral forms of the density and cumulative distribution functions of the parameters α and β are determined. Consider the following three important expressions regarding the probability density function, cumulative density function and the characteristic function of alpha stable random variables respectively:

$$f(-n, \alpha, \beta) = f(n, \alpha, -\beta) \tag{6.9}$$

$$F(-n, \alpha, \beta) = 1 - F(n, \alpha, -\beta) \tag{6.10}$$

$$\phi(-t, \alpha, \beta) = \phi(t, \alpha, -\beta) \tag{6.11}$$

If we assume that $\phi(t, \alpha, \beta)$ and $f(n, \alpha, \beta)$ are the characteristic and density functions of a standard random variable, then, according to the inversion formula of the characteristic function:

$$f(n, \alpha, \beta) = \frac{1}{2\pi} \int_{-\infty}^{\infty} e^{-itn} \phi(t, \alpha, \beta) dt$$

$$= \frac{1}{2\pi} \left(\int_0^{\infty} e^{-itn} \phi(t, \alpha, \beta) dt + \int_0^{\infty} e^{itn} \phi(-t, \alpha, \beta) dt \right) \tag{6.12}$$

And, given that $e^{-itn}\phi(t, \alpha, \beta) = e^{itn}\phi(-t, \alpha, \beta)$, then:

$$f(n, \alpha, \beta) = \frac{1}{\pi} Re \int_{-\infty}^{\infty} e^{-itn} \phi(t, \alpha, \beta) dt$$

$$= \frac{1}{\pi} Re \int_0^{\infty} e^{-itn} \phi(-t, \alpha, \beta) dt = \frac{1}{\pi} Re \int_0^{\infty} e^{itn} \phi(t, \alpha, -\beta) dt \tag{6.13}$$

From which the stable density function in integral form, for $\alpha \neq 1$ is given by:

$$f(n,\alpha,\beta)=\frac{1}{\pi}Re\int_0^{\infty}exp\left(-itn-t^{\alpha}exp\left(-i\beta\frac{\pi K(\alpha)}{2}\right)\right)dt \tag{6.14}$$

And for $\alpha = 1$:

$$f(n,1,\beta)=\frac{1}{\pi}Re\int_0^{\infty}exp\left(-itn-\frac{\pi}{2}t-i\beta t\ln t\right)dt \tag{6.15}$$

The cumulative function of a standard stable random variable for $\alpha = 1$, $\beta_2 > 0$ is then given by:

$$F(n,1,\beta_2)=\frac{1}{\pi}\int_{-\frac{\pi}{2}}^{\frac{\pi}{2}}exp\left(-exp\left(-\frac{n}{\beta_2}\right)U_1(\gamma,\beta_2)\right)d\gamma \tag{6.16}$$

And for $\alpha \neq 1, n > 1$,

$$F(n,\alpha,\beta_2)=C(\alpha,\beta_2)+\frac{\epsilon(\alpha)}{\pi}\int_{\gamma_o}^{\frac{\pi}{2}}exp\left(-N^{\frac{\alpha}{1-\alpha}}U_{\alpha}(\gamma,\gamma_o)\right)d\gamma \tag{6.17}$$

Where:

$$\epsilon(\alpha)=sgn(1-\alpha),\ \gamma_o=-\beta_2\frac{\pi}{2}\frac{K(\alpha)}{\alpha} \tag{6.18}$$

$$C(\alpha,\beta_2)=1-\frac{1}{4}\left(1+\beta\frac{K(\alpha)}{\alpha}\right)\left(1+\epsilon(\alpha)\right) \tag{6.19}$$

$$U_{\alpha}(\gamma,\gamma_o)=\left(\frac{\sin(\gamma-\gamma_o)}{\cos\gamma}\right)^{\frac{\alpha}{1-\alpha}}\frac{\cos\left(\gamma-\alpha(\gamma-\gamma_o)\right)}{cos\,\gamma} \tag{6.20}$$

$$U_1(\gamma,\beta_2)=\frac{\frac{\pi}{2}+\beta_2\gamma}{cos\,\gamma}exp\left(\frac{1}{\beta_2}\left(\frac{\pi}{2}+\beta_2\gamma\right)\tan\gamma\right) \tag{6.21}$$

From the above definitions, the random variable N is said to be a $S_{\alpha}(1,\beta_2,0)$ random variable if and only if for $\gamma_o < \gamma < \frac{\pi}{2}$ and $n > 0$:

$$\frac{1}{\pi}\int_{\gamma_o}^{\frac{\pi}{2}}exp\left(-N^{\frac{\alpha}{1-\alpha}}U_{\alpha}(\gamma,\gamma_o)\right)d\gamma=\begin{cases}P(0<N\leq n) & \alpha<1\\ P(N\geq n) & \alpha>1\end{cases} \tag{6.22}$$

Which can be proven as follows for $0 < \alpha < 1$:

$$F(n,\alpha,\beta_2)=P(N\leq n)=\frac{1-\beta_2}{2}+\frac{1}{\pi}\int_{\gamma_o}^{\frac{\pi}{2}}exp\left(-N^{\frac{\alpha}{1-\alpha}}U_{\alpha}(\gamma,\gamma_o)\right)d\gamma \tag{6.23}$$

$$= \frac{1-\beta_2}{2} + P(0 < N \leq n)$$

Given that for $\alpha < 1$, $\frac{1-\beta_2}{2} = P(N \leq 0)$. Also for the case when $1 < \alpha < 2$, we have:

$$F(n, \alpha, \beta_2) = P(N \leq n) = 1 - \frac{1}{\pi}\int_{\gamma_o}^{\frac{\pi}{2}} exp\left(-N^{\frac{\alpha}{1-\alpha}} U_\alpha(\gamma, \gamma_o)\right) d\gamma \tag{6.24}$$

$$= 1 - P(N \geq n)$$

Now, for γ_o as defined above, we define the following theorem: If γ is uniformly distributed on $\left(-\frac{\pi}{2}, \frac{\pi}{2}\right)$, and Z is another independent random variable that is exponentially distributed with a mean equal to 1, then, we can write:

$$K = \frac{\sin\alpha(\gamma-\gamma_o)}{(\cos\gamma)^{\frac{1}{\alpha}}} \left(\frac{\cos\left(\gamma - \alpha(\gamma-\gamma_o)\right)}{Z}\right)^{\frac{1-\alpha}{\alpha}} \tag{6.25}$$

Where $K \sim S_\alpha(1, \beta_2, 0)$ for $\alpha \neq 1$, while for $\alpha = 1$:

$$K = \left(\frac{\pi}{2} + \beta_2\gamma\right)\tan\gamma - \beta_2 \log\left(\frac{Z\cos\gamma}{\frac{\pi}{2} + \beta_2\gamma}\right) \tag{6.26}$$

Where $K \sim S_1(1, \beta_2, 0)$.

To prove the theorems represented by Equations (6.25) and (6.26), we proceed as follows: From Equations (6.25), we can have:

$$K = \left(a(\gamma)/_Z\right)^{\frac{1-\alpha}{\alpha}} \tag{6.27}$$

where

$$a(\gamma) = \frac{\sin\alpha(\gamma-\gamma_o)^{\frac{\alpha}{1-\alpha}}}{\cos\gamma} \frac{\cos\left(\gamma - \alpha(\gamma-\gamma_o)\right)}{\cos\gamma} \tag{6.28}$$

For $0 < \alpha < 1$, Equation (6.25) has the implication that N is greater than zero if and only if $\gamma > \gamma_o$, and, since $\frac{1-\alpha}{\alpha} > 0$, then:

$$P(0 < N \leq n) = P(0 < N \leq n, \gamma > \gamma_o\ ) \tag{6.29}$$

$$= P\left(0 < \left(a(\gamma)/Z\right)^{\frac{1-\alpha}{\alpha}} \leq n, \gamma > \gamma_o\right) = P\left(Z \geq n^{\frac{\alpha}{\alpha-1}} a(\gamma), \gamma > \gamma_o\right)$$

Therefore,

$$P\left(Z \geq n^{\frac{\alpha}{\alpha-1}} a(\gamma)\right) P(\gamma > \gamma_o) = E_\gamma exp\left(-n^{\frac{\alpha}{\alpha-1}} a(\gamma)\right) 1_{\{\gamma > \gamma_o\}} \tag{6.30}$$

$$= \frac{1}{\pi} \int_{\gamma_o}^{\frac{\pi}{2}} exp\left(-n^{\frac{\alpha}{\alpha-1}} a(\gamma)\right) d\gamma$$

Given that $a(\gamma) = U_\alpha(\gamma, \gamma_o)$, this completes the proof that $N \sim S_\alpha(1, \beta_2, 0)$.

Also, for the case of $1 < \alpha \leq 2$, since $\frac{1-\alpha}{\alpha} > 0$, for $n > 0$, we can write that:

$$P(N \geq n) = P(N \geq n, \gamma > \gamma_o) \tag{6.31}$$

$$P\left(0 < \left(a(\gamma)/Z\right)^{\frac{1-\alpha}{\alpha}} \geq n, \gamma > \gamma_o\right) = P\left(0 < \left(Z/a(\gamma)\right)^{\frac{\alpha-1}{\alpha}} \geq n, \gamma > \gamma_o\right) \tag{6.32}$$

$$= P\left(Z \geq n^{\frac{\alpha}{\alpha-1}} a(\gamma), \gamma > \gamma_o\right)$$

$$= E_\gamma exp\left(-n^{\frac{\alpha}{\alpha-1}} a(\gamma)\right) 1_{\{\gamma > \gamma_o\}}$$

$$= \frac{1}{\pi} \int_{\gamma_o}^{\frac{\pi}{2}} exp\left(-n^{\frac{\alpha}{\alpha-1}} a(\gamma)\right) d\gamma$$

From which we conclude that $N \sim S_\alpha(1, \beta_2, 0)$.

From the case of $\alpha = 1$, the right hand side of Equation (6.26) reduces to $\frac{\pi}{2} \tan \gamma$ with a Cauchy distribution. When $\beta_2 \neq 0$, Equation (6.26) can be written as:

$$\beta_2 \log\left(a_1(\gamma)/Z\right) \tag{6.33}$$

Where

$$a_1(\gamma) = \frac{\frac{\pi}{2}+\beta_2\gamma}{\cos\gamma} exp\left(\frac{1}{\beta_2}\left(\frac{\pi}{2}+\beta_2\gamma\right)\tan\gamma\right) \tag{6.34}$$

For $\beta_2 > 0$ we can then write:

$$P(N \leq n) = P\left(\beta_2 \log\left(a_1(\gamma)/_Z\right) \leq n\right) \tag{6.35}$$

$$= P\left(Z \geq e^{\frac{-n}{\beta_2}} a_1(\gamma)\right)$$

$$= E_\gamma exp\left(-e^{\frac{-n}{\beta_2}} a_1(\gamma)\right)$$

$$= \frac{1}{\pi}\int_{-\frac{\pi}{2}}^{\frac{\pi}{2}} exp\left(-e^{\frac{-n}{\beta_2}} a_1(\gamma)\right) d\gamma$$

From which we draw the conclusion that for all admissible values of β_2, $N \sim S_1(1, \beta_2, 0)$, which completes the proof.

6.3. Proposed algorithm and noise synthesis results

From Equations (6.25) and (6.26) and the proofs thereof, a method for the synthesis of the PLC noise is proposed. The model is tested using the stable non-Gaussian noise models (and their parameters) developed in Chapter five. The following algorithm is proposed, after the Chambers *et al.* method:

1. For a standard alpha stable noise process with $\alpha \in [0,2]$ and $\beta \in [-1,1]$, generate V, which is a randomly distributed uniform variable on $\left(-\frac{\pi}{2}, \frac{\pi}{2}\right)$ and Z, which is an independent random variable that is exponentially distributed with a mean equal to 1.
2. For $\alpha \neq 1$, compute

$$N = S_{\alpha,\beta} \frac{\sin\left(\alpha\left(V+B_{\alpha,\beta}\right)\right)}{(\cos V)^{\frac{1}{\alpha}}} \left(\frac{\cos\left(V-\alpha\left(V+B_{\alpha,\beta}\right)\right)}{Z}\right)^{\frac{1-\alpha}{\alpha}} \tag{6.36}$$

Where N is the variable that defines the standard stochastic power line noise process, and:

$$S_{\alpha,\beta} = \left(1+\beta^2\tan^2\frac{\pi\alpha}{2}\right)^{\frac{1}{2\alpha}} \tag{6.37}$$

$$B_{\alpha,\beta} = \frac{\tan^{-1}\left(\beta\tan\left(\frac{\pi\alpha}{2}\right)\right)}{\alpha} \tag{6.38}$$

3. Else, for $\alpha = 1$, compute:

$$N = \frac{\pi}{2}\left(\frac{\pi}{2} + \beta_2 V\right)\tan V - \beta_2 \log\left(\frac{\frac{\pi}{2} Z \cos V}{\frac{\pi}{2} + \beta_2 V}\right) \tag{6.39}$$

4. Generalize the stochastic alpha stable power line noise process by transforming the standard stable noise process as follows:

$$N_1 = \begin{cases} \sigma N + \mu & \alpha \neq 1 \\ \sigma N + \dfrac{2}{\pi}\beta\sigma \log \sigma + \mu & \alpha = 1 \end{cases} \tag{6.40}$$

Where $N_1 \sim S_\alpha(\sigma, \beta_2, \mu)$ defines the alpha stable powerline noise synthesis process.

From the alpha stable noise model parameters obtained in Chapter five, the synthesis of the power line noise process as a stochastic process is carried out for different random number of alpha stable noise samples *N*. Results for 100, 1000, and 10000 alpha stable noise samples are presented here. The time domain synthesised power line noise series for 100, 1000 and 10000 noise samples are shown in Figures 6-1 to 6-3 respectively.

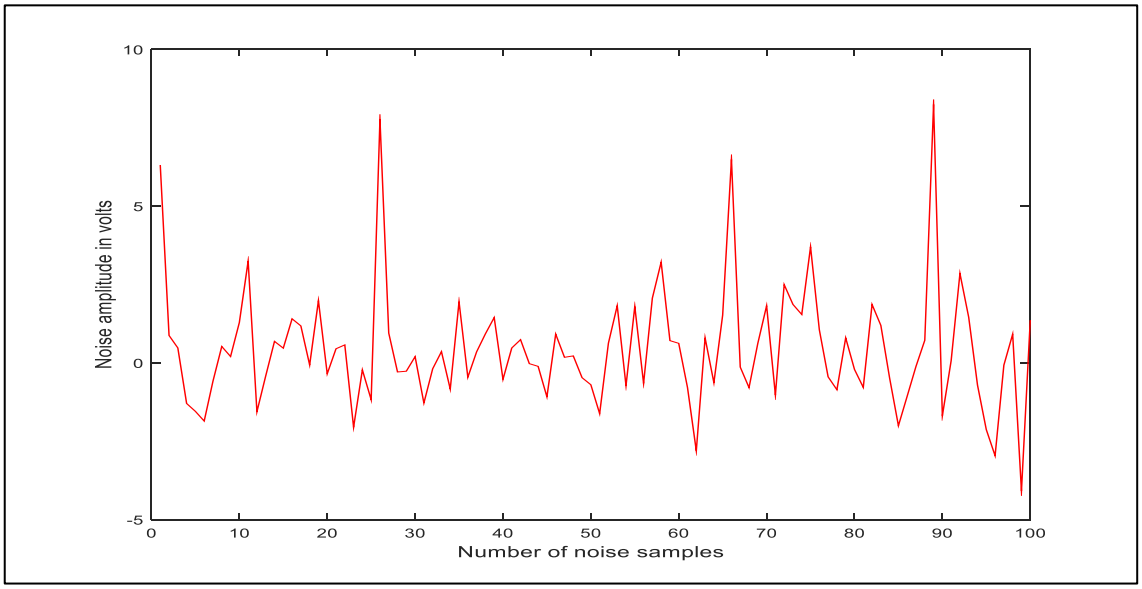

Figure 6- 1: Sythesised time domain alpha stable power line noise for 100 noise samples

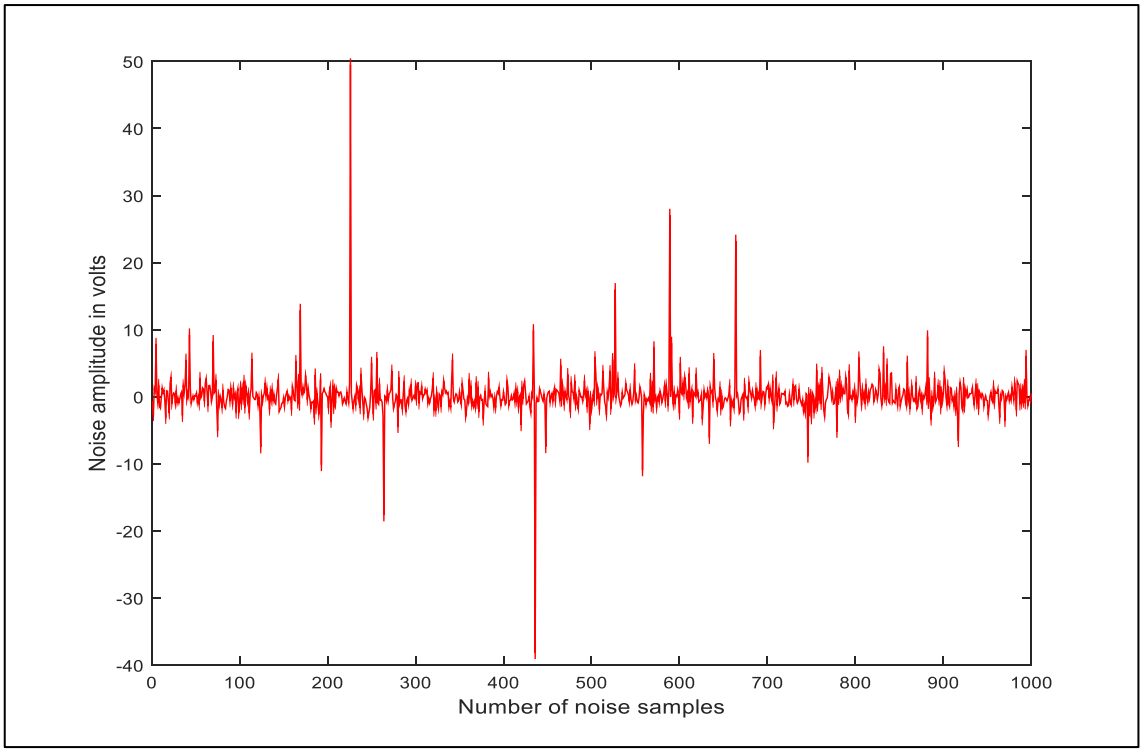

Figure 6- 2: Sythesised time domain alpha stable power line noise for 1000 noise samples

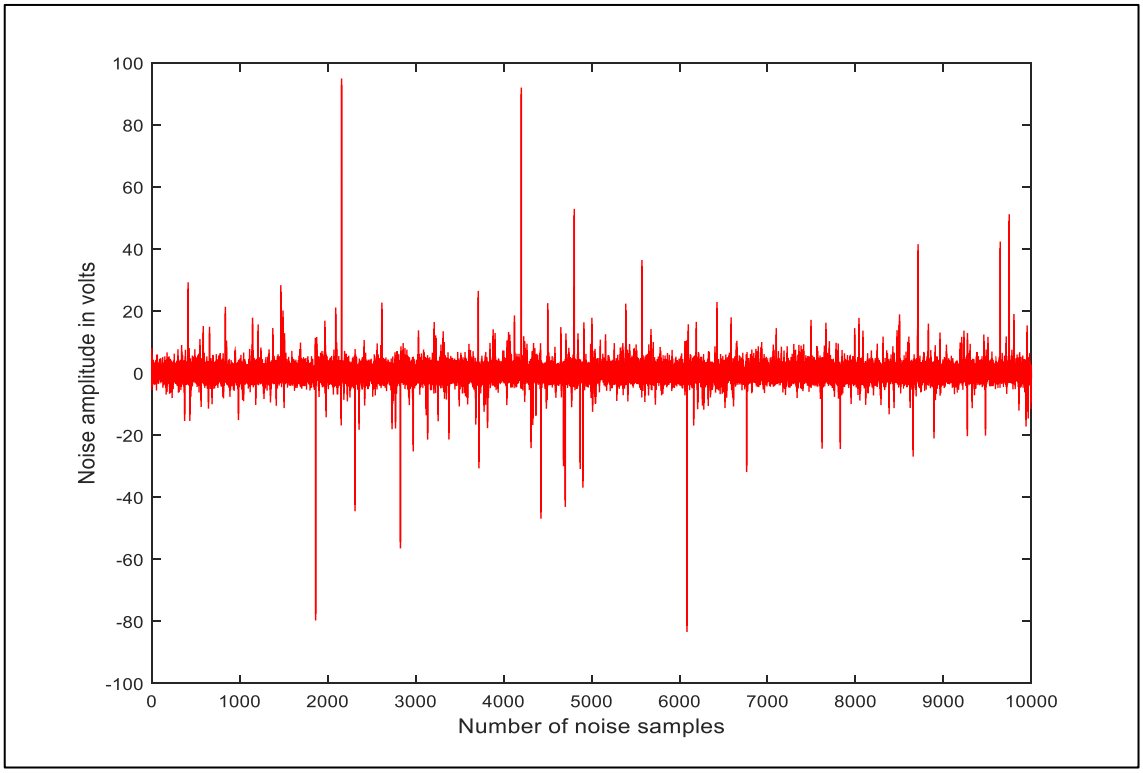

Figure 6- 3: Sythesised time domain alpha stable power line noise for 10000 noise samples

Similarly, the synthesised frequency domain power line noise series for 100, 1000 and 10000 noise samples are shown in Figs. 6-4 to 6-7 respectively.

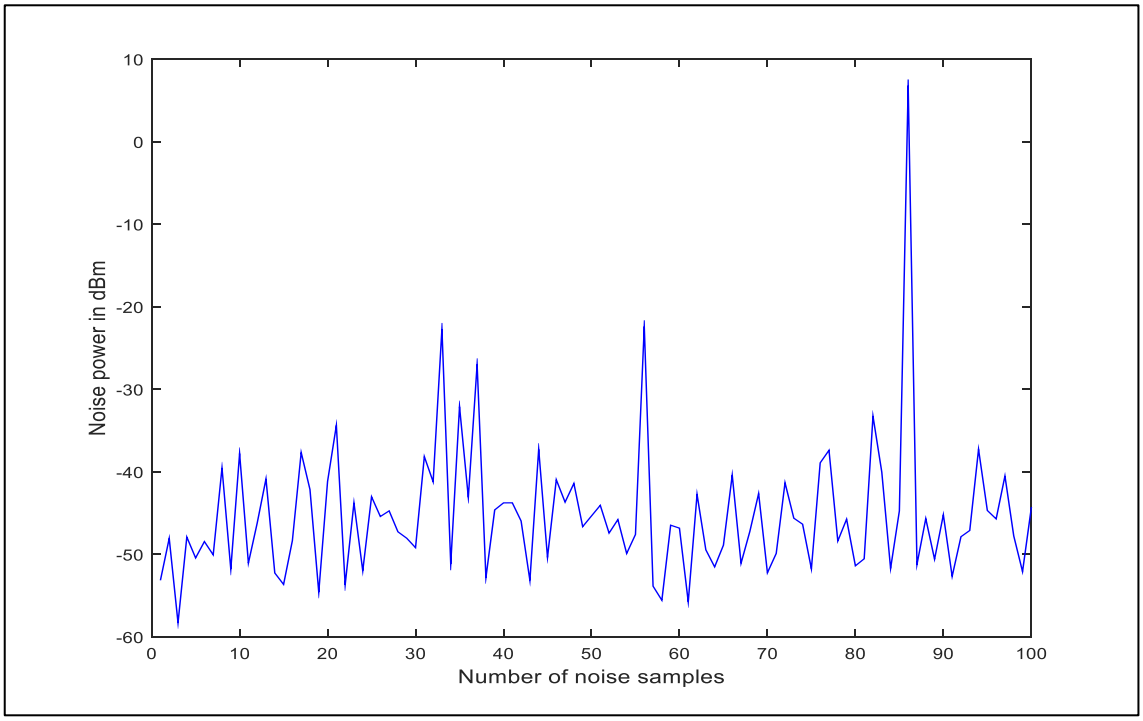

Figure 6- 4: Sythesised frequency domain alpha stable power line noise for 100 noise samples

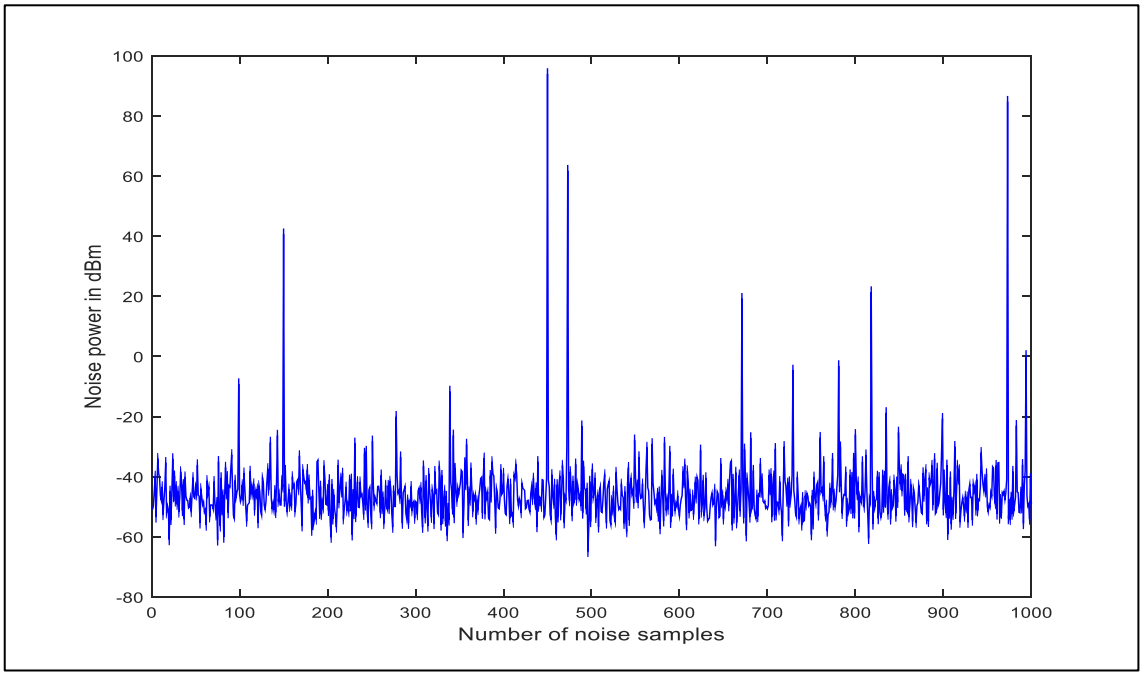

Figure 6- 5: Sythesised frequency domain alpha stable power line noise for 1000 noise samples

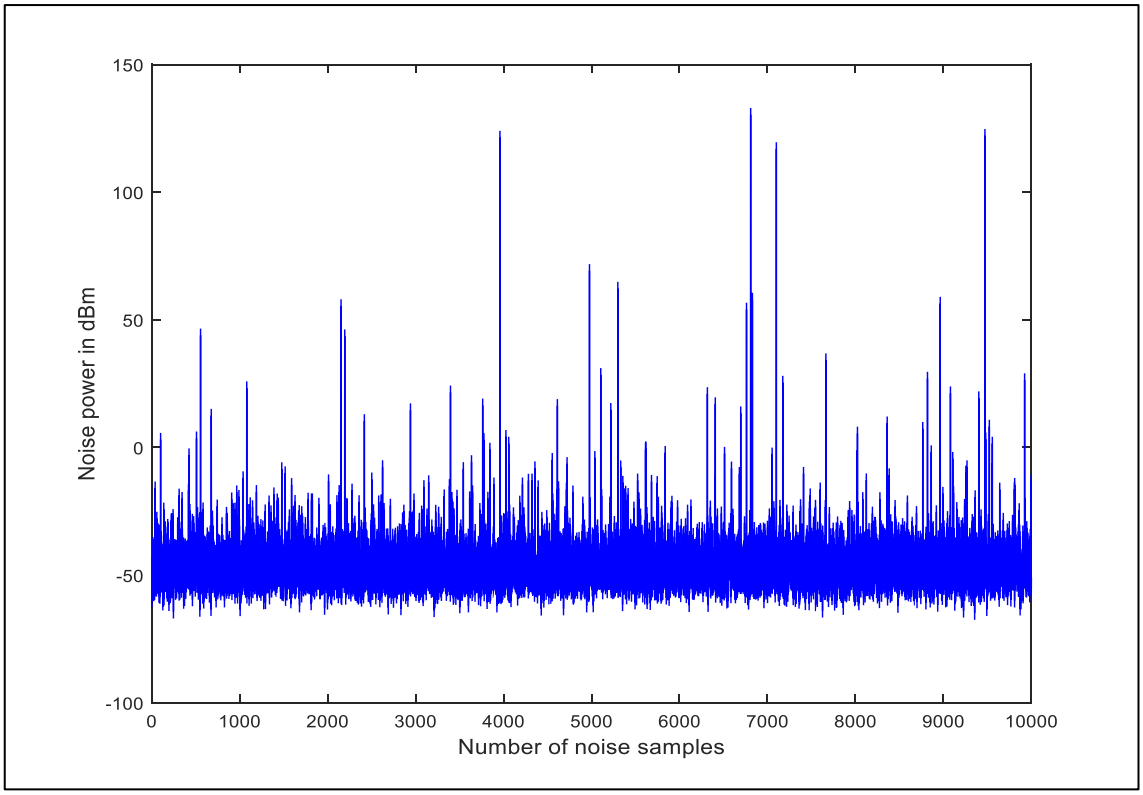

Figure 6- 6: Sythesised frequency domain alpha stable power line noise for 10000 noise samples

From both the time and frequency domain power line noise series, we see that high variability is observed in the synthesised noise series for the noise parameters that were obtained from our noise measurements. This kind of high variability is an indication of the impulsive nature of power line noise. Moreover, most of the noise power appears to be constrained to a small range, which indicates the background noise component in PLC systems. Also, we observe that the high power impulses are fewer compared to the background noise that is more prevalent. The background noise is known to be Gaussian distributed, characterized by a fairly flat spectrum, while impulsive noise is characterized by high variability, which leads to a long-tailed characteristic of its marginal distribution. The fact that the synthesised noise for all random samples in both domains clearly shows both background and impulsive noise events confirms that the framework developed is robust. The algorithm proposed is applicable for all admissible values of the alpha stable noise parameters; meaning it can be used for the study of highly impulsive to weakly impulsive PLC systems. Thus, using this algorithm, it is now possible to generate impulsive noise for the study and development of PLC systems without necessarily resorting to noise measurements. Overall, we observe that the higher the number of noise samples considered, the higher the variability (range) in the overall noise power or voltage. Also, a higher number of noise samples results in more powerful noise power/voltage

spikes, an indication that the framework developed produces meaningful results. Thus,the algorithm works very well for our noise results in Chapter five. Also, the similarities between the synthesised noise and those obtained in the measurements in Chapter three cannot go unnoticed.

To prove that the algorithm works well for the noise results in Chapter five, the determination of the alpha stable parameters for the noise results shown in Figs. 6-1 to 6.6 was done, using the parameter estimation techniques in Chapter five. The alpha stable noise parameters obtained from the sythesised noise in Figs. 6-1 to 6-6 are shown in Tables 6.1 and 6.2 below.

Table 6. 1: Sythesised time domain noise alpha stable parameters

Time domain Levy synthesis parameters				
Number of noise samples	α	β	γ	δ
100	1.58	0.531	0.928	0.478
1000	1.48	0.208	0.828	0.163
10000	1.47	0.254	0.822	0.231

Table 6. 2: Sythesised frequency domain noise alpha stable parameters

Frequency domain Levy synthesis parameters				
Number of noise samples	α	β	γ	δ
100	1.848	1	4.167	-45.80
1000	1.90	1	4.334	-46.41
10000	1.733	1	4.248	-45.86

From these tables, we observe that the parameters obtained are close to those in Chapter five. Also we observe that a higher number of noise samples produces parameters that are closer to those in Chapter five; which in itself is a more practical scenario. To confirm that the synthesised noise has the same distribution as the one obtained from the measured noise, the pdfs and the cdfs of the synthesised noise parameters and those from measurements are plotted together. These are shown in Figs. 6-7 to 6-10.

From these figures, we observe that there is a very close match between the synthesised plots and the measured ones (those in Chapter five). Also, from the time domain plots, we see that the plot for the 100 noise samples provides the least match to the measured one. The frequency domain plots seem to all fit very well. Overall, the same shape and long-tailed behaviour of the pdfs as well as the cdfs is retained. However, to ascertain the accuaracy of the overall noise synthesis process, RMSE analysis and Chi-square tests were done. These results present a

comparison between the alpha stable models in Chapter five and those developed from the noise synthesis in this chapter. The results of the tests are shown in Tables 6.3 and 6.4.

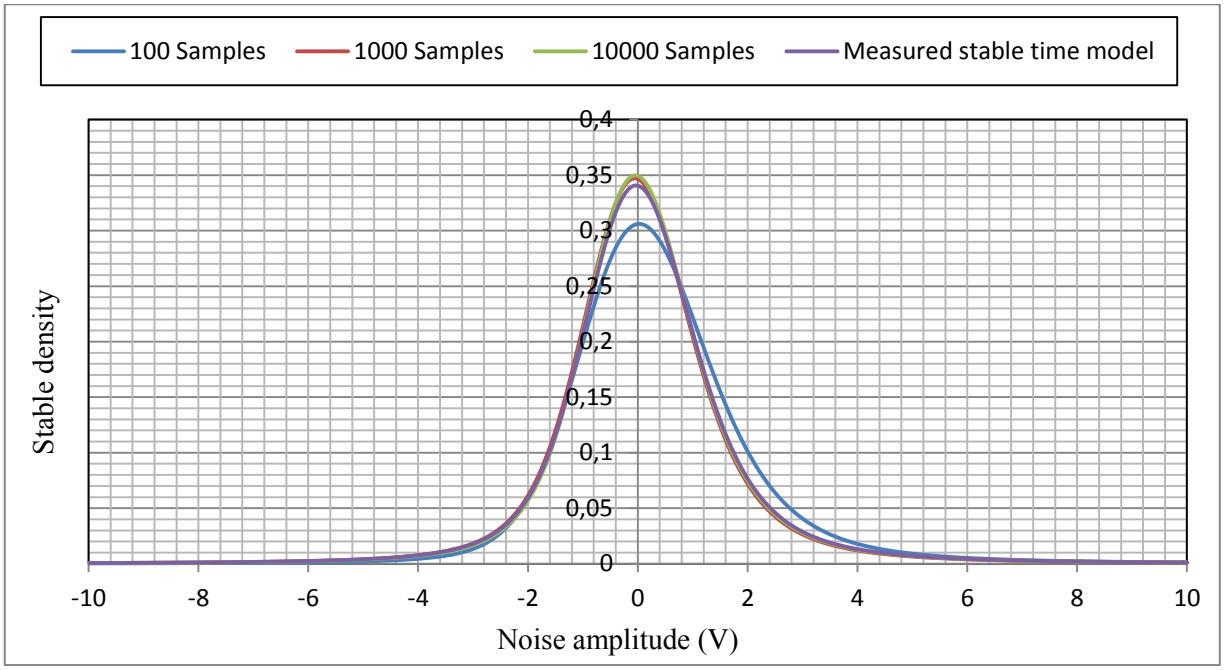

Figure 6- 7: Time domain alpha stable power line noise models

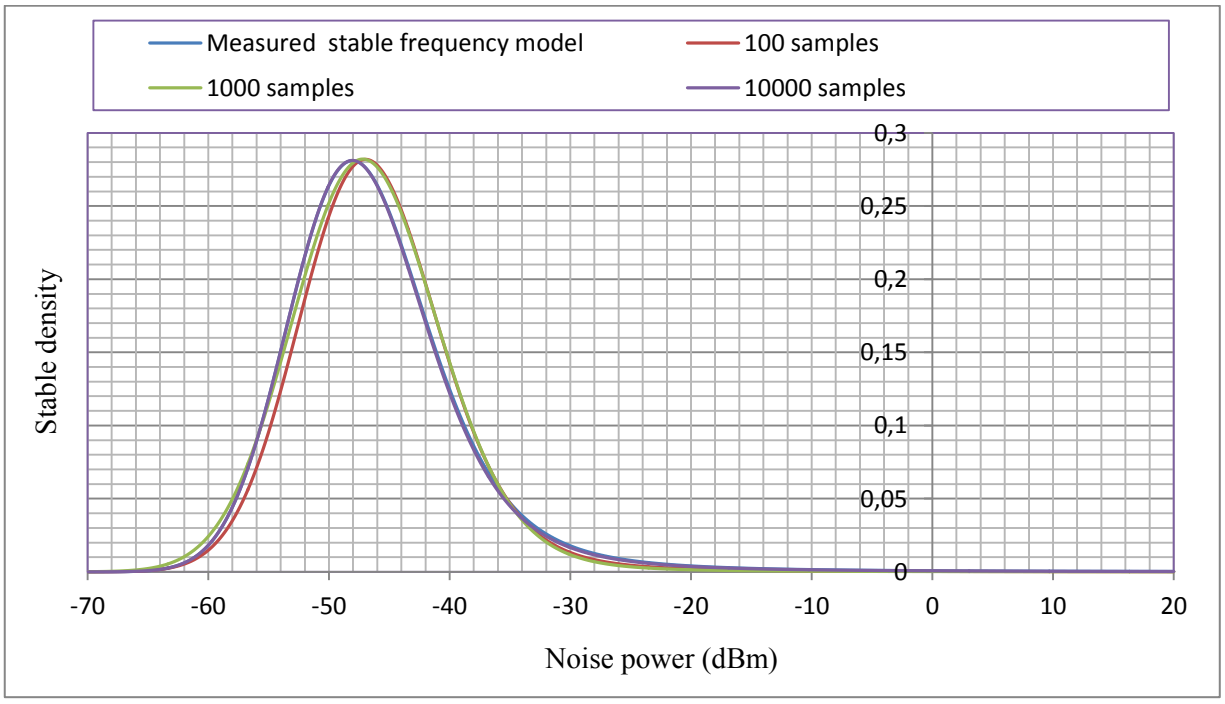

Figure 6- 8: Frequency domain alpha stable power line noise models

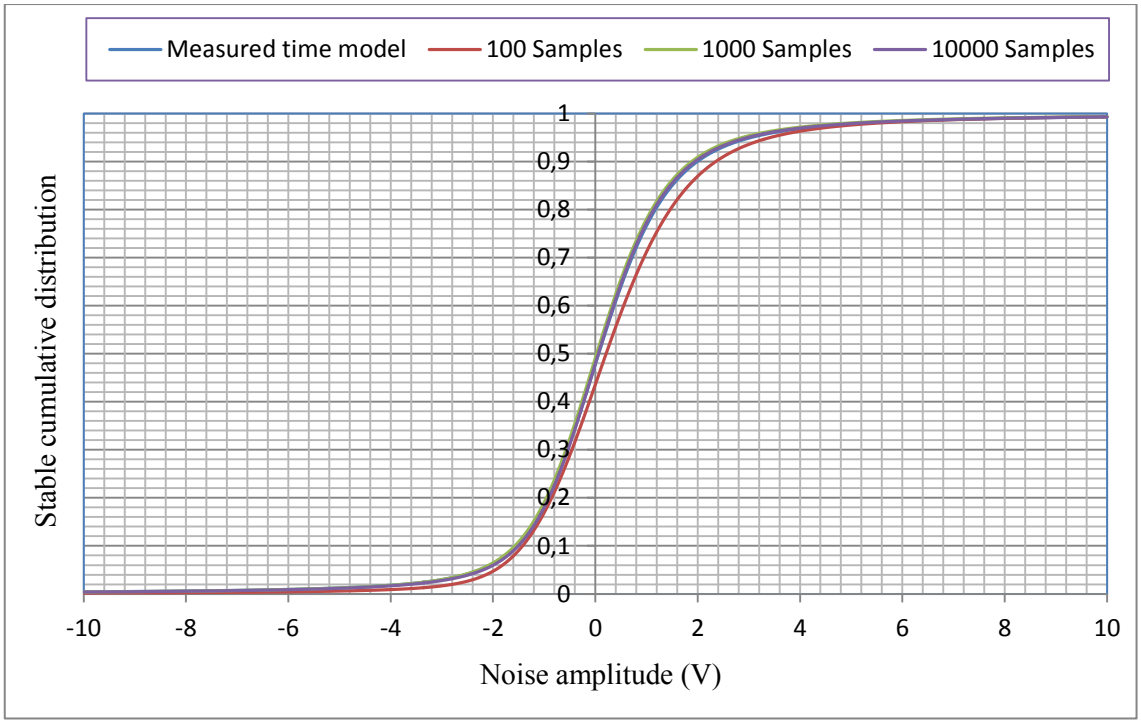

Figure 6- 9: Time domain alpha stable power line noise cdf plots

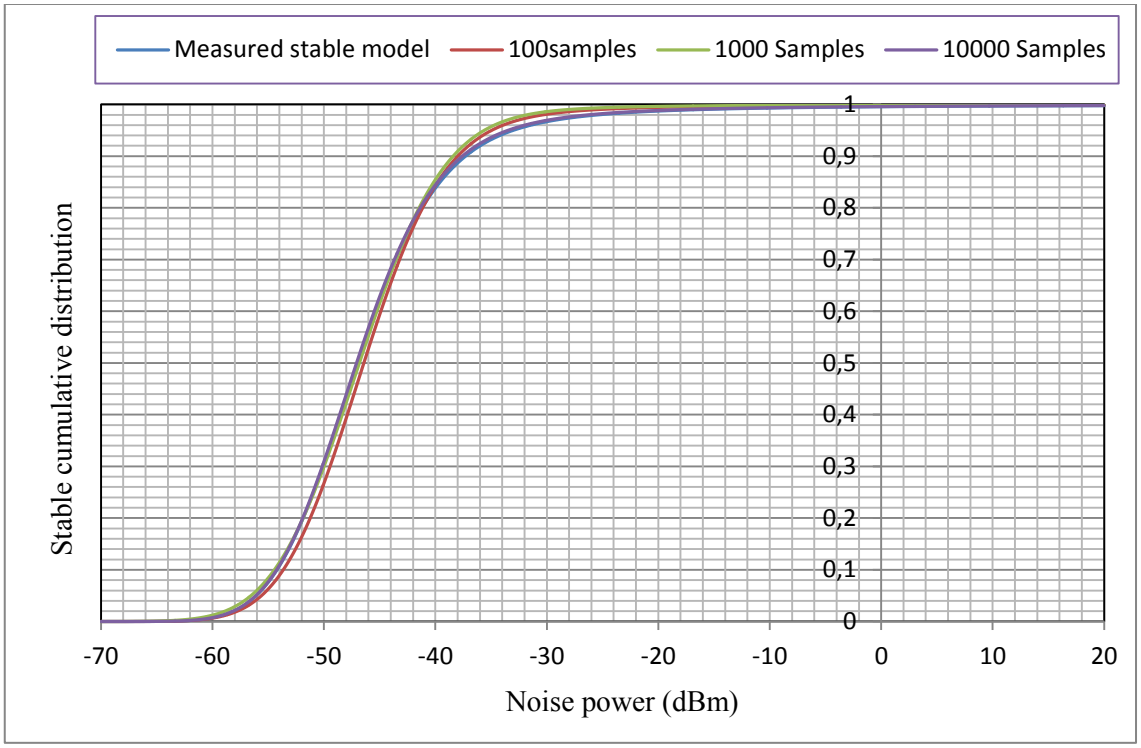

Figure 6- 10: Frequency domain alpha stable power line noise cdf plots

Table 6. 3: Time domain noise goodness of fit results

Number of noise samples	Time domain			
	RMSE	χ^2	DF	CV
100	0.0104	0.34	450	500.456
1000	0.0026	0.00003	450	500.456
10000	0.0022	0.003	450	500.456

Table 6. 4: Frequency domain noise goodness of fit results

Number of noise samples	Frequency domain			
	RMSE	χ^2	DF	CV
100	0.0109	1.254	450	500.456
1000	0.0079	0.270	450	500.456
10000	0.001	0.00006	450	500.456

From the results in Tables 6.3 and 6.4, we see that the least RMSE is obtained for 10000 random noise samples, which means that a higher number of noise samples improves the algorithm prediction accuracy. Also, the highest χ^2 values are obtained for 100 noise samples which means that the alogrithm reliability is slightly reduced when the noise samples are very small. The smallest χ^2 values are obtained for 1000 noise samples for the time domain while the same is obtained for 10000 noise samples for the frequency domain. However, at the 0.05 significance level used for this test, we see that the critical values (CVs) are much much higher than the computed χ^2 values, for the same degrees of freedom (DF). Therefore, the null hypothesis is accepted for all cases. Thus for all random noise samples, the PLC noise synthesis framework developed proves to be very reliable. Overall, we also see that all RMSEs are very small, which means the noise distribution prediction accuracy of the algorithm proposed is very high.

6.4 Chapter summary and conclusion

In this chapter, a framework for synthesizing noise in PLC systems has been developed. The mathematical background for the algorithm proposed has been presented as well. Results from the synthesis of the power line noise as an alpha stable stochastic process show that the random nature of the power line noise is well captured. High variability is observed in the synthesised noise series for both time and frequency domains, for a random number of alpha stable noise samples. Also, an ever present low power background noise component is observed in the

synthesised noise, coupled with a lesser number of high power impulses. The Levy stable noise parameters obtained from the synthesised power line noise are very close to those in Chapter five, for all random number of samples considered, an indication that the algorithm prediction accuracy is very good. Also, the synthesised noise has the same distribution as the measured noise. All goodness of fit and reliability test results obtained show that the algorithm accuracy is very satisfactory. Also, the algorithm is applicable for all admissible values of alpha stable parameters.Thus, the proposed algorithm is able to synthesise any level of impulsiveness raging from very impulsive noise processes to background noise cases, by considering the PLC noise process as a Levy stable stochastic process. Overall, the long-tailed behaviour as well as overall shape of the pdfs and cdfs is retained in all the synthesized noise models. Therefore, the PLC noise synthesis framework developed here is very crucial in the study and development of high performing and reliable PLC systems, as well as stimulating further research in PLC noise in general (for LV, MV and HV networks) in line with the outcomes presented in this chapter.

Chapter references

[1] J.M. Chambers, C.L. Mallows, and B.W. Stuck, "A method for simulating stable random variables," *Journal of the American Statistical Association*, vol. 71, no. 354, pp. 340-344, 1976.

[2] M. Kanter, "Stable densities under change of scale and total variation inequalities," *The Annals of Probability*, vol. 3, no. 4, pp. 697-707, 1975.

[3] L. Devroye, "A triptych of discrete distributions related to the stable law," *Statistics & Probability Letters,* vol. 18, pp. 349-351, 1993.

[4] L. Devroye, "A note on Linnik's distribution," *Statistics & Probability Letters*, vol. 9, Issue 4, pp. 305–306, April 1990.

[5] R. Weron, "On the Chambers-Mallows-Stuck method for simulating skewed stable random variables," *Statistics and Probability Letters,* vol. 28, Issue 2, pp. 165-171, 1996.

[6] R. Weron, "Correction to: On the Chambers-Mallows-Stuck method for simulating skewed stable random variables," *MPRA Paper* No. 20761, posted 17th February 2010.

[7] S. Borak, W. Hardle, and R. Weron, "Stable distributions," *Statistical tools for finance and insurance*, pp. 21-44. Berlin: Springer, 2005.

[8] R. Weron, "Levy-stable distributions revisited: Tail index > 2 does not exclude the Levy-stable regime," *International Journal of Modern Physics,* C12: pp. 209–223, 2001.

[9] R. Weron, "Computationally intensive value at risk calculations, in J. E. Gentle, W. H¨ardle, Y. Mori (eds.)," *Handbook of Computational Statistics*, Springer, Berlin, pp. 911–950, 2004.

[10] E. Taufer, *A note on the empirical process of strongly dependent stable random variables*, Department of Economics and Management, University of Trento, October 2014, Available: http://arxiv.org/abs/1410.8050v1.

[11] L. Devroye, and L. James, "On simulation and properties of the stable law," *Statistical Methods and Applications*, vol. 23, pp. 307–343, 2014.

[12] A. Janicki and A. Weron, *Simulation and chaotic behavior of α-stable stochastic processes*, (Marcel Dekker, New York), 1994.

[13] A. Weron and R. Weron, "Computer simulation of Levy alpha-stable variables and processes," *The Interplay Between Stochastic and Deterministic Behaviour: Proceedings of the XXXIst Winter School of Theoretical Physics,* Karpacz, Poland, 13-24 February 1995. Lecture Notes in Physics, vol. 457, p.379-392.

[14] V. M. Zolotarev, "One-dimensional stable distributions," *Translations of Mathematical Monographs, vol. 65, American Mathematical Society,* pp. 270-277, 1986.

Chapter Seven

7. Conclusion

7.1 Executive summary

In this thesis, a framework has been developed for PLC noise modelling, characterization and synthesis based on measurements, and parametric and nonparametric stochastic processes. The work covered in every chapter is summarized next.

In Chapter one, a general introduction about what power line communications entails was given; its definition, challenges, advantages and applications. A brief motivation for the research presented here was also presented. Also, outline of the research questions, objectives, methodology, as well as a list of both major and minor contributions that have been made to this research field were given.

In Chapter two, a survey of powerline communications in terms of the characteristics that define it was presented. A thorough review of the channel frequency response, noise as well as multipath propagation was given. The different channel modelling approaches were surveyed, where multipath propagation phenomena (echo scenario) was noted as the major contributor to the channel models proposed so far. This multipath propagation results in different copies of the signal that was send from the transmitter getting to the receiver through different paths, attenuated and delayed in different proportions. The channel models fall into two main categories: the top-down and bottom-up models. This classification is based on whether or not the PLC channel is considered as a black-box or not. On the other hand, PLC noise is divided into three major groups: narrowband interference, coloured background noise and impulsive noise. Various parametric models have been previously fronted in literature for the study of PLC noise; key among them Middleton's Class-A model and the two-term Gaussian mixture model. These models are however rigid and limited in their applicability. The choice of appropriate modulation schemes for PLC was also discussed. Additionally, a study on the impact of the impulsive noise on an OFDM-based BPSK system was also presented based on the elementary parameters that define impulsive noise. Finally, EMC/EMI issues that pertain to PLC technology were presented; the key point being the fact that PLC systems must co-exist with other systems without causing interference to them and vice versa.

In Chapter three, a presentation was done on the noise measurements carried out in this study. The measurement environment was discussed together with the coupling circuitry used. Also, the noise measurement set up and the measurement equipment description was also presented.

Finally, sample noise measurements results in both time and frequency domains were also presented.

In Chapter four, models of measured indoor low voltage powerline noise in Chapter three are developed based on a nonparametric approach that is based on the kernel density estimation technique. These models were developed through a direct estimation of the density estimate from the data. That is, no assumptions were made as to the particular shape of the underlying data structure, neither were any restrictions imposed on the data structure. These models are highly flexible and overcome the rigidity associated with former parametric models of PLC noise. The kernel method estimation accuracy is determined more by the smoothing parameter than the kernel function, as seen from the results obtained. For this reason, a simple iterative procedure was adopted that ensured that optimal bandwidth value was used for each of the four kernels used. Thus optimal kernel models of the noise measured in both time and frequency domains were developed. For comparison purposes, both over-smoothed and under-smoothed models were also presented alongside the optimal ones. Error analysis and Chi-square tests were applied to ascertain the modelling certainty and accuracy. Since this approach models the data as it is, such models act as an excellent reference point for the development of parametric models of the same PLC noise. Also, a long-tailed characteristic was also observed on the pdfs developed, and therefore there was need to futher investigate this behaviour of the noise process. Thus, a choice of a very flexible modelling tool for the development of appropriate parametric models of the noise data that captures this heavy/long tailed behaviour was necessary.This was also important in confirming the well-known fact that noise in PLC systems is non-Gaussian. Thus, this formed the task in Chapter five.

In Chapter five, a very flexible stochastic modelling tool (stable distribution) was employed in the development of parametric models of the noise measured in Chapter three. These models are referenced on the optimal kernel models developed in Chapter four. The highly flexible stable distribution was employed in the derivation of appropriate simple and tractable models of the measured noise characteristics. Two methods were used to determine the alpha stable noise models parameters; McCulloch's quantile based and Koutrouvelis' Fourier based iterative method. The four alpha stable noise parameters obtained using both methods were the same; an indication of the robustness of the estimation methodology adopted. The probability density as well as the cumulative distribution plots were then developed using the noise parameters obtained. The models developed showed non-Gaussian behaviour as witnessed from the parameters also. The long-tailed characteristic of the models developed is also clearly visible, something that results from the impulsive nature of the PLC noise. Alpha stable distributions are defined by heavier tails than those of the Gaussian distribution and were therefore best suited in modelling this impulsive phenomenon. Upon confirmation that the noise process in

PLC can be considered as an alpha stable process, there was need to develop an appropriate framework for the noise generation in PLC systems as an alpha stable process. This was the focus in Chapter six.

In Chapter six, a PLC noise synthesis framework as a Levy stable process was developed. This framework is based on the method proposed by Chambers *et al.* Also, the method is based on the equality in law for a skewed stable random variable. The important proof of the nonlinear transformation of an independent exponential variable and an independent uniform variable was also presented. Based on the above method and the proofs thereof, an algorithm for the noise synthesis in power line networks was proposed. This algorithm is applicable for all admissible values of the alpha stable noise parameters and can therefore be used to synthesise PLC noise for any level of impulsiveness. PLC noise synthesis results for the alpha stable noise parameters obtained in Chapter five were presented, where a random number of noise samples were chosen. It was noted that a higher number of noise samples results in higher impulsive power, and this confirms that the algorithm works well. For comparison purposes, results for a Gaussian alpha stable distribution were also presented. A fairly constant impulse power was observed in the Gaussian case as opposed to the high variability noted in the impulsive noise process generated using the parameters in Chapter five.

All in all, a full framework for the modelling, characterization and synthesis of low voltage (applicable to other power networks as well) power line noise has been developed; where a very flexible nonparametric approach starts off the modelling and characterization process followed by a very flexible parametric modelling of the same noise using Levy stable distributions, and finally a general PLC noise synthesis framework has been developed. This synthesis framework implies that it will no longer be necessary to perform noise measurements for one to understand the marginal distribution aspects of PLC noise.

7.2 Future work

Possible avenues for future research are:

1. A performance study of the developed noise models through their application in different coding and modulation schemes for PLC systems optimization and/or redesign purposes.
2. The application of the PLC noise framework developed here for the actual characterization of PLC noise in MV and HV networks through measurements.
3. The incorporation of a memory aspect in the models developed here is an interesting research to look into.